Addis Ababa University

College of Natural and Computational Sciences

Center For Environmental sciences

Modeling Soil Erosion and Mapping its Risk in the Dura Watershed of the Upper Blue Nile Basin in North Western Ethiopia

By:- Yitbarek Aemro Tegegne

Addis Ababa, Ethiopia

June, 2024

Addis Ababa University

College of Natural and Computational Sciences

Center for Environmental Science

Modeling Soil Erosion and Mapping its Risk in the Dura Watershed of the Upper Blue Nile Basin in North Western Ethiopia

By: Yitbarek Aemro

Advisor:- Prof. Mekuria Argaw

A Thesis Submitted to School of Graduate Studies, Addis Ababa University, In Partial Fulfilment of The Requirement for The Degree of Master of Science in Environmental Science, Specializing in Natural Resource Management

Thesis approval form

This is to certify that the Thesis entitled as “Modeling Soil Erosion and Mapping Risk in Dura Watershed of Upper Blue Nile Basin in North Western Ethiopia” has been approved by Center for Environmental science for post graduate in Natural Resource management.

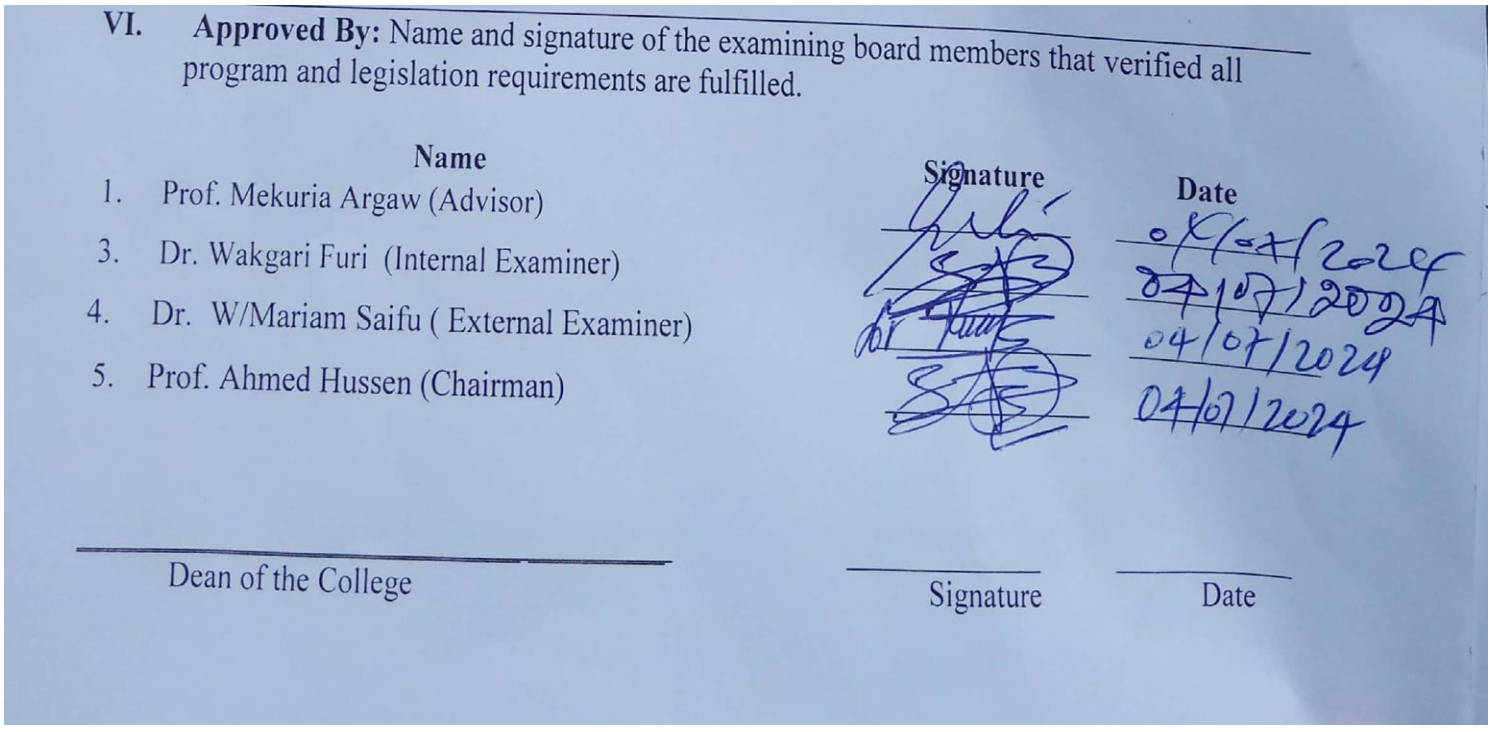

VI. **Approved By:** Name and signature of the examining board members that verified all program and legislation requirements are fulfilled.

	Name	Signature	Date
1.	Prof. Mekuria Argaw (Advisor)		04/07/2024
3.	Dr. Wakgari Furi (Internal Examiner)		04/07/2024
4.	Dr. W/Mariam Saifu (External Examiner)		04/07/2024
5.	Prof. Ahmed Hussen (Chairman)		04/07/2024

Dean of the College — Signature — Date

Acknowledgements

First and foremost, all praise and glory to the Merciful Almighty God.

First of all, I would like to express my deep sense of gratitude to my advisors, Prof. Mekuria Argaw for their leading and constructive comments, generous financial support, continuous guidance, and feedback throughout the thesis process and this study. My special thanks go to Dr. Alemu Beyene for his special guidance on HEC-HMS software and the GIS part of the study.

I would like to express my special thanks to my family (their support, love, and care) for the opportunity to teach me how to use my money without having to pay for throughout the whole study period. I would like to thank Dr. Tadesse Alemu for their generous financial support and continuous guidance. I would like to thank Dr. Eyale Bayabel and Dr. Andualem Mekonen, Eng. Tarekegn Assay, Birelew Azimeraw for their financial support and guidance. I would like to thank Bireda Alemayehu (a PhD student) and his wife, Sirawdinke, for their continued encouragement, cooperation, and critical financial support that enabled me to finish my study. I would like to thank my best friends Belay Tafachu for their special guidance on GIS and remote sensing software for image processing. And, I would like to thanks Gebayaw Ayele, Jerbaw Tirunh, Amare Temesgen, Endashaw Abyneh, Degu Abirham for their independent encouragement, guidance and cooperation.

I am grateful to Addis Ababa University for sponsoring me to pursue my post-graduate study at the Addis Ababa University College of Natural and Computational Science. This is a great opportunity to thank College of Natural and Computational Science Center for Environmental Sciences staff members, directly or indirectly, for their generous support during my study period. My appreciation also goes to the Ministry of Water and Energy for providing me with stream gauges and sediment data and to the National Meteorological Authority for providing climate data. The technical support of the university and all other persons who have helped me on various stages since elementary school until this study are gratefully acknowledged.

I would like to express my deep gratitude to Arat Kilo Gibe Gubbay for allowing me to learn a spiritual lesson, all the students of Addis Ababa University, instructors, Earth Science students, and Center for Environmental Science, who have both served as valuable classmates and close friends. I would like Center for Environmental Science, instructors, coordinators and Secretaries for them brief explanation and orientation on our learning journey and for their guidance in every manner as much as they can.

Finally, I would like to thank all my friends; they were close to me in all aspects of my life. All names could not be mentioned separately because of their independent encouragement and cooperation. Thank you very much!!!

Table of Contents

List of Figures

List of Tables

Acronyms and Abbreviations

ANRS	Amhara National Regional State
DEM	Digital Elevation Model
NASA	National Aeronautics and Space Administration
SRTM	Shuttle Radar Topography Mission
USGS	United Satas Geological Survey
GPS	Geographical Positioning System
ASTER_GDEM	ASTER- Global Digital Elevation Model
USACE	United States Army Corps of Engineers
HEC-HMS	Hydrologic Engineering Centers Hydrologic Modeling System
GIS	Geographic Information System
MUSLE	Modified Universal Soil Loss Equation
RUSLE	Revised Universal Soil Loss Equation
SWAT	Soil and Water Assessment Tool
SWC	Soil and Water Conservation
USLE	Universal Soil Loss Equation
PWRMSE	Peak-Weighted Root Mean Square Error
NSE	Nash-Sutcliffe Efficiency
RMSE	Root Mean Square Error
R^2	Coefficient of Determination
SB	Sub-basin
SMA	Soil Moisture Accounting
DC	Deficit and Constant
LULCC	Land Use Land Cover Change

LCC	Land Use Land Cover
FAO	Food and Agricultural Organization of the United Nation
Km	Kilometer
ha	hectare
t ha–1yr–1	ton per hectare per year
SCS-CN	Soil Conservation Services Curve Number
HWSD	Harmonized World Soil Data
Tc	Time of Concentration
Sc	Storage Coefficient
GW. F	Ground water Fraction
m.a.s.l	meter above sea level

ABSTRACT

Modeling soil erosion and mapping land use and land cover dynamics is critical for the estimation, management, and sustainability of current and future natural resources and improving the quality and quantity of agricultural products. It emphasizes soil erosion as a major environmental threat, causing significant economic losses and reduced agricultural productivity. The main objective of this study was to model soil erosion and map its risk in order to determine erosion vulnerability in the Dura watershed on the upper Blue Nile basin using the HEC_HMS model integrated with GIS and remote sensing. The impact of LULC change on the magnitude of surface runoff and soil erosion was assessed using MUSLE model and statistical tools in HEC-HMS. The effect of LULC change, on surface runoff, sediment load for the water and soil resources, and watershed management for sustainable Natural resource management was evaluated. The result showed that, forest area experienced a decline of 10.9% from 1993 to 2013, followed by a noteworthy recovery of 26.2% by 2023. Notably, bush land displayed the most substantial growth rate (84.9%) across the entire period, with a particularly sharp increase (45.5%) from 2013 to 2023. Agricultural land exhibited a peak in 2013, with a 46.4% increase from 1993, but then decreased by 23% by 2023. The area of bare land witnessed the most dramatic decline (95.8%) from 1993 to 2023, demonstrating a consistent decrease across each decade. Higher values indicate better agreement between model predictions and observations. These findings validate the suitability of the HEC-HMS model for runoff simulation. Notably, the upper sub-watershed exhibited higher surface runoff, soil erosion rates, and sediment yield compared to the lower sub-watershed in 1993. Specifically, SB1 experienced an erosion rate of 4.56 t/yr, which more than doubled to 11.76 t/yr by 2010. Similarly, SB2 witnessed a substantial increase from 8.27 t/yr in 1993 to 10.79 t/yr in 2010. The sediment yields for Sub-Basins 1, 2, and 3 were 45.15 t ha^{-1} yr^{-1}, 28.9 t ha^{-1} yr^{-1}, and 5.81 t ha^{-1} yr^{-1}, respectively. In contrast, Sub-Basin 13 had a lower sediment yield of 0.031 t ha^{-1} yr^{-1}. These results underscore the combined impact of land use/land cover changes, topography, rainfall patterns, and agricultural activities within the watersheds. Generally, LULC increases the watershed, decreases the traction power of rainfall, reduces soil loss and sediment yield in the watershed, increases the infiltration rate of the soil, reduces the magnitude of surface runoff. In order to enhance the quality and quantity of soil and hydrological components, it is important to expand reforestation efforts and consistently monitor shifting patterns. This will help identify areas that are particularly susceptible to erosion. By doing so, we can improve water absorption into the groundwater system, which will have positive impacts on agricultural productivity, water resources, and ecological sustainability in the surrounding area. Additionally, these efforts will also have social, economic, and environmental benefits, as they directly influence soil and water resources and watershed management in the Dura River watershed.

Key Words: LULC change, Mapping land, MUSEL model, Soil Erosion, Sediment HEC-HMS Model, GIS, Dura Watershed

CHAPTER ONE

INTRODUCTION

1.1. Background

One of the biggest environmental issues facing the planet today is soil erosion, which threatened sustainable development and results in significant yearly economic losses. Soil erosion has a long-term impact as its cause loss of fertile top soil and reduce the productivities capacity of the land there by creates risk to global food security (Gomiero, 2016; Mosbahi et al., 2013; Rhodes, 2014). However, Soil is the fundamental resource for economic development and for maintaining sustainable productive landscapes and people's livelihoods especially for countries with agrarian economy like Ethiopian (Gashaw et al., 2017; Wassie, 2020). Forest clearance on mountain slopes for wood charcool and agricultural purposes is the most likely cause of soil erosion in Ethiopian highlands (Teketay, 2001).

In Ethiopia's highlands, soils are at serious risk due to traditional farming, poor management, heavy rains falling on steep slopes with fragile soils, and low vegetation cover that leads to high soil erosion. The high soil erosion rates are mainly a problem in developing countries due to intensive cultivation, deforestation, ploughing of marginal lands, and extreme climate hazards (Jemal, 2021). Globally, about 80% of the agricultural land degradation is caused by soil erosion (Jemal, 2021). Among the various forms of land degradation, soil erosion is the most serious problem, which results in soil nutrient depletion and the loss of the productivity capacity of land.

Some 50% of the highlands of Ethiopia were already significantly eroded in the mid-1980s, and erosion was causing a decline in land productivity at the rate of 2.2% per year and also could reduce per capita incomes of the highland population by 30% in the year 2010 (FAO, 1986). Ethiopia losses over 1.5 billion tons of soil each year from the highlands by erosion resulting in the reduction of about 1.5 million tons of grain from the countries annual harvest (Jemal, 2021). Deforestation, overgrazing and poor land management accelerates the rate soil erosion and sedimentation affects downstream water reservoirs in developing countries like Ethiopia (Kidane & Alemu, 2018). Soil erosion has long term impacts as its cause loss of fertile top soil and reduce the productive capacity of the land and there by creates risk to global food security (Gomiero, 2016). Sedimentation is a major problem in reservoirs and dams as it reduces water storage

capacity, thus indirectly reducing electricity production besides shortening the life time and increasing the maintenance cost (Borji, 2013). The most prevalent issue in Ethiopia's highlands is land degradation brought on by erosion, where a significant amount of fertile soil is lost annually (Wang et al., 2018; Yesuph & Dagnew, 2019). The erodible and poorly structured soils of the Blue Nile Basin could contribute to greater soil erosion and sedimentation in the river basin due to its higher discharge than the White Nile across the catchment region (Haregeweyn et al., 2017; D. Kidane & Alemu, 2018). Poor land-use practices and a lack of soil conservation techniques in the upper Blue Nile Basin have a significant role in the sedimentation of downstream reservoirs (Ali, 2014; D. Kidane & Alemu, 2018).

In Ethiopia's highlands, soil and water resources are at risk, as nearly 80% of the population depends on subsistence agriculture (Jemal, 2021). One process that threatens the resource base is soil erosion (Easton et al., 2010). In Ethiopia's highlands, which provide a living space for more than 90% of the country's human population and for 75% of the livestock population, the country suffers from soil erosion and 42% t/ha/year average soil loss on cultivated land (Hans Hurni, et al., 1998). Besides its impact on onsite land productivity, soil erosion causes rapid siltation of downstream streams and reservoirs by accelerating the storage capacity loss of water harvesting schemes. The rapid water storage capacity losses of the dam reservoirs result in the waste of considerable investments incurred in their construction, in addition to the failure to achieve food security through surface water harvesting (Borji, 2013; Devi et al., 2008; Jemal, 2021).

1.2. Statement of the problem

Soil erosion is a major environmental concern, especially in Ethiopia where the rugged landscape intensifies the erosion process. Therefore, it is crucial to gain a comprehensive understanding of erosion's mechanisms and outcomes in order to effectively regulate water quantity and quality, as well as soil and land utilization. Erosion has significant negative effects on agricultural productivity and infrastructure in both the upstream and downstream areas of the watershed. It also leads to sedimentation, particularly in the downstream region of the watershed. Despite limited research, the potential consequences of soil erosion on environmental resources, infrastructure, agricultural productivity, and economic development are significant (Hans Hurni, et al, 1998, Wassie, 2020). The rapid increase in population has resulted in the expansion of agriculture, which

in turn has caused soil degradation and deforestation. This disrupts the ecological balance of the watershed system (Wassie, 2020; Zegeye, 2017). Traditional farming practices, especially in upper watersheds and marginal lands, exacerbate environmental degradation (Wassie, 2020). Inappropriate land management practices have increased the Dura watershed's vulnerability to soil erosion and negatively impacting its health and sustainability.

This study employs the HEC-HMS model for simulating various factors, including surface runoff, soil loss, sediment yield, climate change, crop development, and land management practices. While other soil erosion prediction models exist, HEC-HMS offers valuable features for simulating these diverse aspects. It has a proven track record in simulating erosion, runoff, and sediment load across various catchments and climatic conditions, including semi-arid regions. The primary objective is to evaluate the effectiveness of HEC-HMS in predicting water, soil, and sediment movement within the Dura watershed. This will facilitate the modeling, mapping, and prioritization of the most degraded sub-catchments based on estimated rainfall, runoff, and sediment yield. Additionally, the study aims to classify land use and land cover within the watershed.

Although some studies have been conducted on soil erosion and LULCC, the relationships between these factors and their impact on hydrological components have not been fully explored. According to (Dibaba et al., 2020), While techniques for analyzing the impact of Land Use Land Cover Change (LULCC) on modeled hydrological components are still under development, and future change predictions are limited, the historical influence of LULCC and soil erosion on agricultural productivity, hydrological processes, and overall watershed health has been recognized and quantified. For instance, the connection between deforestation and increased Soil erosion is well-established, but the connection between deforestation and increased surface runoff and the specific impact on downstream water quality and aquatic ecosystems in the Dura watershed remains unclear. Therefore, modeling the hydrological significance of surface runoff and sediment load remains crucial for estimating, planning, and managing current and future water resources to ensure the long-term sustainability of the Dura watershed.

1.3. Objectives of the study

1.3.1. General objective

The main objective of this study is to model soil erosion and map its risk in order to determine the vulnerability to erosion in the Dura watershed on the upper Blue Nile basin.

1.3.2. Specific objectives

- To analyze the LULC change and dynamics of Dura watershed in the last four decades (1993 to 2023)
- To model the rate of soil erosion, sedimentation and surface water availability in Dura Watershed
- To map the soil erosion risk of Dura watershed

1.4. Research questions

- How has LULC change occurred in Dura watershed over the last four decades (1993 to 2023)?
- What is the impact of LULC on surface runoff and soil erosion in Dura watershed?
- What is the magnitude if LULC change have an impact on soil erosion in Dura watershed
- Which sub-watersheds of Dura watershed are facing serious risk of soil erosion?

1.5. Significance of the research

- The study creates risk maps that identify areas prone to soil erosion. These maps guide decision-making for effective erosion control measures. Decision-makers can prioritize interventions based on the severity of erosion risk in different parts of the watershed
- provide a better understanding of soil erosion and sedimentation process, its upstream and downstream effects as a result of upstream land management systems in Ethiopia.
- The research will add considerable contribution to the benefit of the region in the natural
- resource development, soil and water conservation, and landscape restoration.
- The final output data will be available as a digital map and associated spatial database that will be part of the future national and/or regional Soil Erosion Database and can be used for governmental and/or non-governmental organizations engaged in practical
- implementation and/or further scientific research work in Dura watershed.

- In summary, this research provides valuable insights into soil erosion dynamics, risk assessment, and management strategies in the Dura Watershed. It empowers stakeholders to take informed actions for sustainable land use and environmental conservation.

1.6. Limitations of the research

The study encountered limitations, including the lack of precise secondary data for sediment yield validation in the study area, the challenge of analyzing all data in the catchment due to the large extent of the study area covering a large area of the Dura River basin, and the lack of historical data of the study area and previous research work. Additionally, meteorology data interpolation was performed for the whole study area, but only three-gauge stations in the catchment had data availability, and there was incompleteness of the data record. Furthermore, processing huge satellite image could propagate errors in the result.

1.7. Outline of the thesis

This thesis work consists of five main chapters. The first chapter provides general information about the study area and the purpose of this study. The second chapter briefly discusses previous work, while the third chapter introduces the methodology and data acquisition and provides a brief description of the study area. Chapter four deals with modeling and mapping attributes of analyzing hydrogeological data and spatial data, along with their output description. Finally, in chapter five, the soil erosion modeling and its risk mapping are concluded, along with an analysis of land use land cover change on soil, and recommendations for soil erosion and its risk are provided.

CHAPTER TWO

LITERATURE REVIEW

2.1. Soil Erosion

Soil erosion is a form of soil degradation caused by the dynamic activity of erosive agents such as water, glaciers, snow, wind, plants, and animals (including humans) (Kumarasinghe, 2021; Shah, 1998). Soil erosion is a natural landscape process of critical concern to many land management agencies (Sidle et al., 2006). Soil erosion can be generally defined as the detachment and transport of in-situ soil particles by three natural agents' water wind, and gravity (down slope movement) (Bryan, 2000; William W. and Russell Harmon, 2022). Beside of this, Soil erosion is a basic social and economic problem and an important factor in assessing soil quality, quantities and health, ecosystem health and their function (Balasubramanian, 2017). One of the main causes of land degradation in Ethiopia Highland is soil erosion, which has a variety of negative on-site and off-site effects (Tilahun, 2013, Majoro et al., n.d.,2020).

In many developing nations, like Ethiopia, soil erosion is a significant source of watershed issues that result in significant loss of soil fertility, decreased productivity, and environmental degradation (Ananda & Herath, 2003). Soil erosion and sediment movement are the results of numerous mechanisms, such as water erosion, wind erosion, etc. Soil erosion by water is a serious and continuous environmental problem in parts of the world (Arekhi & Niazi, 2012). In Ethiopia's Highlands, the major environmental risk associated with agricultural productivity is mainly water erosion in the form of sheet, and rill, erosion, in terms of both its economic costs and the areas affected (Abiye, 2022; Esa et al., 2018; Wassie, 2020). However, Due to improper land use, gully and rill erosion increase, and agriculture areas become fragmented. This leads to both socioeconomic and environmental problems in the country (Bekele, 2019; Wassie, 2020).

2.2. Soil Erosion in Ethiopia Highlands

2.2.1. Process of Soil Erosion

Soil erosion is a critical problem affecting rural livelihoods in Ethiopia, and it is mainly caused by human activities, land use change, and topography(Tadesse et al., 2022;Haregeweyn et al., 2015). Soil erosion processes include sheet, rill, and gully erosion, and they vary across different Agro-

ecological zones (Tadesse et al., 2022). The average gross soil erosion rate in Ethiopia is estimated to be 38 t /ha/1/ yr, while the net sediment yield is about 26 t/ ha/ yr (Tamene et al., 2022). Various soil and water conservation measures have been implemented to reduce soil erosion and improve land productivity, but they face many challenges such as limited resources, land tenure insecurity, and poor community participation (Haregeweyn et al., 2015).

2.2.2 Soil Erosion by Water

Soil erosion by water is a major cause of land degradation in the highlands of Ethiopia, where rainfall is erosive and slopes are steep (Balabathina et al., 2020; Ebabu et al., 2023). The dominant erosion processes are sheet, rill, and gully erosion, and they vary across different land uses and management practices (Balabathina et al., 2020). The average soil loss rate in the highlands of Ethiopia is estimated to be 42 t/ha/year for croplands, and up to 300 t/ha/year in extreme cases(Bekele, 2019). Water erosion is estimated to cause 4 billion tons of gross soil loss per year in East Africa, with a mean soil loss rate of 6.3t/ha/year, half of this accounting for Ethiopia (Tadesse et al., 2022).

2.3. Causes of Soil Erosion in Ethiopia

The primary reasons that assist (accelerate) soil erosion in the Ethiopian highlands are fast population growth, cultivation of steep slopes, traditional farming, clearance of vegetation, free grazing, and overgrazing (Gashaw, 2015). Particularly in the northern, Northwestern, and central Ethiopian highlands, the type of soil, the variability of topography, deforestation, intense rainfall, inadequate land management, and the kind of land cover and land use practices have all contributed to runoff that results in soil erosion (Esa et al., 2018; Taddese, 2001). Cultivation of steep slopes, free grazing, clearing of vegetation, and limited knowledge in the community about soil erosion risk have accelerated erosion in the highlands (Alemu, 2015; Mekuria et al., 2009). In the northwest Ethiopia highlands, soil erosion was primarily caused by intensive farming practices without fallow periods, cultivation on steep slopes, inadequate water and soil conservation measures, a lack of ownership awareness, deforestation, overgrazing, utilization of crop yields for animals feed and fuel, and heavy rainfall (Alemayehu, 2015; Wordofa et al., 2020).

Ethiopia loses nearly 1.5 billion tons of soil from its highlands every year due to erosion, which could have produced an additional 1 to 1.5 million tons of grain (Taddese, 2001).

2.3.1 Land use and Land cover change

The reason why people use a piece of land has been used to define land use. It involves both the technique used to modify the biophysical characteristics of the land and the motivation behind that technique. The characteristics of the Earth's immediate subsurface (lithosphere, biosphere, and hydrosphere) and land surface have been referred to as land cover. using land Anthropogenic and natural adjustments to the land surface are indicated by land cover change (LCC). Changes in land use and land cover, namely the biggest human-caused issues in Ethiopia, which have significantly accelerated soil erosion, are the conversion of the natural plant cover into arable land (Negese, 2021). The natural ecosystem is being severely impacted by the expansion of cultivated and grazing areas at the expense of native plants (Negese, 2021). This ongoing expansion of cultivated and grazing land is a significant factor in land degradation, which puts the fertility of the soils in Ethiopia's highlands at greater risk (M. Kidane et al., 2019; Taddese, 2001).

2.3.2 Cause of Land use Land cover change

In Ethiopia, the combination of diverse demographic, social, institutional, and biophysical factors is the main driver of land use and land cover (LULC) change (Dibaba et al., 2020a). According to earlier research, the main causes of land use and land cover change in the Ethiopian highlands were high population pressure, extensive agricultural expansion, settlement expansion, poverty, a lack of common resource management, land tenure insecurity brought on by institutional and policy reforms, and a high demand for fuel wood and building supplies(Negese, 2021). The transition from a natural forest to grassland and cultivated land has always been the cause of deforestation. The primary change in Ethiopia's land use and land cover (LULC) is shifting forested areas to farm land (Berihun et al., 2019). The primary direct causes of deforestation are believed to be agriculture, timber extraction, fuel wood gathering, and charcoal manufacture. Indirect causes of deforestation include population expansion, commodity demand, economic growth, and poor governance(Tsegaye, 2019).

Population expansion is accelerating, which exacerbates land degradation due to the extreme pressure on land resources (M. Kidane et al., 2019). Similar to the above studies, the cause of land cover conversion to agricultural lands and urban areas to meet the increasing demands for food, water consumption of goods and services, and land use conversion due to increasing human and

livestock populations is a common experience in Ethiopia. Inappropriate agricultural practices and high human and livestock population pressure lead to severe land degradation in the highlands of the country (Tsegaye, 2019).

2.3.3 Effect of Land use Land cover change on Soil erosion

Land use and land cover change (LULCC) is a major factor that affects soil erosion and land degradation, especially in arid and semi-arid regions (Kgaphola et al., 2023). LULCC can alter the natural vegetation cover, soil properties, hydrological processes, and climatic conditions that influence soil erosion by water and wind (Aneseyee et al., 2020; Eskandari Damaneh et al., 2022). Some of the common LULCC that increase soil erosion are deforestation, urbanization, intensification of agriculture, overgrazing, and desertification(Kgaphola et al., 2023). LULCC can also affect the sediment delivery ratio and the downstream water quality and quantity (Demissie, 2022; Szatten & Habel, 2020).

2.3.4. Effect of upper stream Land use practices on soil erosion in Ethiopia

The Ethiopian Highlands are the water towers of most East and North African countries, especially Egypt and Sudan, with various international rivers originating from these highlands (D. Kidane & Alemu, 2015). Ethiopia is characterized by rugged and steep ground slopes, intensively cultivated, high intensity and amount of rainfall, a sparse vegetation cover, mismanage soil resource and significant direct runoff generation leading to accelerated soil erosion and high risk of ecological degradation (Durán Zuazo & Rodríguez Pleguezuelo, 2008, D. Kidane & Alemu, 2015).

For downstream water users, the effects of excessive surface runoff include altered flow patterns and increased surface runoff that causes springs to dry up during the dry season (Bewket & Sterk, 2005). The transboundary rivers that flow out of the highlands of Ethiopia are thought to transport 1.3 billion tons of sediment each year to the bordering nations, compared to the 131 million tons carried by the Blue Nile alone (D. Kidane & Alemu, 2015). These rates are the result of traditional conservation methods and poor upstream watershed management. Sedimentation as an ecological and environmental phenomenon is increasingly affecting the sustainable development of human societies in the Ethiopian highlands, especially in the Blue Nile and Tekeze Basins (D. Kidane & Alemu, 2015). Deforestation and soil surface thinning brought on by these are enabling and increasing water erosion. As a result, it causes soil degradation in the upper catchment, decreased

reservoir capacity, flooding, obstruction of hydropower inlets, sedimentation of irrigation canals, and deterioration of downstream water quality (Ahmed & Ismail, 2008; D. Kidane & Alemu, 2018)

In Ethiopia, nutrient loss on-site and off-site water resource sedimentation are both consequences of soil erosion, which is a significant contributor to land degradation (Hurni, et al., 1998). Increased rates of soil erosion are caused by rapid land use change brought on by intensive agriculture techniques in the Ethiopian highlands (Meshesha et al., 2012). This has resulted in major downstream effects, including decreased reservoir storage capacity and costly irrigation canal desilting expenditures Basins (Wang et al., 2018, D. Kidane & Alemu, 2015). Therefore, planning for catchment management and the judicious use of water resources in the upper Blue Nile Basin can benefit from understanding soil erosion, sedimentation, upland management, and its associated implications.

2.3.5 Effects of Soil erosion on Agricultural productivities, Infrastructures and Natural Resource of Ethiopia

Soil erosion is a serious problem in Ethiopia that affects the rural livelihoods and the environment. According to a review by Wassie, (2020), soil erosion in Ethiopia is caused by various factors such as population pressure, agricultural expansion, overgrazing, deforestation, climate change, and environmental pollution. Some of the effects of soil erosion are on-site and off-site effect:

The onsite effect of soil erosion is the effect that occurs on the site where the soil is eroded. According to a review by Zewide & Achame,(2021), some of the onsite effects of soil erosion in Ethiopia are: Loss of soil organic matter, nutrients, and water holding capacity, Reduction of soil depth, structure, and porosity, decrease of soil fertility and productivity, increase of soil acidity, salinity, and compaction, Decline of crop yield and quality.

Soil erosion have negative impacts on the livelihoods of the farmers and the food security of the country. Therefore, it is important to implement effective soil and water conservation measures to prevent or reduce soil erosion and enhance soil quality (Zewide & Achame, 2021 Wassie, 2020). The offsite effect of soil erosion is the effect that occurs downstream or away from the site where the soil is eroded. According to a review by Wassie, (2020), some of the offsite effects of soil erosion in Ethiopia are: - Sedimentation of rivers, lakes, reservoirs, and dams, Reduction of water storage capacity and hydropower generation, Deterioration of water quality and aquatic habitats,

Flooding and landslides, Loss of downstream agricultural land and infrastructure. These effects have negative impacts on the environment, the economy, and the society. Therefore, it is important to implement integrated watershed management and sediment control measures to prevent or reduce soil erosion and its offsite effects (Haregeweyn et al., 2015; Wassie, 2020; Zewide & Achame, 2021).

Approximately 70% of the world's arid regions have been destroyed, according to the United Nations Convention to Combat Desertification, and 24 billion tons of soil are lost each year due to erosion (Kum et al., 2022). A global estimate indicates that by mid-1990 s, soil degradation affected around two billion hectares of cultivated land of which water induced soil erosion accounting for about 55% a and one billion people affected by soil erosion globally, 50% are founded in Africa contents(Gashaw et al., 2021). According to various studies, water-induced soil erosion affects 80% of the world's arable land at moderate to severe rates(Barakat et al., 2023; Senamaw et al., 2022; Walling et al., 1999). In the Ethiopian Highlands, many resources are at risk, like soil, water, infrastructure, and the environment. As nearly 80% of the population depends on subsistence agriculture, it threatens the resource base through soil erosion (Easton et al., 2010).

To address this problem, Ethiopia has implemented several soil and water conservation (SWC) programs since the 1970s, such as soil bunds, trenches, check dams, and tree planting (Haregeweyn et al., 2015; Tamene et al., 2022). However, these programs have faced many challenges such as limited access to capital, land tenure insecurity, limited technology choices and technical support, and poor community participation (Bewket, 2007; Haregeweyn et al., 2015). Therefore, there is a need for more comprehensive and participatory research and extension of soil and water conservation interventions in Ethiopia.

2.4. Soil Erosion modeling by MUSLE

Soil erosion modeling is the process of mathematically describing soil particle detachment, transport, and deposition on land surface (Lisle et al., 2017; William and Russell, 2022). There are basically three types of erosion models: empirical, conceptual, and physically-based (Pandey et al., 2016). Empirical models are based on statistical relationships derived from observed data, such as the Universal Soil Loss Equation (USLE) and its revisions. They are simple and easy to use, but they are limited to the conditions and locations where they were developed Soil erosion models are useful to estimate soil loss and runoff rates from agricultural land, to plan land use

strategies, to provide relative soil loss indices and to guide government policy and strategy on soil and water conservation (P.U. et al., 2017).

2.5. HEC_HMS Model

Hydrological models are essential tools for water resources, environmental planning, and management. The Hydrologic Engineering Center-Hydrologic Modeling System (HEC-HMS) is one such model that has been widely used for hydrological modelling. A recent review article by(Sahu et al., 2023) provides a comprehensive state of the art technology hydrological modelling by briefly discussing different hydrological models and evaluating their application based on Nexus assessment. The review suggests that the HEC-HMS is feasible compared to other models and performs well for dendritic watershed drainage patterns. According to Soil Conservation Service Curve Number (SCS-CN) method and the Soil Moisture Accounting (SMA) method are the most widely used methods for event-based and continuous modelling. Compared to other models, the Deficit and constant (D.C.) loss approach of the HEC-HMS is the least utilized but found to be straightforward and provide accurate results (Ismail et al., 2022; Sahu et al., 2023). The review guides modelers in identifying the type of hydrological models that need to employ to a particular catchment for a specific problem. It also equally helps water resources managers and policymakers by providing them with an executive summary of hydrological studies and sustainable development.

2.6. GIS and Remote Sensing

Although different types of maps have been used for thousands of years, Geographic Information Systems (GIS) have only been possible in the last few decades because the technology that combines maps with databases and computer graphics (Andreev, 2020; Manson et al., 1999). Many databases are made up of layers, which are collections of data. Each layer is a specific sort of geographic information. For instance, one layer can reflect the area's soil information, while other layers might have data on elevation or the slope nearby, among other things. These layers can be combined by the GIS into a single image that illustrates the relationships between the soil, slope, and elevation (Dobos et al., 2000). In contrast to in situ or on-site observation, remote sensing is the process of gathering data about a phenomenon or object without actually coming into touch with it (Bartolini et al., 2018; Denil, 2006). The majority of earth science disciplines, geography, land surveying, the military, intelligence, weather forecasting, and drought monitoring are just a

few of the fields where remote sensing is used Woldai, (2020). In addition to controlling forest fires, detecting land use and land cover, estimating forest supplies, and locating construction and building modifications, some of its applications include assessing the condition of rural roads, developing a base map for visual reference, computing snowpack, gathering images of the earth from space, and computing snowpack.

CHAPTER THREE

METHODOLOGY

3.1. Location and Watershed Descriptions

3.1.1. Location of the Study Area

The Dura watershed is found in both Amhara regional state in Awi zone and Benishangul Gomez regional state which is located between10°20’0”–11º10’0” North latitude and 36°20’0”–36º50’0” East longitude. Upper stream of Dura watershed is found in Awi zone of Amhara National Regional state (ANRS) and downstream of Dura watershed is located Benishangul Gomez regional state of Ethiopia. The Dura watershed covers 2246 km² and the upper catchment of Dura watershed is situated about 460 kilometers Northwest of Addis Ababa and 100 kilometers Southwest of Bahir Dare the capital city of ANRS in Awi zone and downstream is situated 659 kilometers Northwest of Addis Ababa in Benishangul Gomez regional state, in Ethiopia (Figure 1). The dura watershed is connecting two regional states (Amhara regional state and Benishangul Gomez regional state). According to Hurni H, et al.,(2016), the agroecological zone of the study area is classified in to three zone depending on the elevation above sea level :500 m to 1500 m kola, 1500 m to 2300 Weyna Dega and 2300 to 2915 m Dega.

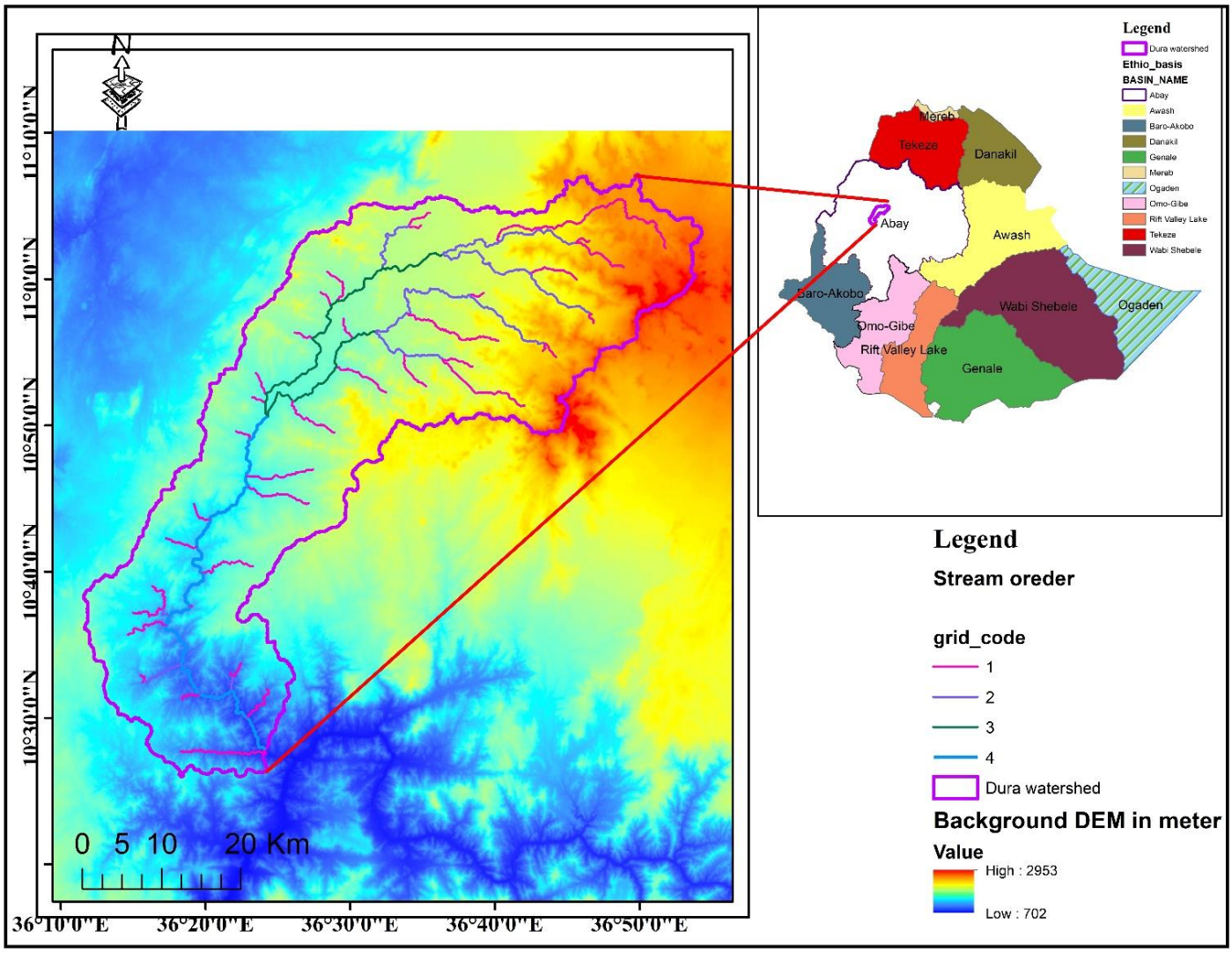

Figure 1: Map of the Study Area, Dura watershed in the left of the map and the right side is the Ethiopian Basins and the polygon location of Dura watershed. The background is the elevation of Dura watershed in meters. (Source: generated from DEM in NASA shuttle Radar Topography Mission (SRTM) (2013)). https://doi.org/10.5069/G9445JDF

3.1.2. Physiography

The altitude of the study area ranges from 768 to 2915 m above sea level (m.a.s.l.) (Figure 2). The graph represents a 3D topographic map showing the elevation of a specific geographical area of Dura Watershed. Elevation is color-coded, with red areas indicating higher elevations (reaching up to 2,900 meters) and blue areas representing lower elevations (around 800 meters). The higher elevation ranges are located in the northern and northeastern parts of the watershed. The watershed

includes a range of topographic conditions, size, climate conditions, slops, geological features, drainage patterns, vegetation covers, soils, and anthropogenic activities. The topography of the watershed is split into two distinct features: The first comprises mixed flat and mountainous topography in the lowland of Benishangul Gomez regional state, and the second includes flat and more mountainous topography in the Amhara region, Awi Zone. The watershed relief type consists of 30% flat (plain), 65% mountains, and 5% others. The slope gradient of the watershed ranges from 2 to >35%. Generally, this map visually depicts the varying elevations in the specified area, highlighting peaks and valleys.

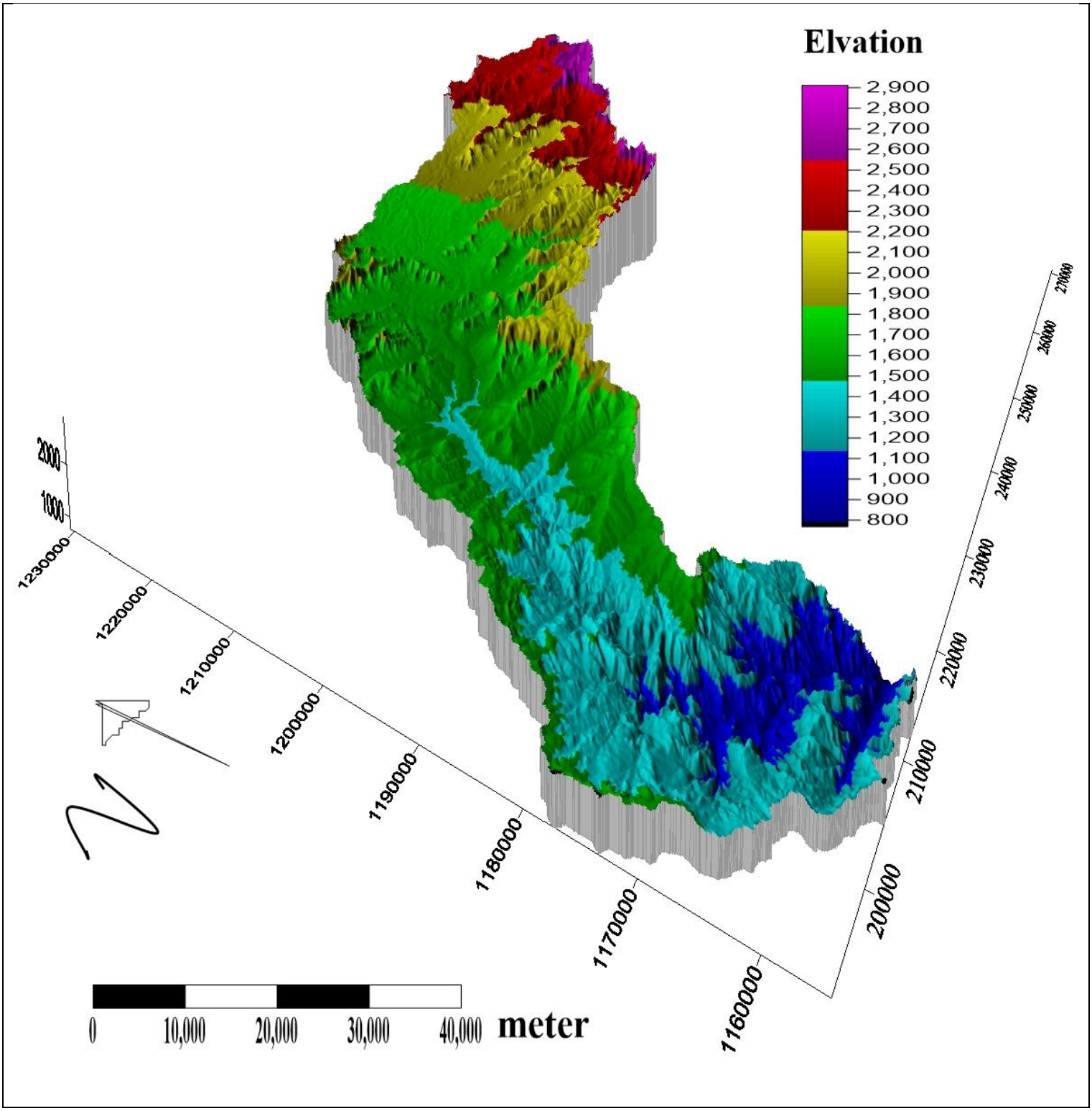

Figure 2: 3D physiographic map of Dura watershed

3.1.3. Slope and Drainage of Dura watershed

Figure 3. and Table 1 show the distribution of area and percentage of different slope gradients in the Dura watershed. The slope gradient is a measure of how steep the land is. The results indicate that the most common slope gradient in the watershed is 5-10%, which covers 25% of the total area. The least common slope gradient is 0-2%, which covers only 6% of the total area. The results also show that as the slope gradient increases, the area and percentage decrease, except for the 15-25% slope gradient, which has a slightly higher area and percentage than the 10-15% slope gradient. This suggests that the Dura watershed has a high drainage density and a high potential for soil erosion, especially in the areas with slope gradients greater than 15%.

Table 1 Slop class of the Dura watershed

Slop Gradient (%)	Area_(ha)	Area-Precent (%)
0-2	12269	6
2-5	32653	15
5-10	54713	25
10-15	37002	17
15-25	43613	20
25-35	22490	10
>35	15928	7

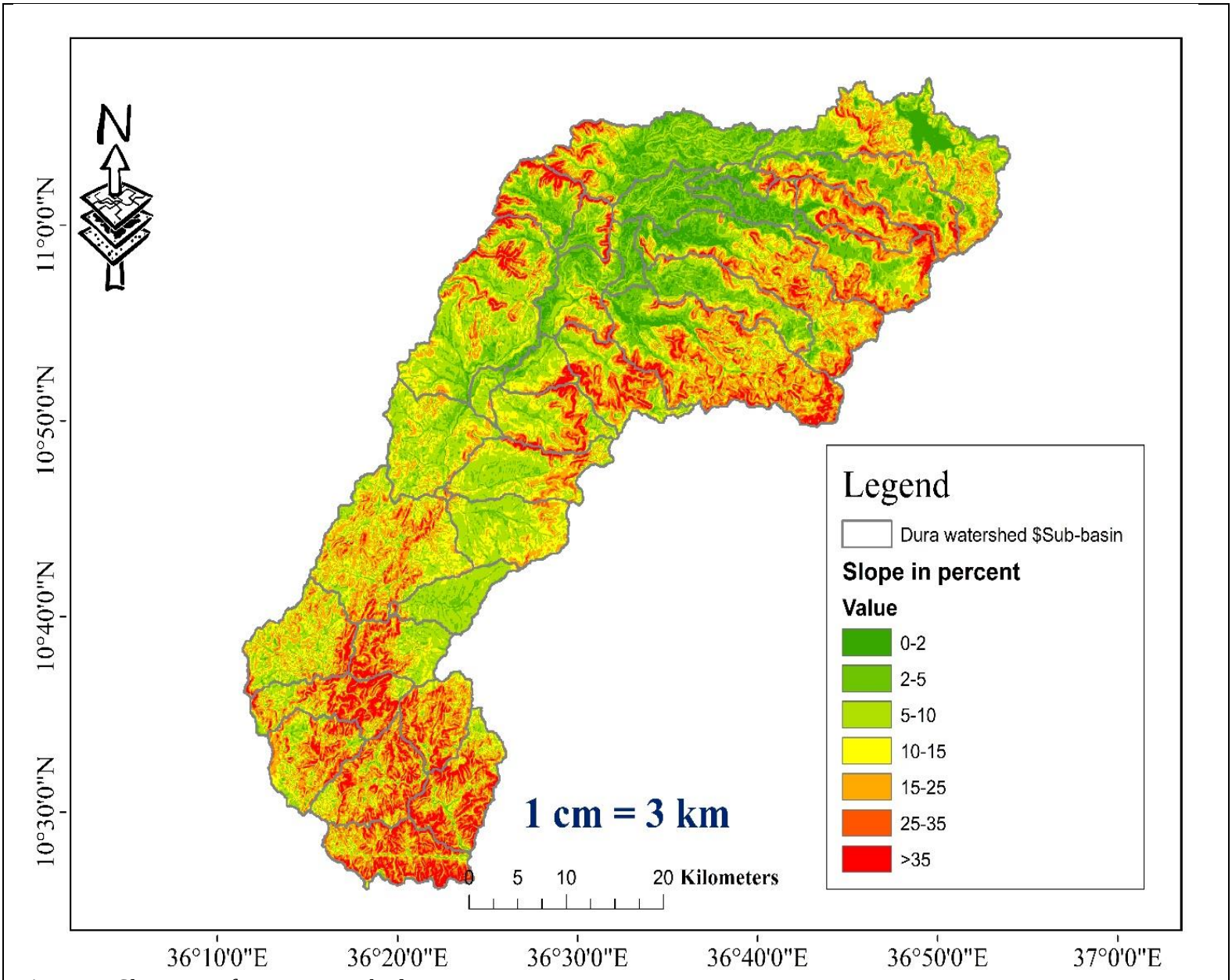

Figure 3: Slop map of Dura watershed

Drainage density is higher in relatively elevated areas, especially when the watershed stations are thick or when the pattern of structures crossing the rocks is higher (Figure 4). In the highlands, narrow deep to shallow gorges are generally found, while relatively wider river channels are found in the lowlands of the watershed. Most of the major rivers are tectonically controlled and follow regional and sub-regional liniments. The main high discharge streams are aligned along regional faults. The lowest elevated areas are found near the Abay River, at the confluence of Dura and Abay rivers. Generally, the direction of river flow is controlled by topography. The highlands, from where the streams flow, are humid and rugged, while the surrounding lowlands into which the streams flow are mostly arid and relatively flat. These topographic differences induce rapid runoff, low retention in soil layers, and increase soil erosion rate on the highlands.

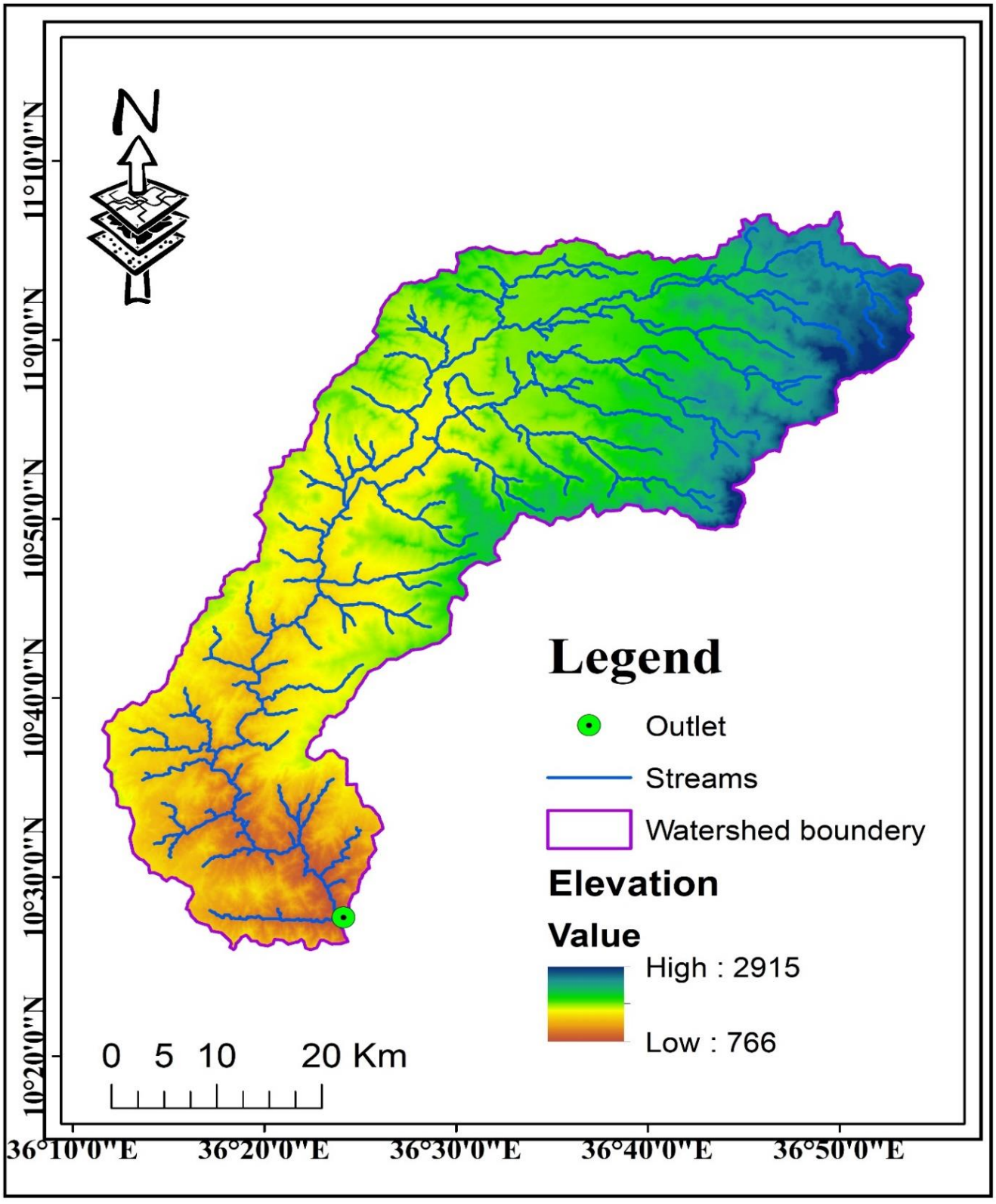

Figure 4: Drainage Map of Dura watershed

Strahler stream order is a way of classifying streams and rivers based on their position and hierarchy in a drainage network. It is an important aspect of a drainage basin, as it reflects the size, shape, and complexity of the watershed (Strahler, 1957). According to Strahler stream order, all streams without any tributaries are assigned an order of 1 and are referred to as first-order streams. The stream order increases by one whenever two streams of the same order join. In Figure 5, when two first-order streams come together, they form a second-order stream. When two second-order streams come together, they form a third-order stream, and when two third-order streams come together, they form a fourth-order stream. The Dura River is the largest river in the study area and a fourth-order waterway. First- through third-order streams in the Dura watershed are called headwater streams.

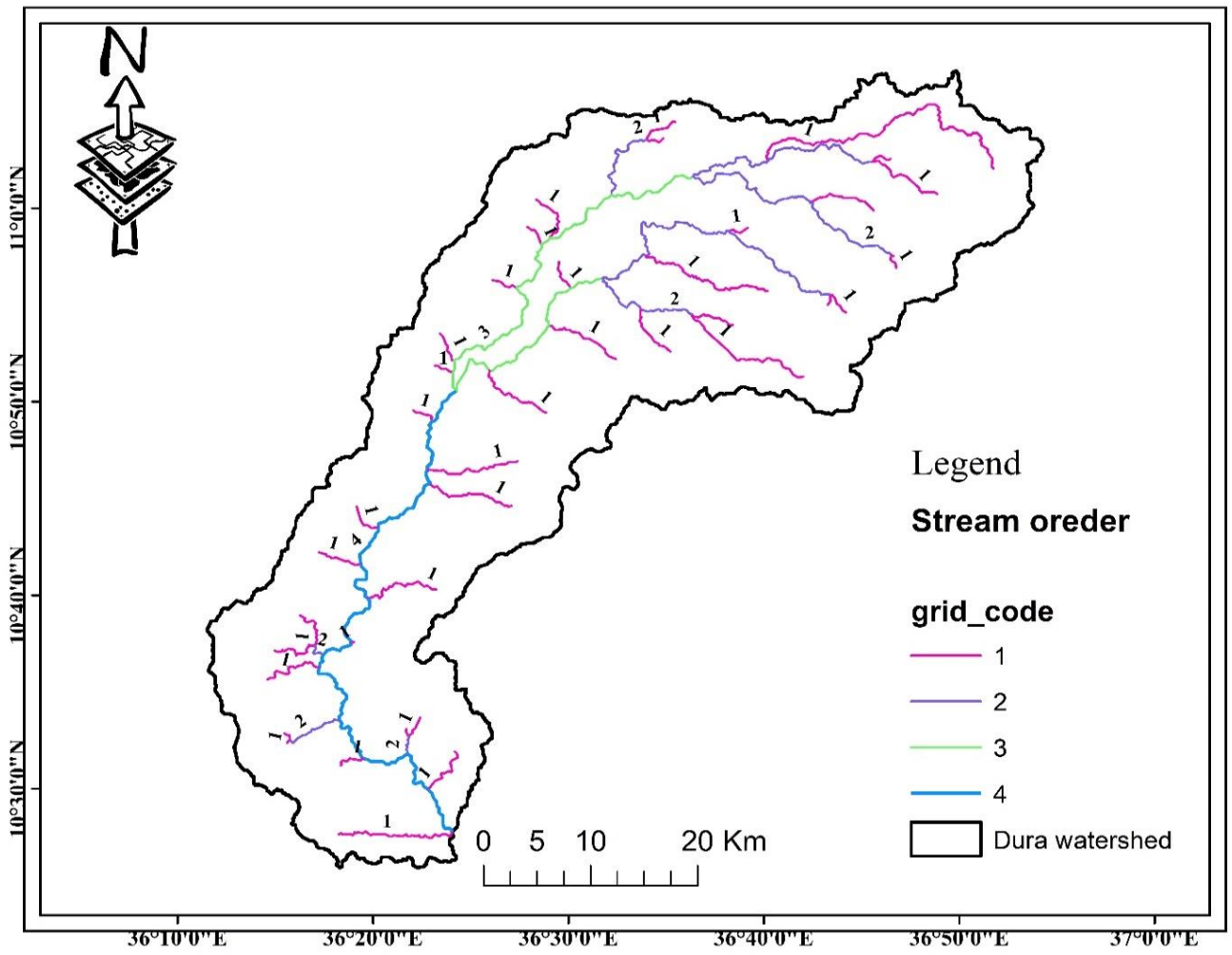

Figure 5: Map of stream flow order of Dura watershed

3.1.4. Climate of the Study area

The Dura watershed is subject to two separate seasons: the Kiremt wet season, which occurs from June to September, and the Belg minor rainy season, which occurs from mid-February to May, which adds moisture to the watershed. The Figure 3.6 shows the average maximum temperature in Celsius for three different stations in Dura watershed, Northwestern Ethiopia, namely Addis Kidame, Chagni, and Bullen, for each month of the year. For example, the average maximum temperature in Addis Kidame station is **5.7°C** in January, **6.98°C** in February, **8.76°C** in March, and so on. Similarly, the average maximum temperature in Chagni station is **30.5°C** in January, **32.15°C** in February, **32.77°C** in March, and so on. Finally, the average maximum temperature in Bullen station is **29.7°C** in January, **31.6°C** in February, **32.4°C** in March, and so on. The data can be used to compare the average maximum temperatures of the three stations across different months of the year. For instance, we can see that Addis Kidame station has a much lower average maximum temperature than Chagni and Bullen stations throughout the year in the Dura watershed. We can also observe that all three stations experience their highest average maximum temperatures during March and April.

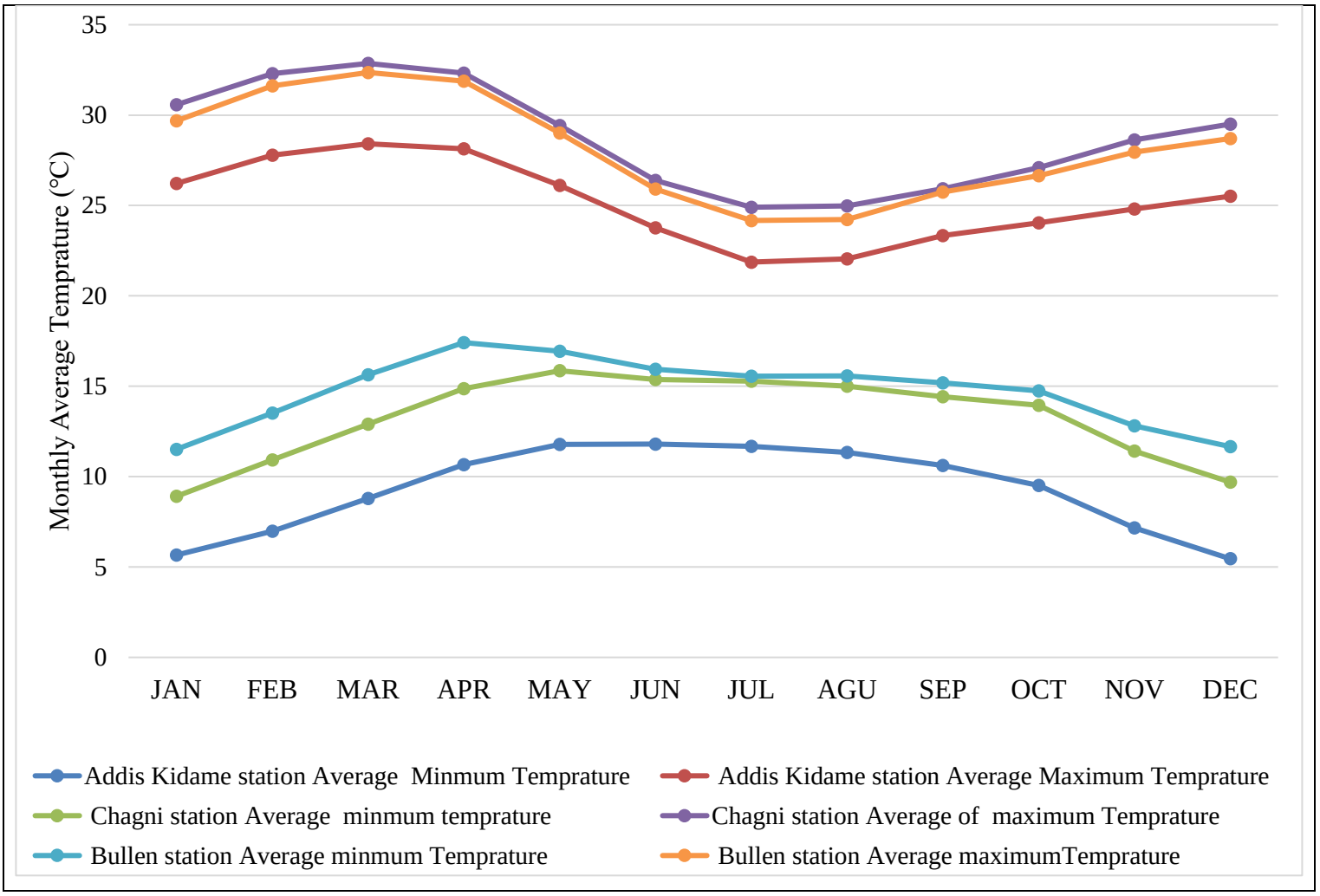

Figure 6: Monthly average minimum and maximum Temperature for Addis Kidame Station, Chagni Station, and Bullen Station in Ethiopia:-(Source: National Meteorological Agency 1991_2020)

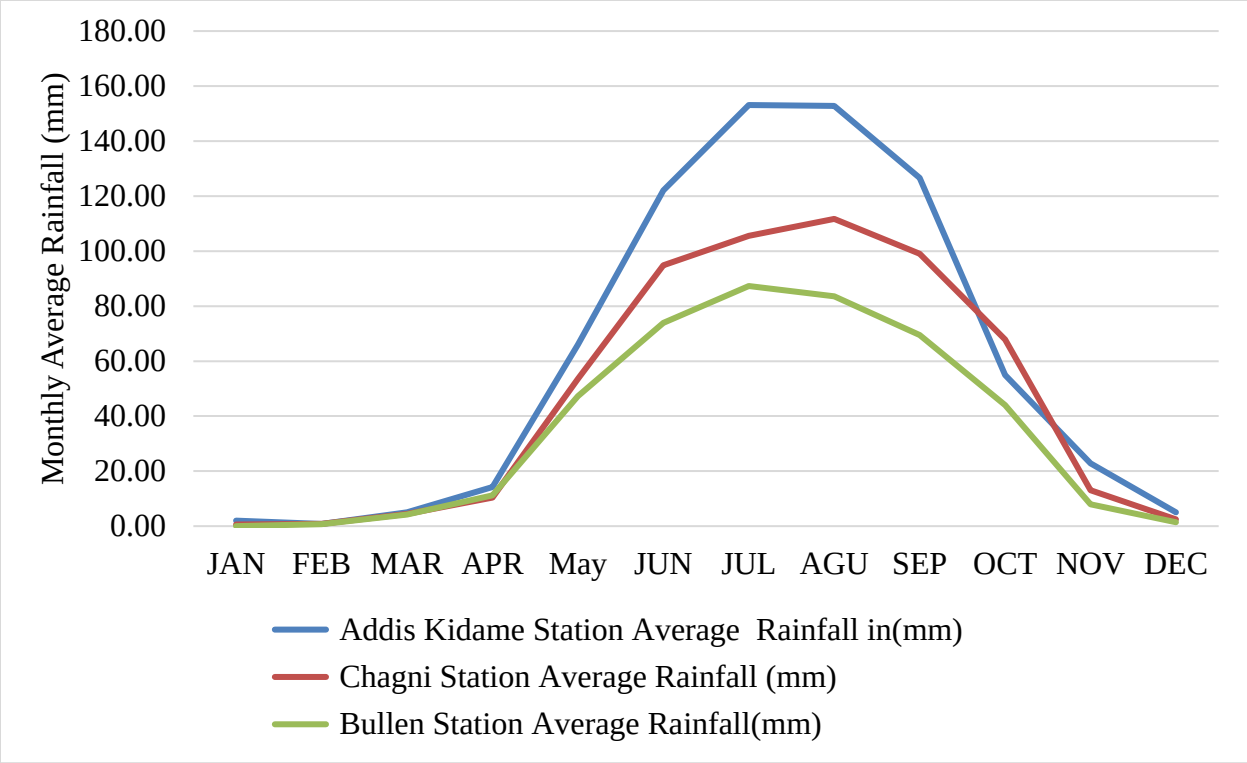

Figure 7: Average Rainfall of Dura watershed in Addis Kidame, Chagni, Bullen Gauge Station (source: - National Meteorological Agency 1990_2020)

The rainy season in the study area extends from the beginning of May to the end of October. During this period, the region experiences increased precipitation. Addis Kidame Station encounters the highest rainfall during the months of June, July, and August. Specifically, the peak rainfall occurs in July (Figure 8). Rainfall at Chagni station is more evenly distributed throughout the year. Similar to Addis Kidame, Chagni also observes higher rainfall in June, July, and August. Bullen station receives minimal rainfall consistently throughout the year. There are slight increases in rainfall during April and May. Overall Comparison of station in the study area: Addis Kidame receives the highest total rainfall, followed by Chagni. Bullen remains relatively dry compared to the other two stations. The farming system in the study area is a mixed agriculture approach. It primarily relies on rain-fed farming, supplemented by traditional irrigation. However, irrigation facilities are limited and available only in specific locations, depending on suitable sites within the upper watershed of the study area (Awi zone).

3.1.5. Geology

Regional Geology

Generally, the geology of Northwestern Ethiopia is very complex. This vast lowland region, adjoining the western and Northwestern highlands, is characterized by Basement complex Precambrian rocks with relatively wide coverage of Quaternary sediments. These elevated adjacent highlands and transitional areas are covered with Tertiary and Quaternary volcanic rocks. According to Mengesha Tefera et al.'s (1996) Second Edition Geologic Map of Ethiopia report, the general regional succession of rocks from the oldest to the youngest is Precambrian rocks, Triassic Sandstone, Mesozoic sediments, Tertiary basalts, Cretaceous sandstone, Quaternary basalt, and recent alluvial sediments (Girma Addisu, 2010).

The characterization of different geological units was done based on various geological maps, their explanatory notes and reports, and Field observation. The general description of the lithostratigraphic units of all the rocks in the basin is given below; most of this description has been taken from the geologic map of Ethiopia compiled at the scale of 1:2000.000 (Mengesha et al, 1996).

Archaean Age Formation

Lower Complex: high-grade metamorphic rocks in the pan-African Mozambique Belt with amphibolite to granulite facies that include mainly gneisses Although usually coarse-grained and well foliated, the gneisses and migmatites merge into more homogenous varieties of granitic appearance. In the Blue Nile Basin, this group includes rocks that, generally, have not been assigned to a particular lithological unit. Only the Konso gneisses were differentiated and mapped in the south of the Dangur mountain in the Western part of the Dura basin. It consists of dark, weakly foliated pyroxene, amphibole pyroxene, and pyroxene-garnet gneisses.

Alghe Group: This group developed in the Alghe. This rock group is found in the southern Dura watershed and extends into the Guder, Anger, and Didesa watersheds, where it consists of biotite, hornblende, gneisses, granulite, and migmatite with minor metasedimentary gneiss.

Lete Proterozoic age Formation

Tulu Dimtu group: This group developed at Tulu Dimtu in Wonbera, Guba, Bullen, Galesa, and Dibate and extended to Beles Basin. It Consists of Meta basalt, meta-andesite, green schist phyllite, Meta conglomerate, quartzite, and marble. Marble rocks are fine-grained and dark green, weathering to brown or yellow. In a few places, they can easily be identified as white patches. Generally, they are massive, dense, and cut by numerous quartz veins.

Quaternary age Formation

Plateau Basalt: This rock group covers a large area of the Dura watershed in the Northern part of the watershed and extends to Bahir Dare. It consists of alkaline basalt, Scorious basalt, and Trachyte.

3.1.6. Soil of the Study Area

For soil type identification of the Dura watershed FAO soil data base was used. The stated soil data base shows that the watershed have soil type of calcic cambisols, calcic xerosols, chromic luvisols, dystric fluvisols, dystric gleysols, dystric nitisols, leptosols, orthic acrisols, orthic solonchaks (Figure 8). The soil texture of the watershed is clay dominated followed by, sandy clay, clay loam, and sandy clay loam. The soil texture proportion of the watershed is 74%, 0.07%, 25.8%, 0.13%, respectively.

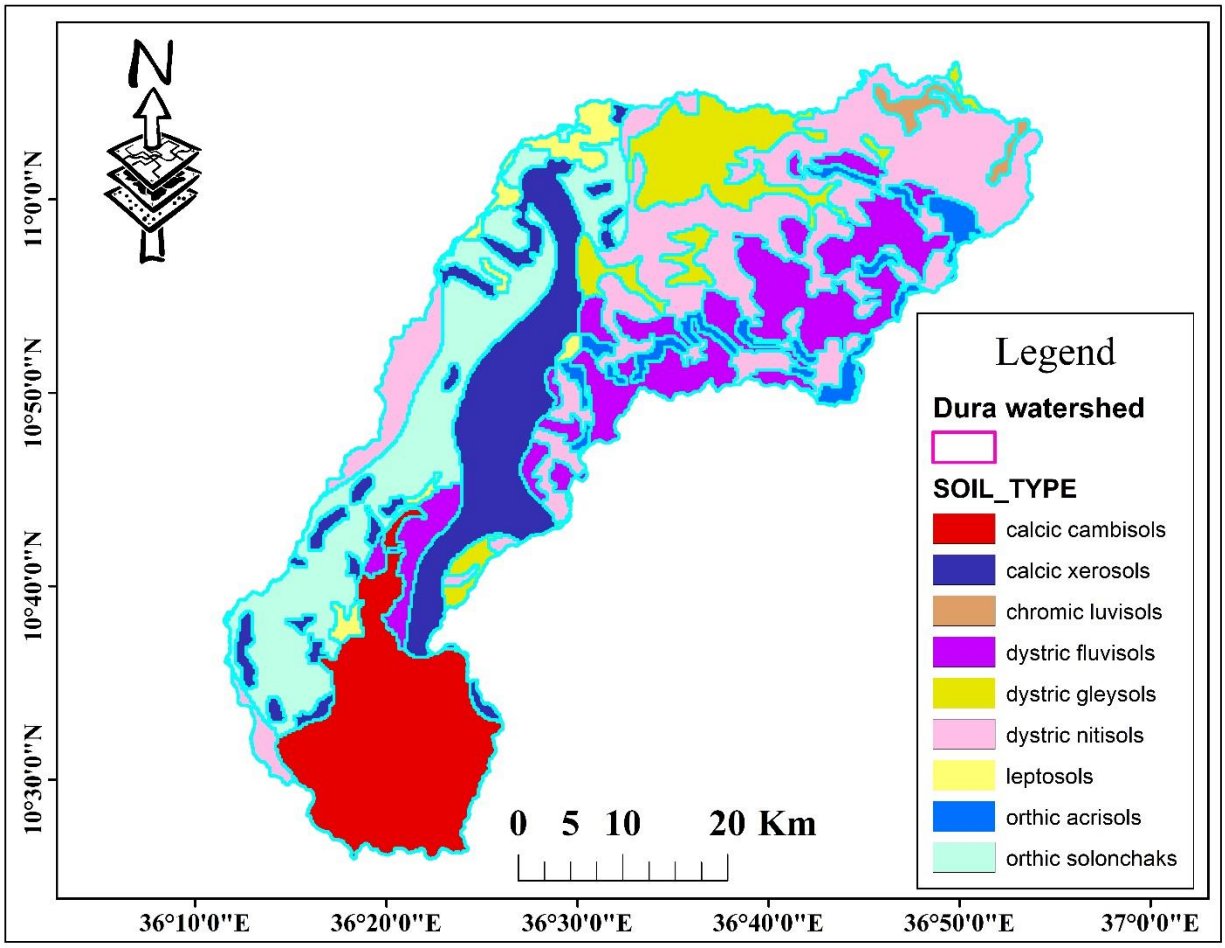

Figure 9: Soil map of dura watershed (Sources: Minster of Agriculture)

3.1.7. Population Settlement in the Study Area

The study area is part of the Amhara and Benishangul Gumuz National Regional States. The population distribution is variable from place to place due to several factors. The main factors are the suitability of the climate, the presence or absence of perennial water bodies, the Suitability of the land for farming and cattle breeding, and the proximity of the villages to roads, markets, and other social infrastructure. A relatively large number of people live in the highlands of the Awi Zone (Addis Kidame, Enjabera, and Chagni) and the lowlands of Mandura, Dibate, Bullen, and Galesa. The Gumuz, Shinasha, Agew, and Amhara are the major tribes in the area, while the Oromo and Tigre represent a minority. The people of the Gumuz tribe inhabit only the lowlands, and these people sometimes engage in subsistence farming, cultivating sorghum and maize. They raise goats and occasionally pan for gold along some of the rivers in the lowland of the study area in the Benishangul Gumuz region. And also harvest wood to produce incense, honey, and wood

charcoal. The Amhara, Agew, and Shinasha people populate the highlands and lowlands. They grow Teff, Wheat, Barley, potatoes, Maize, Degussa, and Nuge. Rice and raise Cattle, Horses, Sheep, and Goats.

3.1.8. Land Use and Vegetation cover

Mixed Cereal-livestock farming system is the primary source of income for those who reside in the study region. The main crops farmed in the research region include barley, wheat, beans and peas, sorghum, Tef, Maize, Potato in the upper stream watershed, Sesame, Almonds (ለውዝ፡), Soy sauce, and Rice including Maize in doween stream watershed of the Study area. The marginal lands between the farm fields are getting much smaller as crop lands are growing at the expense of pasture and vegetative lands. Since there is no custom of integrating perennial income crops with these cereal crops, the ground will be left bare and subsequently exposed to erosion after the crop products are gathered.

About 48.85% of the land is devoted to cultivated and settlement land, 27.47% of it is bushland and 22.47% of the watershed is forest, 1.32% of the watershed is bare land in 2023 land use land cover (Figure 4.1,). Most part of the bushland is covered by grass which serves as grazing in both dray and wet season, some parts to cut and sell in the rainy season. The most familiar plantation in the study area is NechBahirzaf and KeyBahirzaf (Eucalyptus globules) and Chigegn (Acacia decurrens), and some natural pants in the watershed are Injory (Morus mesozygia), Qoba (Mytemus arbutifolia) and Kerkeha or Bamboo Forest (Arundinaria alpine), Wanza (Cordia Africana), Girare (Acacia tortilis) etc. Small Scale NechBahirzaf and KeyBahirzaf (Eucalyptus globules) and Chigegn (Acacia decurrens) stands near to the settlement and at agricultural field edges, but the amount of this planted vegetation is increasing in alarming rate from year to year in the upper catchment of the watershed. In a study conducted by According (Alemayehu, 2015), it was found that in the years 2013 and 2014, a total of approximately 900 hectares and 17,500 hectares were used for growing seedlings, resulting in the growth of around 18 million and 33 million seedlings, respectively. These findings indicate a significant decrease in natural vegetation throughout the entire watershed.

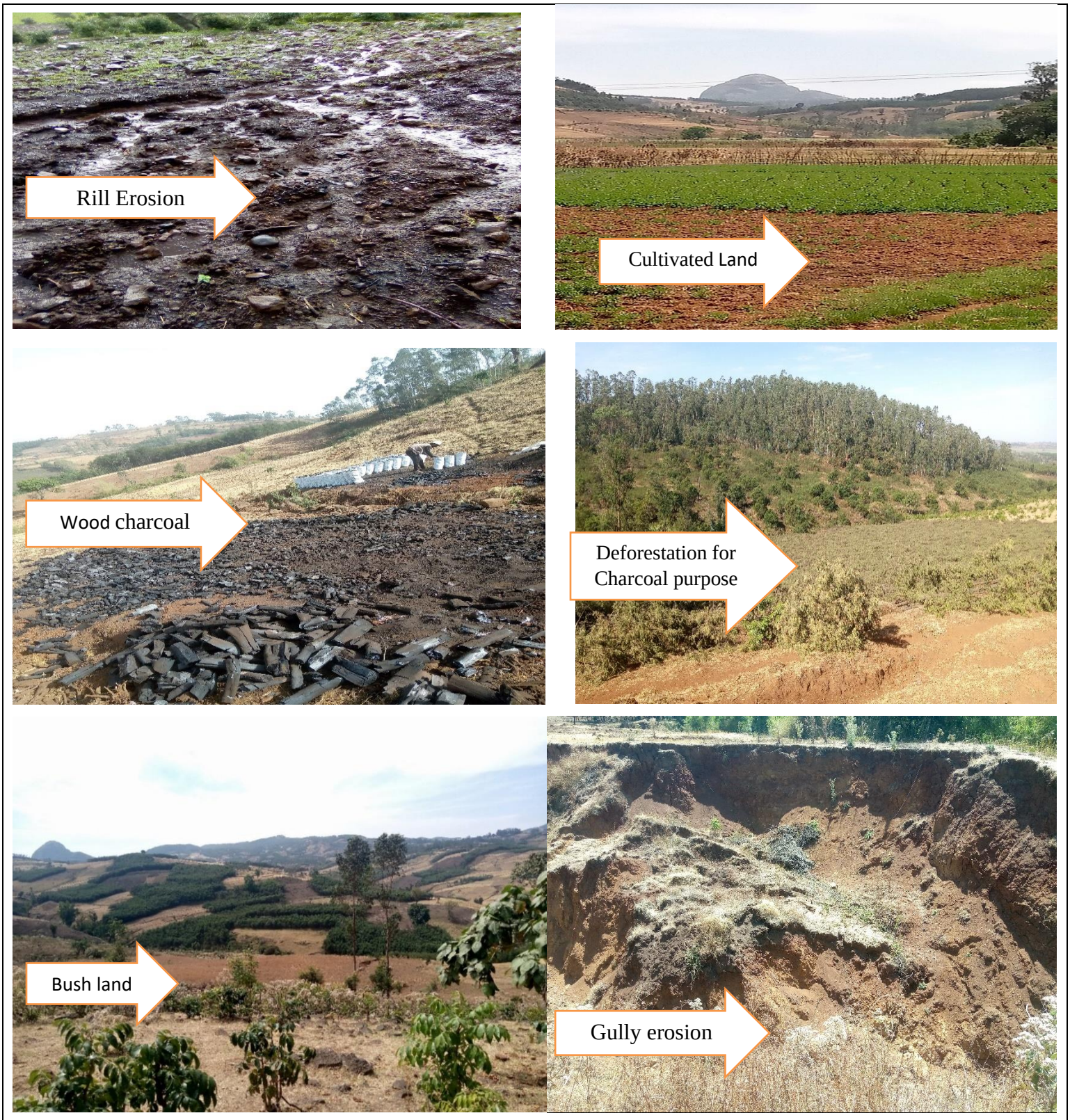

Figure 10: Photographs of some Dura watershed.

3.1.9. Study Design

3.1.9.1 General Research Framework

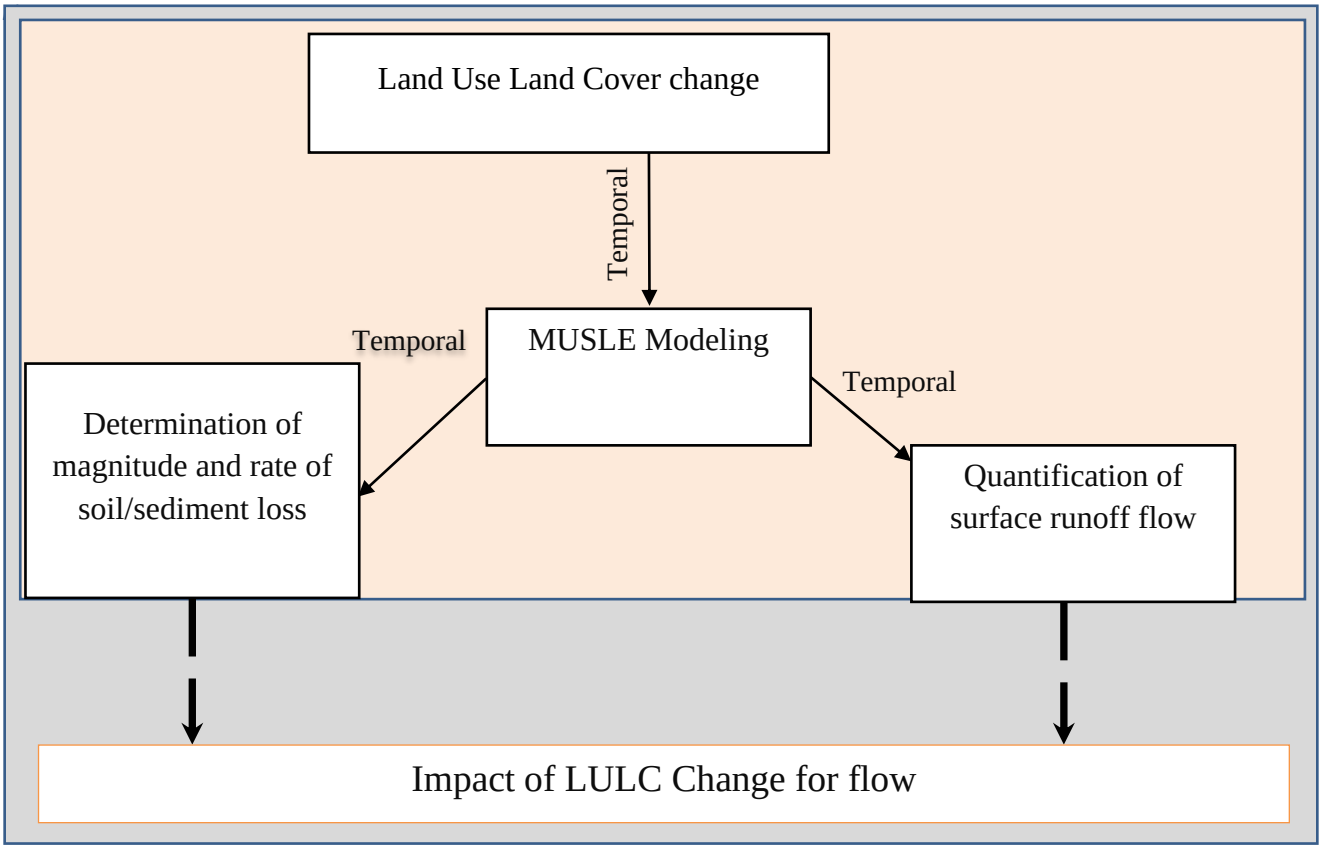

Figure 10. *Flow diagram showing impact of LULCC on Soil loss, sediment yield and surface runoff*

There are two fundamental reasons for the selection of the Dura watershed as the site of this research study;(I) it is typical of the Northwestern highlands of the country in terms of the different environmental attributes Such as topography, climate, soil type, and socio-economic activity of the environment, and (ii) the Dura watershed is part of the highlands that are known to be surplus producing regions, but currently threatened by natural resource degradation and impending food insecurity. Dura watershed is part of the Blue Nile Basin.

3.1.9.2 Data Acquisitions and Sources

Spatial and temporal data are the two types of input data that HEC_HMS requires. The spatial data includes slope maps Digital Elevation Model (DEM)), soil maps, and land use maps. The temporal data also includes information on the hydrology (streamflow and sediment yield) and the climate

(solar radiation, relative humidity, air temperature, precipitation, and wind speed). land use map, Satellite images are downloaded from USGS and reclassified the land use map of the area and used to identify land use land cover change trends.

Satellite Image

This research involved primary and secondary data collection techniques. Landsat satellite images of the study area were acquired for four time series epochs viz: 1993, 2003, 2013, and 2023. This image was obtained from the USGS (United States Geological Survey). The images were extracted to tiff formats for processing, and the details of image properties are summarized in table 2. The image was acquired from the period January, as this is a clear dry season in the region, which is important for reducing atmospheric and radiometric problems. Images were composed in different ways in order to identify surface features in the study area. During field work to collect GPS data, those are ground control points used to accuracy assessment.

A digital elevation model (DEM) of the Dura watershed will be utilized to represent the relief of the study area, which will be extracted from the ASTER-GDEM (Global Digital Elevation Model from the ASTER) data. The DEM integrated into the HEC_HMS model and used to delineate the sub-basins. DEM will be used to derive topographic parameters such as slope and length of slope for the sub-basins.

Table 2: Characteristics of Data sources

Path/Row	Landsat/Sensor	Data Acquired	Source	Resolution
170/053 170/052	Landsat-5/ TMC2L2	1993/01/06	USGS	30m
170/053 170/052	Landsat-7/ ETM+C2L2	2003/01/26	USGS	30m
170/053 170/052	Landsat-7/ ETM+C2L2	2013/01/05	USGS	30m
170/053 170/052	Landsat-8/ OLI/IRSC2L2	2023/01/01	USGS	30m

Hydro-Metrological Data

Climate data (20 years) are the main input for the hydrological process in HEC-HMS. Data from the National Meteorological Agency (1990-2020) station was used for this, including daily precipitation, maximum and minimum air temperatures, wind speed, sun radiation, and relative air humidity. To assess the effectiveness of the HEC-HMS simulation, daily stream flow data from the Dura Stream Gauging Station was used (Minster of Water and Irrigation). The climatic parameters in HEC-HMS consisted of precipitation and air temperature. Daily precipitations for the period 1990–2020 have been gathered at different rain gauge stations within or in close proximity to the study area by the National Meteorological Agency.

Soil Data

The Harmonized World Soil Database (HWSD), created by the Food and Agriculture Organization (FAO), provide soil maps. The primary characteristics of the different soil types are listed in an attribute table that is attached to a digital map layer in this database (Nachtergaele et al., 2008).

3.2. Land use land cover change analysis

3.2.8. Image processing and Classification Scheme

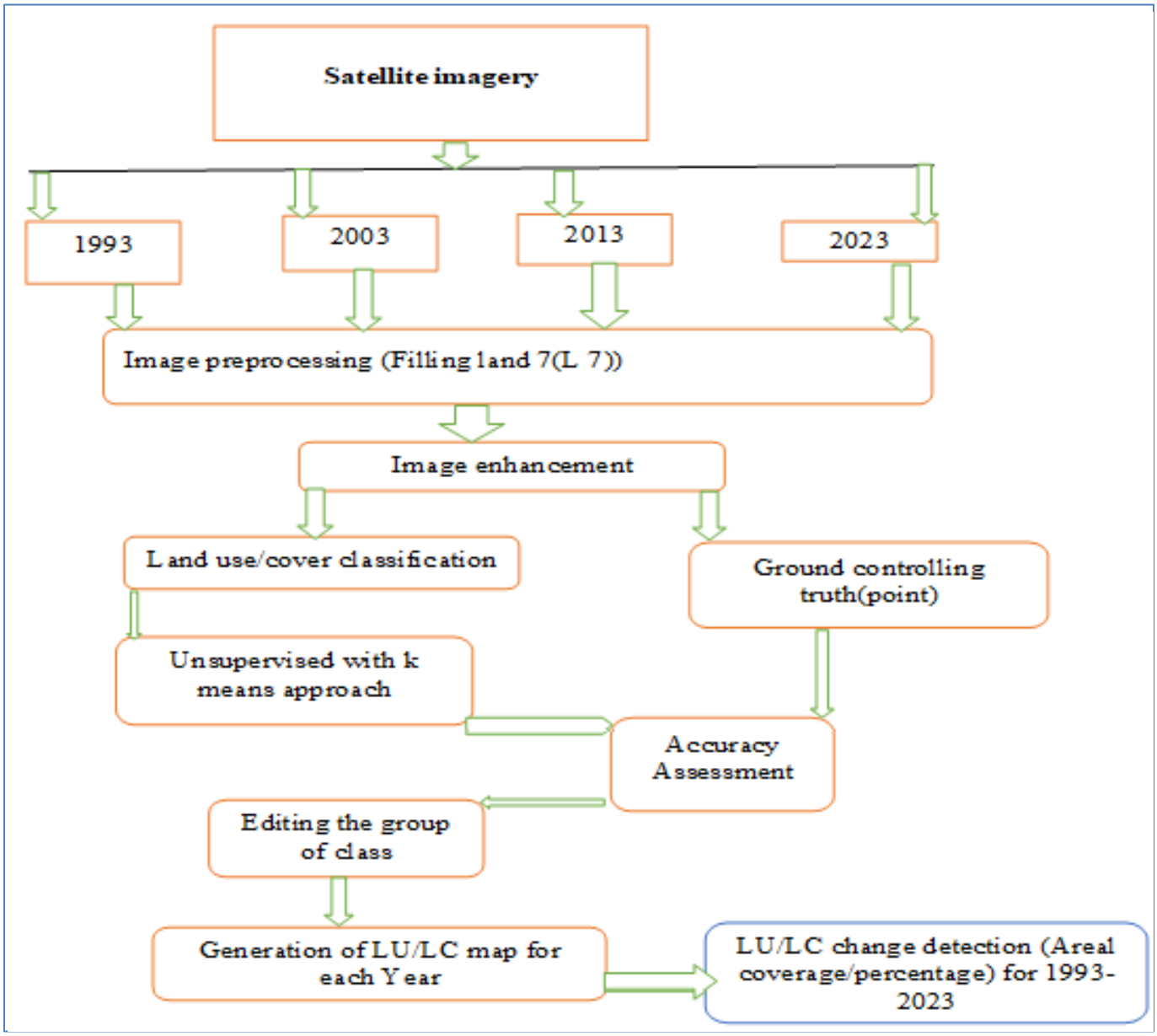

Figure 12: Flowchart of land use land cover map classification and change detection based on improving change vectors analysis.

3.1. Image processing and Classification Scheme

Unless adjusted, a raw digital image cannot be utilized as a map (Tesfaye et al., 2021). Geometrical distortion in a raw digital image can be brought on by two things. Both systematic (predictable) and spontaneous (unpredictable) distortions exist. While the satellite rotates from north to east, the

former is brought about by the Earth's west to east motion. As a result, the entire picture has moved from the south to the wet region and from the north to the east. An image information representation known as a thematic map shows the spatial distribution of a certain land use or land cover class. Meaningful information can be derived from remotely sensed earth data and used for a variety of purposes. The primary goal of image categorization techniques is to automatically classify all pixels in an image into land use and land cover classes. All images were captured during January which is the dry season. The period immediately following harvests may be thought of as the ideal time to differentiate between the various land use and land cover categories. The quality of the topographic map, the amount and kind of human intervention, the amount of time needed to train the classifier, and the complexity of the classifier are a few variables that affect the choice of an acceptable classifier (Tesfaye et al., 2021). Band combination (layer stake) and clustering by K-means were performed on images.

Approaches for supervised and unsupervised images classification were also utilized. While the supervised image classification was computed after the training sample was gathered in the field survey, the unsupervised classification was done before to the field survey. Since unsupervised land use and land cover image classification performs better than supervised image classification for broad areas, unsupervised image classification methodologies were generally used in this image classification. Because the landscapes of our countries vary spatially and temporally. Classification will be lost because we don't get pure pixels for input and output transit. Consequently, unsupervised is a reasonable option for classifying relatively broad areas of land use and land cover classification. Based on the information obtained and the procedures followed, the study adopted a classification scheme consisting of Four land-use land-cover types (Agricultural lands, Forests, Bush lands, and Bare lands) (Table 3 and Figure 3.7).

Table 3: Land use Land cover Classifications and description

Land use/ Land cover type	Descriptions
Forest cover	This refers to areas covered with a thick growth of trees that include evergreen forest, mixed forest, deciduous forest lands, plantation of indigenous species of trees such as NechBahirzaf and KeyBahirzaf (Eucalyptus globules) and Chigegn (Acacia decurrens).
Bush Land	This refers to area covered by small trees, bushes and shrubs, mixed with grasses, less dense than forests, grass land, wetland which are intermittently, mainly in dry season used for grazing and in the watershed area grazing lands area found manly in the highland areas.
Agricultural Land	This refers areas allotted to crop cultivation, mostly of cereals in subsistence farming and the scattered rural settlements including the cultivated fields and Scattered bushes Trees. (Area of land ploughed/ prepared for the growing of rain-fed crops and irrigations crops and Seeds. This includes areas currently under crop and fallow, as well as land under preparation. And rural housing and fencings).
Bare Land	This refers to the areas of land surface without vegetation cover, degraded agricultural lands, or with rock outcrops and quarries as well as large gully erosions. In the watershed, bare land mainly found in mountainous and an appropriate soil and water conservation practices areas which is mainly covered by bare soil and exposed rocks

Figure 13: Photographs of different Land use Land cover types: (A$B) Agricultural Land, (C$D) Bush land, (E) Forest, and (F), Bare Land in the upper Dura Watershed (photo by: Yitbarek Aemro, March, 2023).

3.2.9. Accuracy Assessment of land use land cover classification

Satellite imagery was acquired from Landsat-5 for 1993, Landsat-7 for 2003 and 2013, and Landsat-8 for 2023. Accuracy Assessment of land use and land cover classification is the comparison of a classification with ground controlling truth (points) and a Google Earth historical image to evaluate how well the classification represents the real world. It is performed by comparing a map created by using remote sensing analysis to a reference map based on different information sources such as field surveys, Google Earth, and original mosaic images. An interpretation is then made of how closely the newly produced map from the remotely sensed data matches the reference map. Although the basic approaches to accuracy assessment seem relatively direct and easy, a variety of errors are encountered when evaluating an image classification and capturing remotely sensed data.

In this study, a total of 240 test samples for each image (1993, 2003, 2013, 2023) were randomly selected from the original mosaic images of 1993, 2003, 2013, and Google Earth for the images 2023. In addition, for 1993, 2003, and 2013 images, some of the sample points were supported by local area elders as to what was there at what time, and for 2023, visual observations were carried out. Therefore, the accuracy assessment of the land use and land cover classification validated is greater than 0.80 (80%).

3.2.10. Rate of Land use Land cover Change (LULCC) analysis in Dura watershed

The classified images were compared in four periods, i.e., 1993- 2003, 2003-2013, 2013-2023 and 1993-2023. Land use Land Cover change statistics were determined by comparing image values of one data set with the corresponding value of the second data set in each period. The value was presented in terms of hectares and percentages. The percentage Land Use Land Cover Change between periods were calculated using the following formula (Ebabu et al., 2023; Tesfaye et al., 2021).

$$Percentage\ of\ LULCC = \frac{Area\ final\ year - Area\ of\ intial\ year}{Area\ of\ intial\ year} * 100$$

Where Area is extent of Initial Year: The land area covered by a specific land use or land cover type at the start of the study period. Area of Final Year: The land area covered by the same land use or land cover type at the end of the study period. Percentage of LULCC: The calculated percentage change in land area between the initial and final years. Positive percentage values suggest an increase whereas negative percentage value indicates a decrease in extent.

3.3. To model the volume of surface runoff from the watershed

3.3.8. Workflow diagram for HEC-HMS setup

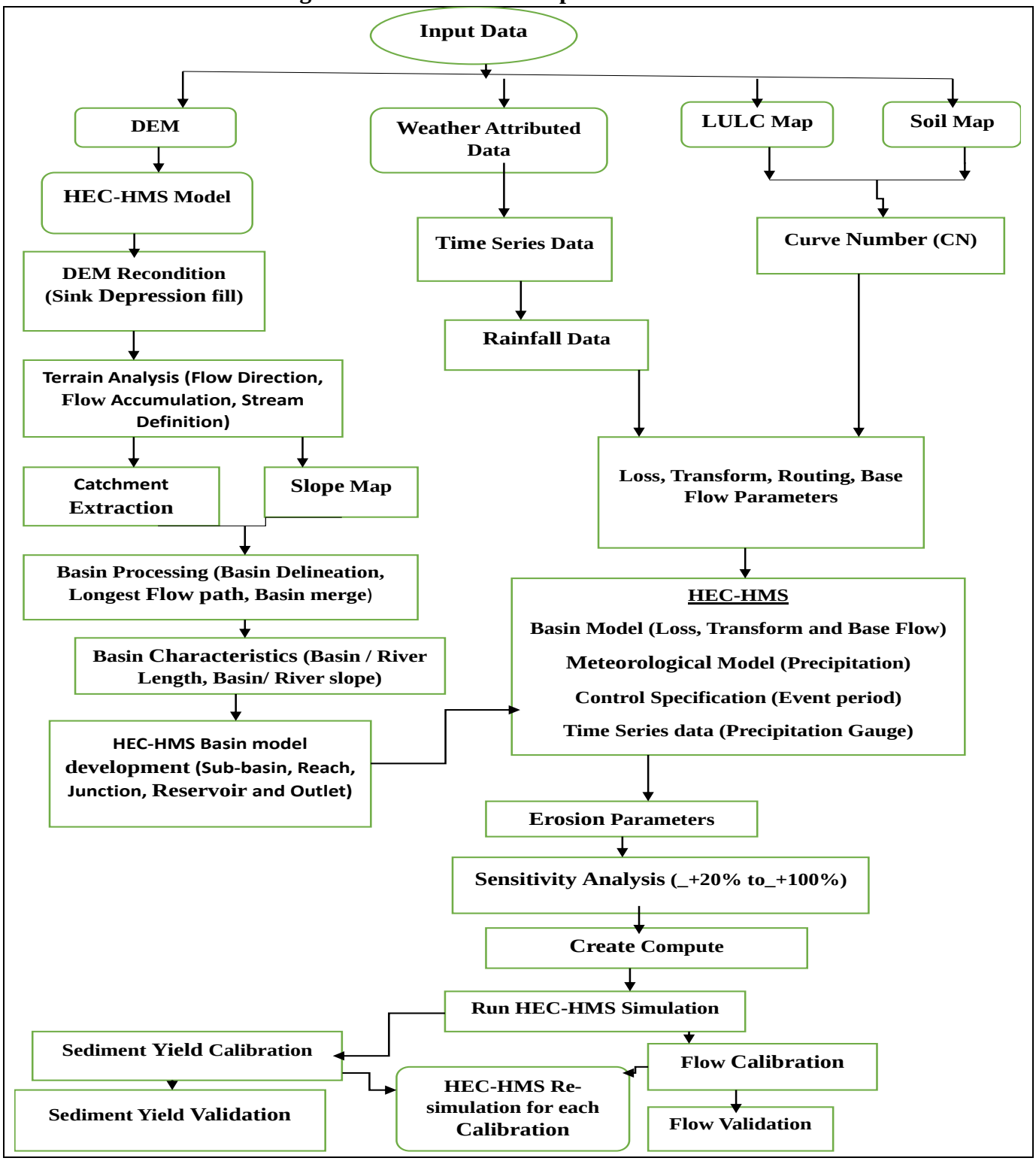

Figure 14: Workflow Diagram for setup and HEC-HMS model run

3.3.9. Parameters of HEC_HMS Model

1.Basin Model

HEC-HMS is hydrological modelling software developed by the US army corps of Engineers Hydrologic Engineering Centre (USACE) (Thangarajah & Saabith, 2021).These modelling tool consist of Basin, Meteorological data, Control specification, Time series, Paired, Terrian. The loss method used in the study was deficit and constant with Clark unit hydrograph transform method. Basin model consist of Sub-basin, reach, junction and outlet. Deficit and constant method are used as a loss method. For the transformation process Clark unit hydrograph method was used as base flow method. Reach is used to convey flow downstream. Muskingum routing method has been used for attenuation. In this method X and K parameters are used. Theoretically, K is the parameter having unit of time, and is passing of a wave in a reach length and X parameter is consist coefficient that its value varies between 0-0.5. Junction and outlet element require the observed flow data. In the beginning of the simulation some initial values were fixed and then adjusted in the calibration and validation stage.

1. Meteorological Model

Meteorological model consists of precipitations methods. Precipitation and Evapotranspiration is required for the continuous simulation. Where the watershed is in cold climates snowmelt is required.

2. Control specifications

Control specification is one of the main components in a project, even though they do not contain much parameter data. Their principal purpose is to control when simulation start and stop, and what time interval is used in the simulation. The model was run for periods of 1990-2000 for calibration and 2001-2010 for validation.

HEC-HMS is a software package designed to simulate the hydrologic cycle. The software requires many different components such as shortwave and longwave radiation, precipitation, potential evapotranspiration, snowmelt, infiltration, surface runoff, baseflow, and channel routing but in this

study used only precipitation. To ensure that the estimates of runoff volumes, peak flow rates, and timing of flows are precise and accurate, the software must be validated.

Calibration is the process of adjusting model parameters to improve model performance by comparing simulated results with observed data (1990-2000). Calibration is an iterative process that involves adjusting parameters until an acceptable level of agreement between simulated and observed data is achieved. Validation is the process of testing a calibrated model against independent data (2001-2010) to determine if it can accurately predict future events. Sensitivity analysis is used to determine which parameters have the greatest impact on model performance.

3. Time Series data: Dailly rainfall data put in time data series.

3.3.10. HEC-HMS Model parameter estimation and processes

The physical characteristics of sub-watersheds (basin slope, longest flow path, basin centroid, centroid elevation, and centroidal longest flow path) and streams (river length, upstream and downstream elevations, and river slope) were extracted from terrain data using HEC-HMS. HEC-HMS used these data with LULC and soil data to generate the model parameters (Deficit and Constant method, Clark Unit Hydrograph, Linear Reservoir, MUSLE) in each sub-watershed (Mewded et al., 2021) and also Muskingham K and X from each reach.

Basin Models (sub-basins, junctions, reach and drainage network of the catchment), Meteorological Models (precipitation), Control Specification (Starting date and time, ending date and time and computational time step for the simulation) and Time series Data (meteorological elements and discharge data which was supplied to the software) (Scharffenberg et al., 2010) were used. For the basin model, metric unit system was adopted and the downstream for each of the sub-watershed, route and junction was assigned automatically. The hydrological procedure of changing rainfall into runoff has been represented by four processes in HEC-HMS: loss, transform, base flow and routing (Alemu Beyene et al, 2020; Jeevika and & Jagritee, 2018) as described below: The model parameters, daily precipitation, and daily observed surface runoff were used to calibrate and validate the HEC-HMS model and the adequate model was used to simulate surface runoff.

i. Precipitation Loss Method

In this research, the Soil Conservation Service-Curve Number (SCS-CN) model (Ramakrishnan et al., 2009) was selected as given by Eqns. (1) to perform the hydrologic modeling of Dura watershed that determined what percentage of precipitation infiltrates through the ground and becomes runoff contributing to the river flow.

$Q = \frac{(P-I_a)^2}{P-I_a-S})$ for $I_a \leq P$ other wise $Q = 0$ (Chow et al., 1998)

$I_a = \lambda S \quad where\ P \geq 0.2S$ Hence, $Q = \frac{(P-0.2S)^2}{(P-1.2S)}$ *(1)*

Where: P is total rainfall (mm), I_a is initial abstraction (mm), Q is direct runoff (mm), S is potential maximum retention (Sorpitivty) (mm) (0, ∞) and λ is the initial abstraction coefficient or ratio (SCS has adopted a standard value of 0.2) (unit less).

ii. Transform Method

The lag time (T_{lag}) of each sub-watershed in Dura watershed is highly related to the characteristics of the main stream (length, slope, and roughness) as shown in Eqn. (2) (USDA, 1972) and Lag time can be related to time of concentration (Tc) as follows (Chow et al., 1998) in Eqn. (3):

$$Tc = \frac{1}{60}\sum\frac{L}{V} \quad (2)$$

$$T_{lag} = \frac{Tt}{2} + 0.6Tc \quad (3)$$

Where: Tc = Time of concentration (Min), L = Longest flow path (Length of flow path) (ft), V = Average velocity in sheet flow and channel (ft/s), Tt = Time of travel (Min), T_{lag} = Lag time (Min), L = Longest flow path (Length of flow path) (ft).

iii. Routing Model

The reach routing process converts a hydrograph at the upstream boundary of the sub-watershed to a resultant hydrograph at the downstream boundary of the sub-watershed for each reach, accounting for gains and losses experienced as the river travels through that particular sub-watershed (US Army Corps of Engineers, 2016; US Army Corps of Engineers Hydrologic Engineering Center, 2000). The routing models available in HEC-HMS account for this attenuation (Bitew G. et al., 2019). The Muskingum method, which was developed by McCarthy (1938), is a popular lumped flow routing technique which was selected for this study.

The Muskingum routing method is a simple approximate method to calculate the outflow hydrograph at the downstream end of the channel reach from the inflow hydrograph at the upstream end (Bitew G. et al., 2019). Among many models used for flood routing in rivers, it is a straightforward hydrological flood routing technique used in natural channels (Bitew G. et al., 2019), In this model calibration, two parameters are needed; travel time (K) of the flood wave through routing reach; and dimensionless weight (X) which corresponds to the attenuation of the flood wave as it moves through the reach.

The routing parameters in the models are usually derived through calibration using measured discharge hydrographs (Baláž et al., 2011) as shown in Eqn. 4.

$$\boldsymbol{S = K[XI + (1 - X)Q]} \qquad (4)$$

Where:

(S) represents the outflow hydrograph at the downstream end of the channel reach.

(K) is the travel time factor (unit hours).

(X) is the dimensionless weighting factor (with $0 \leq X \leq 0.5$).

(I) represents the initial abstraction (mm).

(Q) represents the direct runoff (mm).

The parameter K and X are proportionality factor with the dimension of time or the travel time of a flood wave through the reach and a dimensionless weighting factor with $0 \leq X \leq 0.5$. In natural streams, X is between 0 and 0.3 with a mean value near 0.2 (Chow et al., 1998). Great accuracy in

determining x may not be necessary because the results of the method are relatively insensitive to x (Chow et al., 1998). Both Muskingham K and x was assigned to HEC-HMS model to parameters in the main menu of the software.

iv. Base-flow Method

Sub-surface flow in the catchment was illustrated by base flow in HEC-HMS. There was insignificant contribution of base flow in case of short rainfall event, so it has been ignored. While in case of long rainfall event, the base-flow contributed to the recession limb of hydrograph and had a significant contribution in flood volume (Jeevika and & Jagritee, 2018). Hence, in this research, recession model was used for base flow computation which involved initial discharge and recession constant with a ratio to peak of 0.1 entered to the model using component editor to each sub-watershed.

3.3.11. Sensitivity analysis in HEC-HMS Model

A sensitivity analysis is usually undertaken in most modelling studies (Alemu Beyene, 2023; Bitew G. et al., 2019) to explain how the variation in model output can be attributed to different sources of variation in the model input and it helps in identifying a series of parameters for the HEC-HMS model calibration (Alemu Beyene, 202, Nejadhashemi et al., 2010). It is a necessary process to identify the key parameters for calibration. In this study, the sensitivity analysis was performed by changing the parameter values in the range of ±100% with 10% intervals.

The model was run repeatedly with the baseline value for each parameter multiplied, in turn, by 0.9 and 1.1, while keeping all other parameters constant at their nominal starting values (Juraj M. and Slobodan, 2004). The initial parameter values were used as base values for the evaluation and one parameter at a time was analyzed accordingly.

3.3.12. Calibration and validation processes in HEC-HMS

The model calibration was done with the Simple optimization package and Peak-Weighted Root Mean Square Error (PWRMS) objective function because of their simplicity and performance (Alemu Beyene, 2023; Bitew G. et al., 2019). The selection of rainfall-runoff simulation time step is a critical step for hydrologic modelling and model calibration and validation.

The choice of calibration and validation years were done based on availability and completeness of rainfall and stream monitoring data (Alemu Beyene et al., 2020; Bitew G. et al., 2019) in Dura River watershed. Calibration of the models was performed to obtain the outflow volume, peak flow, Percent bias, RMSE, and time of peak as closely as possible to the observed flow (Sharu, 2020) at Dura Watershed gauging station and calibration involved combination of automated and manual calibration. Both manual algorithms and automated methods have been developed for calibration of HEC-HMS model simulations. An iterative approach is usually used for manual calibration involving the following steps: 1, perform the simulation; 2, compare measured and simulated values; 3, assess if reasonable results have been obtained; 4, if not, adjust input parameters based on expert judgment and other guidance within reasonable parameter value ranges; 5, repeat the process until it is determined that the bast results have been obtained.

The model was validated using the same input parameters as determined by the calibration process but with different simulation time and the Model was calibrated for ten years and validated for ten years at a calibration and validation time step of one day as shown in table 4.

Table 4: Control Specification for calibration and validation of the model

Control Specification	Dura river	Control Specification	Dura river
Calibration period	Jan 01, 1991 - Dec 31, 2000	Validation period	Jan 01, 2001 - Dec 31, 2010
Calibration time step	One day	Validation time step	One day

The peak weighted root mean square error (PWRMSE) with a simple method for search method was the objective function (Eqns. 5 & 6).

3.3.13. Model Efficiency parameters

Model output efficiency is assessed using the determination coefficient (R2), Nash-Sutcliffe efficiency (NSE), root mean square error to the standard deviation of measuring data (RMSE Stdev), and percent bias. The general equations for Nash-Sutcliffe efficiency (NSE) and coefficient of determination (R2) were applied, as proposed by D. N. Moriasi et al. (2007). These measures are computed at daily or monthly time scales.

When validation of the observed and simulated hydrograph was not acceptable, initial parameters were adjusted to provide a better optimization target value for the optimization process (Alemu Beyene et al., 2020).

$$PWRMSE = \sqrt{\frac{\sum_{t=1}^{N} (Qo(t) - Qs(t))^{2\frac{Qo(t)+Qa}{2Qa}}}{N}} \quad (5)$$

$$Qa = \frac{1}{N}\sum_{t=1}^{N} Qo(t) \quad (6)$$

Where: Qo(t), Qs(t), Qa and N are observed flow at time t, Simulated flow at time t, Average of observed flow and Number of data counts respectively.

Statistical evaluation techniques like Nash–Sutcliffe Efficiency (NSE) by Nash and Sutcliffe (1970) (Bettina Schaefl and, 2010) (Eqn. 7) and coefficient of determination (R2) as described in (Barnett et al., 1975) (Landau et al., 2000) were applied to evaluate the performance of the model.

$$NSE = 1 - \left(\frac{\sum_{i=1}^{N} (Oi - QSi)^2}{\sum_{i=1}^{N} (Oi - \bar{O})^2}\right) \quad (7)$$

Where: Q oi, Q si, $\bar{O}$ and N are observed flow, simulated flow, Average of observed flow and Number of data counts respectively.

3.4. To quantify sediment yield and soil erosion from the watershed

3.4.1. Model selection for sediment load modeling

According to (Hajigholizadeh et al., 2018), erosion models delivered the concepts of reality used to simulate and the selection of erosion model depends on several factors such as input data requirements, the objective and scale output of the model, and basin characteristics.

The Modified Universal Soil Loss Equation (MUSLE) is an advanced form of USLE and RUSLE and it is developed by using runoff energy factor instead of the rainfall erosivity used in previous models. MUSLE model estimates the sediment yield based on the runoff energy factor and it is used in HEC-HMS or SWAT models but based on Pak et al., (2015) HEC-HMS predicts a comparatively effective result than SWAT model (Sanjay Shekar & Vinay, 2021).

Table 5: Selected methods in the HEC-HMS

Model Type	**Surface Method**	**Loss Method**	**Transform Method**	**Erosion Method**	**Sediment Transport Method**
Continuous	Simple surface	SCS-CN	SCS Unit Hydrograph	MUSLE	Laursen-Copeland

Table 6: Selected method in a meteorological model

Model Type	**Precipitation**	**Evapotranspiration**	**Snowmelt**
Continuous	Specified Hyetograph	None	None

3.4.2. Factors of Sediment load and erosion method in HEC-HMS

According to Banasik & Walling, (1996) MUSLE is commonly used in the world and its' mathematical equation to estimate the sediment yield is as in Eqn. 8.

$$Sed = 11.8\ (Qsurface * qpeak)\ 0.56 * K * LS * C * P \quad \text{..... (8)}$$

Where, Sed is sediment load in Tons, Q surface is the volume of surface runoff in m3, q peak is Peak discharge in (m3/s), K is Erodibility Factor, the unit is (ton/ha, R), LS is Topographic factor, C is covering management factor, and P is Practice factor. The LS, C, and P are unitless.

- **Erodibility factor (K)**: According to (Addis & Klik, 2015), K factor describes the resistance to soil erosion and is depends on soil properties, organic matter content (OM), bulk density, particle size, and shape and it ranges from 0 to 1 Scholten, (2007) and the calculation can be derived from observed soil parameters, including organic matter content, texture, presence of coarse fragments, structural class, and permeability (Addis & Klik, 2015; Wischmeier, W. H., and Smith, 1978), that based on Eqns (9&10).

$$K = 2.77 * 10{-}7(12 - OM)\ M1.14 + 4.28 * 10{-}3(s - 2) + 3.29 * 10{-}3(p - 3) \text{ ..... (9)}$$

$$M = [(100 - C)\ (L + Armf) \text{ .... (10)}$$

Where, C is the percentage of clay (<0.002 mm), L is the percentage of silt (0.002 mm to 0.05 mm), *Armf* denotes the percentage of very fine sand (0.05mm to 0.1mm), OM is the

percentage of organic matter content, S is code of the structure size, type, and grade based on field observation and P is code of the permeability (Addis & Klik, 2015).

- **Topographic factor (LS)**: The LS is defined as vulnerability to erosion that depends on the length and slope of the terrain. Generally, the value of (LS) ranges from 0.1 (flat slope) to 10 (steep-slope) (Alemu Beyene, 2023; Zhang et al., 2017) and it is computed in detail in MUSLE part of soil loss computation. The LS -factor was calculated based on the following equation (Kebede Wolka et al., 2015) (Alemu Beyene, 2023) is shown in Eqn. 11.

$$\mathbf{LS} = \left(\frac{\boldsymbol{\lambda}^{\mathbf{0.3}}}{\mathbf{22.1}}\right) * \left(\frac{\mathbf{S}}{\mathbf{9}}\right)^{\mathbf{1.3}} \quad \ldots\ldots\ldots\ldots\ldots\ldots \text{(11).}$$

Where λ is signifies the Flow length and S is Slope in percent

- **Cover factor (C):** it defines the impact of vegetation on soil erosion. A higher value of cover factor indicates to the most vulnerable of soil erosion and vice-versa and the value ranges from 1 to 0.1 and it is presented in the soil loss part of the paper.

- **Practice factor (P):** The Practice factor (P) shows the ratio of soil loss based on conservation practice to the soil loss based on certain cultivation. The P-value range from 0 to 1. The lower value 0 indicates higher erosion resistance capacity whereas higher value 1 represents lower erosion resistance capacity Pandey et al., (2021).

- **Exponent:** The exponent in erosion is used to distribute the sediment concentration in time-series sedigraph. The sediment concentration can be calculated by using a power function (Adhikari, 2020, Alemu Beyene, 2023, Pak et al., 2015). The value of exponent is generally range from 0.5 to 1 (Pak et al., 2015).

A total of seven parameters estimated based on terrain, land use, and soil type of the catchment are required to input for the erosion model. These are: K, LS, C, P, Threshold (1m3/s = no sediment transport if flow is >1 m3/s), Exponent and Gradation curve. In this case Erosion method

of MUSLE was chosen and the erosion is on displayed so that K, LS, C, P factors were coded to each of the sub-watersheds for modeling sediment (Table 7).

Table 7: Erosion model parameters assigned to each sub-watershed

Sub-basins	Erodibility Factor	Topographic Factor	Cover Factor	Practice Factor	Threshold Factor (m^3/s)	Exponent	Gradation curve
Subbasin-1	0.1	18.45	0.2	1	1	0.5	Table 1
Subbasin_2	0.1	16.74	0.2	1	1	0.5	Table 1
Subbasin_3	0.1	7.26	0.2	1	1	0.5	Table 1
Subbasin_4	0.2	2.115	0.2	1	1	0.5	Table 1
Subbasin_5	0.1	16.08	0.2	1	1	0.5	Table 1
Subbasin_6	0.2	22.14	0.2	1	1	0.5	Table 1
Subbasin_7	0.2	14.37	0.2	1	0.1	0.5	Table 1
Subbasin_8	0.2	10.47	0.2	1	0.1	0.5	Table 1
Subbasin_9	0.2	4.92	0.2	1	0.1	0.5	Table 1
Subbasin_10	0.2	8.49	0.2	1	0.03	0.5	Table 1
Subbasin_11	0.2	4.92	0.2	1	0.03	0.5	Table 1
Subbasin_12	0.2	14.37	0.2	1	0.03	0.5	Table 1
Subbasin_13	0.2	7.74	0.2	1	0.03	0.5	Table 1
Subbasin_14	0.2	15.81	0.2	1	0.03	0.5	Table 1
Subbasin_15	0.2	9	0.2	1	0.1	0.5	Table 1
Subbasin_16	0.2	19.56	0.2	1	0.1	0.5	Table 1
Subbasin_17	0.2	16.8	0.2	1	0.1	0.5	Table 1

Table 8: Gradation curve of the watershed

Diameter (mm)	Percent finer (%)
0.002	74
0.01	99.8
0.05	99.93
0.2	100

Gradation curve: The gradation curve in HEC-HMS describes the distribution of total sediment load into different grain size classes at the outlet of the sub-basin. The gradation curve is the particle size distribution curve, and it is input as a diameter-percentage function from the Paired Data Manager in HEC-HMS as shown in Table 8. In non-cohesive sediments the particle or grain size and weight were the dominant parameters for sediment movement and transport.

CHAPTER FOUR

RESULTS AND DISCUSSIONS

4.1. Land use Land cover Change

4.1.1. Land Use Land Cover Change

From the research and data obtained from the satellite imagery for Dura watershed (Figure 4.1), the watershed has undergone numerous land use /land cover changes in the last four decades. The land use land cover map of 1993, 2003, 2013, 2023 in (Figure 4.1) in Dura watershed has changed significantly over the years. Table .4 here was a summary of the land use land cover distribution in the years 1993, 2003, 2013, and 2023: The forest cover has experienced a slight increase from approximately 19.98% in 1993 to around 22.47% in the projected year of 2023. Bush land has shown a significant increase from about 26.45% in 1993 to nearly half of the total area at around 48.85% in the projected year of 2023. Agricultural land has also increased from approximately 22.34% in 1993 to around 27.37% in the projected year of 2023. Bare land has seen a substantial decrease from about 31.23% in 1993 to only about 1.32% in the projected year of 2023. These changes reflect shifts in land use land cover patterns over time and highlight the importance of sustainable land management practices to ensure a balance between economic development and environmental conservation.

Among the four land use types identified (Table 9), forest, bush land has showed a growth trend, and Agriculture and bare land are found under shrinking trends. The land use land cover map of 1993, 2003, 2013, 2023 (Figure 14) in Dura watershed has undergone significant changes over the years. The result shows a decrease in bare land and an increase in forest, bush land, and agricultural land. These changes reflect the ongoing efforts to manage land sustainably and strike a balance between economic development and environmental conservation. The increase in forest area is a positive sign as forests play a crucial role in maintaining biodiversity, regulating climate, and providing ecosystem services. It was important to continue efforts to protect and restore forests to ensure their long-term sustainability.

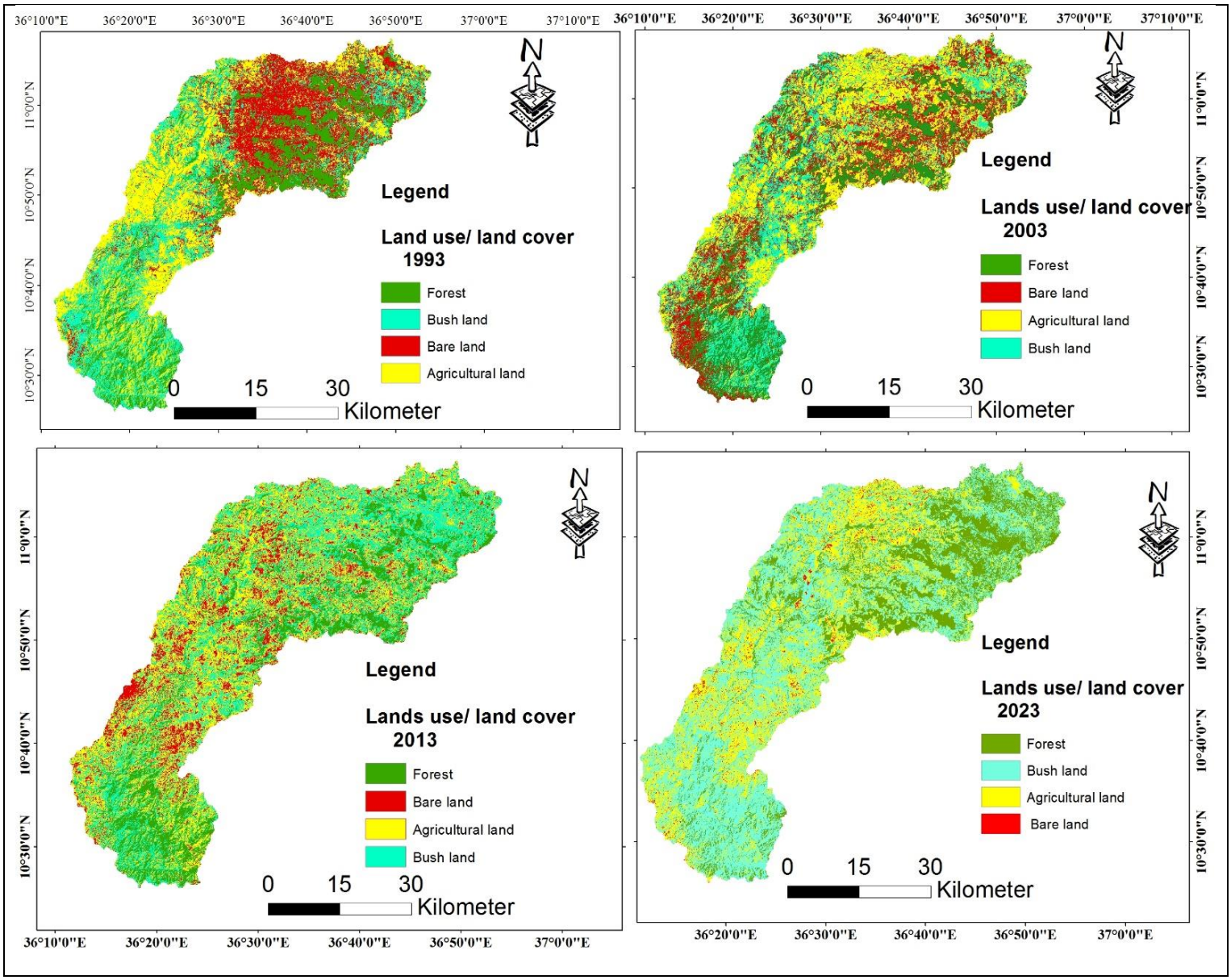

Figure 15: LULCC map of Dura watershed in Four time serious (1993, 2003, 2013 $ 2023)

Table 9: Areal coverage of LULC types at different periods in the Dura watershed

Class Name	1993	2003	2013	2023
Forest	44970.1 ha (19.98%)	47394 ha (21.06%)	40073 ha (17.80%)	50565.6 ha (22.47%)
Bush Land	59528.7 ha (26.45%)	49929.3 ha (22.18%)	75565 ha (33.57%)	109953 ha (48.85%)
Agricultural Land	50282.2 ha (22.34%)	73600.1 ha (32.70%)	80004 ha (35.54%)	61608.1 ha (27.37%)
Bare Land	70306 ha (31.23%)	54163.6 ha (24.06%)	29445 ha (13.08%)	2960.3 ha (1.32%)
Total	225087 ha (100%)	225087 ha (100%)	225087 ha (100%)	225087 ha (100%)

The increase in bush land can be attributed to various factors such as population growth, urbanization, and changes in land use practices. It was essential to monitor and manage bush land effectively to prevent encroachment into natural habitats and protect biodiversity. The increase in agricultural land indicates the expansion of agricultural activities to meet the growing food demand. However, it is important to ensure that agricultural practices are sustainable, minimize environmental impacts, and promote efficient resource management. The decrease in bare land can be seen as a positive outcome of land restoration efforts and reforestation initiatives. Restoring bare land can help prevent soil erosion, improve water quality, and enhance ecosystem resilience. To ensure sustainable land use in the future, it is crucial to implement effective land management strategies, promote conservation practices, and engage local communities in decision-making

processes. This will help preserve natural resources, protect biodiversity, and support the overall well-being of both present and future generations.

4.1.2. Trend of Land use Land cover Change (LULCC)

Table 10: Areal coverage of LULC changes at different periods in the Dura watershed

Class type	1993	2003	change 1993-2003		2013	change 2003-2013		2023	change 2013-2023		change 1993-2023	
		Area (ha)		%	Area (ha)		%	Area (ha)		%	Area (ha)	%
Forest	44970.1	47394	2423.9	54	40073.4	-7320.6	-15	50565.6	10492.2	26	5595.5	12
Bush land	59528.7	49929.3	-9599.4	-16	75565.3	25636	51	109942	34376.7	45	50413.3	85
Agricultural Land	50282.2	73600.1	23317.9	46	80002.7	6402.6	9	61608.1	-18394.6	-23	11325.9	23
Bare land	70305.8	54163.6	-16142.2	-23	29444.5	-24719.1	-46	2960.3	-26484.2	-90	-67345.5	-96

Based on Table 10 the rate of change of LULC in dura watershed is Area of Land Use Land cover types map (Figure 14) in Dura Watershed result shows the changes in the area of different land use land cover classes from 1993 to 2023. Those are, the area of forest decreased by 10.9% from 1993 to 2013, but increased by 26.2% from 2013 to 2023. The area of bush land had the highest growth rate of 84.9% from 1993 to 2023, with a sharp rise of 45.5% from 2013 to 2023. The area of agricultural land peaked in 2013 with a 46.4% increase from 1993, but dropped by 23% from 2013 to 2023. The area of bare land had the largest decline of 95.8% from 1993 to 2023, with a steady decrease in each decade.

The area of forest decreased from 1993 to 2013, but increased slightly in 2023. This might indicate some efforts to restore the forest cover in the recent years. The area of bush land fluctuated over time, but showed a significant increase in 2023. This might suggest that some agricultural land or bare land was converted to bush land due to natural or human factors. The area of agricultural land increased from 1993 to 2013, but decreased in 2023. This might reflect the changes in the demand and supply of agricultural products, or the impact of climate change on crop production. The area of bare land decreased steadily from 1993 to 2023. This might imply that the land was used for other purposes, such as forestation, agriculture, or urbanization.

Table 111: LULCC in hectare (ha)

Change in Hectare (ha)				
Land Use Type	1993-2003	2003-2013	2013-2023	1993-2023
Forest	2423.9	-7320.6	10492.2	5595.5
Bush land	-9599.4	25636	34376.7	50413.3
Agricultural land	23317.9	6402.6	-18394.6	11325.9
Bare land	-16142.2	-24719.1	-26484.2	-67345.5

The table 11 result shows the change in hectares (ha) for different land use types over three time periods: 1993-2003, 2003-2013, and 2013-2023. The forest area increased by 2,423.9 ha from 1993 to 2003, decreased by 7,320.6 ha from 2003 to 2013, and increased by 10,492.2 ha from 2013 to 2023. Overall, there was a net increase of 5,595.5 ha in the forest area from 1993 to 2023. The bush land area decreased by 9,599.4 ha from 1993 to 2003, increased by 25,636 ha from 2003 to 2013, and further increased by 34,376.7 ha from 2013 to 2023. The net change in bush land area from 1993 to 2023 was an increase of 50,413.3 ha. The agricultural land area increased by 23,317.9 ha from 1993 to 2003, further increased by 6,402.6 ha from 2003 to 2013, and then decreased by 18,394.6 ha from 2013 to 2023. The net change in agricultural land area from 1993 to 2023 was an increase of 11,325.9 ha. The bare land area decreased by 16,142.2 ha from 1993 to 2003, further decreased by 24,719.1 ha from 2003 to 2013, and continued to decrease by 26,484.2 ha from 2013 to 2023. The net change in bare land area from 1993 to 2023 was a significant decrease of 67,345.5 ha. These changes reflect the dynamic nature of land use over time and can be influenced by various factors such as urbanization, deforestation, agricultural practices, and natural processes.

Between 1993 and 2023, the forest area experienced a net increase of 5595.5 ha**.** However, it was important to note that the forest area initially decreased by 7320.6 hectares from 1993 to 2003 and then increased by 10492.2 ha from 2003 to 2013. The bush land area experienced significant changes over the years. It decreased by 9599.4 hectares from 1993 to 2003, followed by a

substantial increase of 25636 ha from 2003 to 2013. Finally, it further increased by 34376.7 ha from 2013 to 2023, resulting in total net increase of 50413.3 ha. The agricultural land area increased by 23317.9 ha from 1993 to 2003, followed by a smaller increase of 6402.6 ha from 2003 to 2013. However, it experienced a significant decrease of 18394.6 ha from 2013 to 2023, resulting in a net increase of 11325.9 ha. The bare land area experienced a net decrease of 67345.5 ha from 1993 to 2023. It initially decreased by -16142.2 ha from 1993 to 2003, followed by a further decrease of -24719.1 ha from 2003 to 2013, and finally decreased by -26484.2 ha from 20013 to 2023. Generally, between 1993 and 2023, the bare land cover experienced a net decrease of -67345.5 ha.

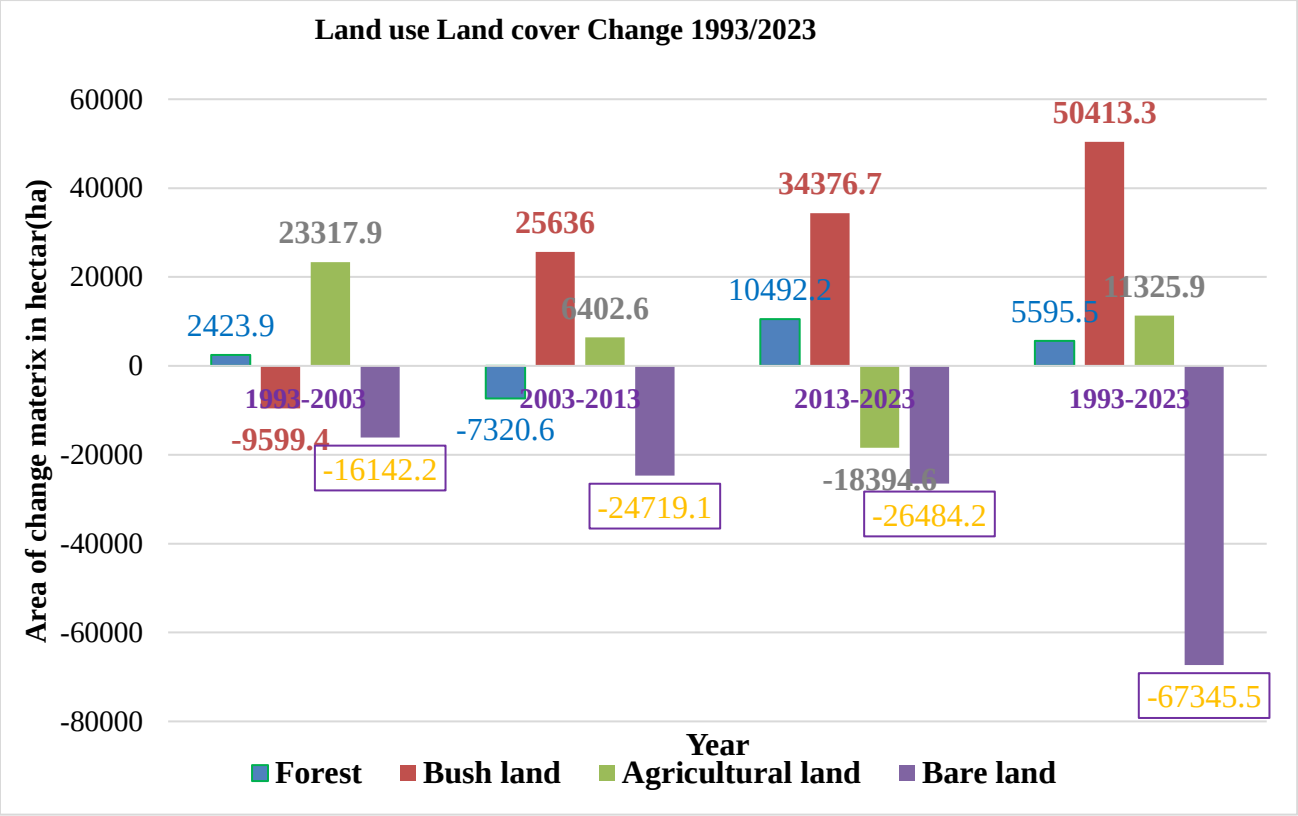

Figure 16: Land use Land cover Change in Dura Watershed 1993/ 2023

4.2. Surface runoff and soil Erosion

4.2.1. Model adequacy evaluation

Table 122: Modeling result and adequacy of HEC-HMS model in Dura watershed

Simulation type	Parameters	Daily	Monthly	Best range	Adequacy	Confirmed Source
Calibration (1990-2000)	Nash (%)	64.2	80.8	>50	Adequate	Mewded, et al 2021
	RMSE Stdev	0.6	0.6	<1	Adequate	
	Percent Bias	-3.66	-3.66	±10	Adequate	
	R square (%)	64	64	>60	Adequate	
Validation (2001-2010)	Nash (%)	60.4	63.8	>50	Adequate	
	RMSE Stdev	0.6	0.6	<1	Adequate	
	Percent Bias	6.54	6.54	±10	Adequate	
	R square (%)	62	62	>60	Adequate	

In this study, we evaluated the performance of the HEC-HMS simulation model over a period of 20 years (1990-2010) using daily hydro-meteorological data. The results, summarized in Table 12, provide insights into the model's effectiveness. The Nash coefficient indicates the goodness of fit between the simulated and observed data. RMSE Stdev represents the standard deviation of the root mean square error. Percent Bias reflects any systematic bias present in the model. R square measures the proportion of variance explained by the model. Our analysis involved sensitivity analysis, calibration, and validation. We calibrated and validated the model using observed stream flow data for two distinct 10-year periods: 1990-2000 and 2001-2010. Overall, the model performs reasonably well, with an NSF (Nash-Sutcliffe Efficiency) value between 0.5 and 0.65, and R square values of 0.62 in validation and 0.64 in calibration both close to 1.0 are adequate model performance. However, there are some variations between the calibration and validation periods.

4.2.2. Model parameters

1. **Loss**

Initial Deficit: The initial amount of water deficit (in millimeters) in this subbasin. Maximum Storage: The maximum storage capacity (in millimeters) of water that this subbasin can hold. Constant Rate: The constant rate of water inflow (in millimeters per hour) into this subbasin. These values represent hydrological characteristics for each subbasin in a model. The initial deficit indicates how much water needs to be filled to reach the maximum storage capacity. The constant rate represents the inflow rate. The impervious area percentage reflects the impermeable surfaces in the subbasin. Overall, these values are essential for understanding water flow and management in each subbasin.

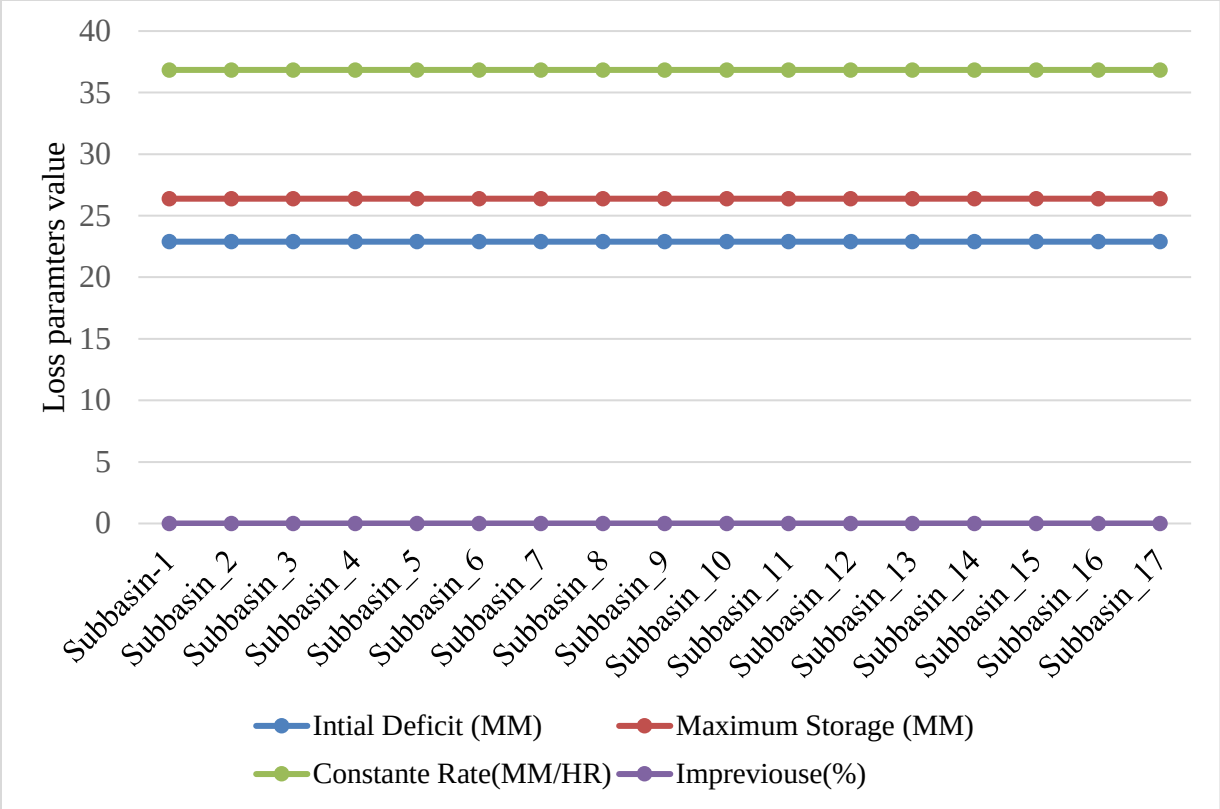

Figure 17: loss parameters

2.Transform

The Time of Concentration for Subbasin-1 was approximately 55.35 hours, indicating the duration it takes for water to flow from the farthest point in the subbasin to the outlet. The Storage Coefficient for Subbasin-1 was approximately 55.16 hours, representing the time it takes for the entire subbasin to drain completely. Subbasin-2 has a Time of Concentration of 48.16 hours and a Storage Coefficient of 48 hours. Subbasin-3 exhibits a Time of Concentration of 40.18 hours and a Storage Coefficient of 40.21 hours. For Subbasin-4, the Time of Concentration is 32.44 hours, and the Storage Coefficient is 32.46 hours. Subbasin-5 has a Time of Concentration of 54.02 hours and a Storage Coefficient of 53.90 hours. The Time of Concentration for Subbasin-6 is 48.63 hours, and the Storage Coefficient is 48.84 hours. Subbasin-7 shows a Time of Concentration of 51.60 hours and a Storage Coefficient of 51.79 hours. Subbasin-8's Time of Concentration is 34.01 hours, and its Storage Coefficient is 34.02 hours. Subbasin-9 has a Time of Concentration of 28.38 hours and a Storage Coefficient of 28.34 hours. Subbasin-10 exhibits a Time of Concentration of 30.65 hours and a Storage Coefficient of 30.61 hours. For Subbasin-11, the Time of Concentration is 25.88 hours, and the Storage Coefficient is 25.90 hours. Subbasin-12's Time of Concentration

is 40.65 hours, and its Storage Coefficient is 40.67 hours. Subbasin-13 has a Time of Concentration of 26.89 hours and a Storage Coefficient of 26.95 hours. The Time of Concentration for Subbasin-14 is 27.36 hours, and the Storage Coefficient is 27.41 hours. Subbasin-15 has a consistent Time of Concentration and Storage Coefficient, both at 24 hours. Subbasin-16's Time of Concentration is 34.48 hours, and its Storage Coefficient is 34.53 hours. Subbasin-17 exhibits a Time of Concentration of 29.47 hours and a Storage Coefficient of 29.47 hours.

Subbasin-1 has a relatively long Time of Concentration (55.35 hours) and a high Storage Coefficient (55.16 hours). Water in Subbasin-1 takes a significant amount of time to flow to the outlet, and its storage capacity contributes significantly to direct runoff. Consider implementing flood control measures or managing the storage capacity effectively to mitigate potential erosion risks. Subbasin-2 has moderate values for both Time of Concentration (48.16 hours) and Storage Coefficient (48 hours). It exhibits balanced characteristics in terms of runoff timing and storage. Continue monitoring and maintain existing drainage infrastructure. Subbasin-3 has a shorter Time of Concentration (40.18 hours) and slightly higher Storage Coefficient (40.21 hours). It responds relatively quickly to rainfall events. Subbasin-4 has a shorter Time of Concentration (32.44 hours) and a similar Storage Coefficient (32.46 hours). It has a rapid response to rainfall, potentially leading to flash floods. Subbasin-5 has a long Time of Concentration (54.02 hours) and a high Storage Coefficient (53.90 hours). It combines delayed runoff with substantial storage capacity. Subbasin-6 exhibits balanced values for both parameters. It maintains a reasonable balance between runoff timing and storage. Subbasin-7 has moderate values for both parameters. It behaves predictably in terms of runoff and storage. Subbasin_8 to Subbasin_17: These subbasins show varying characteristics but generally fall within acceptable ranges. Each subbasin has unique hydrological behavior. Overall, a comprehensive watershed management approach should consider the interplay between time of concentration, storage coefficient, land use, and climate conditions to ensure effective flood control, water resource utilization, and sustainable development.

Land use has a significant impact on various hydrological parameters, influencing water flow, runoff patterns, and overall watershed behavior. Time of Concentration (Tc): Tc represents the time it takes for water to flow from the farthest point in a watershed (or subbasin) to the outlet. Land Use Impact: Urbanization: Increased impervious surfaces (roads, buildings) reduce

infiltration, leading to shorter Tc. Deforestation: Removal of vegetation decreases interception and evapotranspiration, potentially shortening Tc. Agricultural Practices: Altered land cover affects surface roughness and runoff pathways, impacting Tc. Storage Coefficient: R represents the fraction of total watershed storage contributing to direct runoff during a storm. Land Use Impact: Urbanization: Increased impervious areas reduce storage capacity, elevating R. Forests: Forested areas enhance storage through soil and vegetation, lowering R. Wetlands: Preserving wetlands increases storage, reducing R. Tc and R are interconnected. Longer Tc values often correspond to higher R values because more storage contributes to direct runoff. Accurate estimation of both parameters ensures better representation of watershed response to rainfall events.

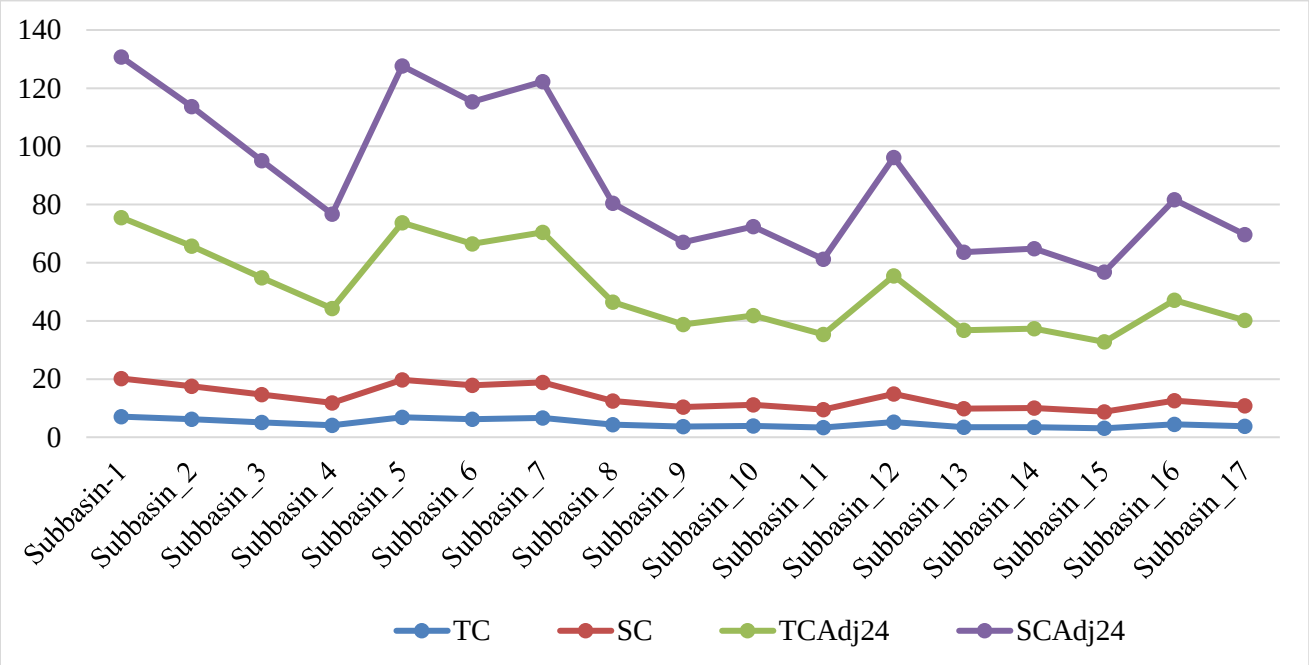

Figure 18. Before and after optimization HEC_HMS Model of Transform

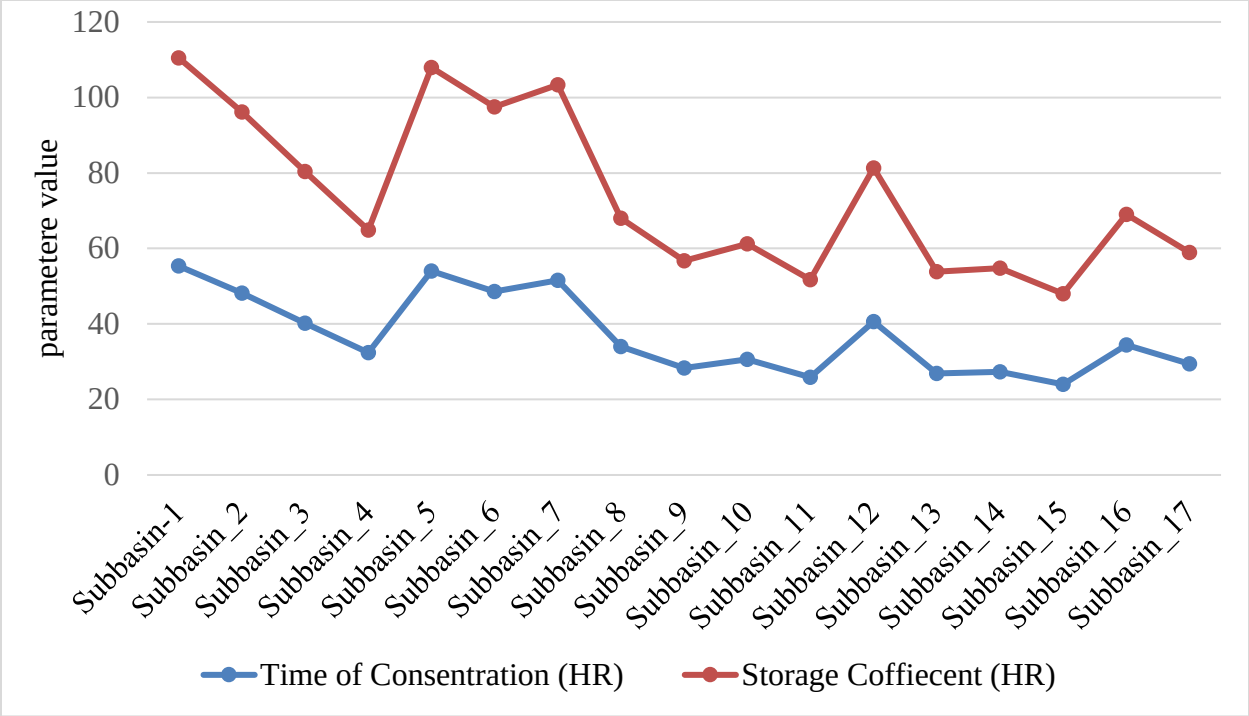

Figure 19: Time of concentration and Storage coefficient

3. Routing model

The hydrological assessment of the Dura watershed reveals a complex interplay of various factors influencing the discharge rates across different reaches. The study utilizes a systematic approach to quantify the initial discharge, Muskingum routing parameters (Mus K and Mus X), and adjustment factors (KAdj2 and XAdj2) for each reach (Figure: 20). The results demonstrate a range of discharge values, with Reach_2 exhibiting the highest initial discharge of 3.3674 hours and Reach_12 showing the lowest at 0.10742 hours. The Muskingum routing parameters remain constant across all reaches, with a Mus K value of 0.01 and Mus X value of 1, indicating a standardized approach to modeling the flow within the watershed. The adjustment factors, represented by KAdj2, vary significantly, reflecting the unique characteristics of each reach. Reach_2 has the highest KAdj2 value of 62.7 hours, suggesting a greater need for adjustment in the model to accurately simulate the flow dynamics. Conversely, reach_7 has the lowest KAdj2 value of 2.24 hours, indicating a lesser degree of modification from the standard parameters.

This analysis underscores the importance of tailored hydrological models that account for the specific conditions of each reach. Such models are essential for effective water resource

management, enabling the prediction of flow rates and the identification of potential areas of concern within the watershed. The study's findings contribute valuable data for the ongoing efforts to manage the Dura watershed sustainably and ensure the balance between economic development and environmental conservation.

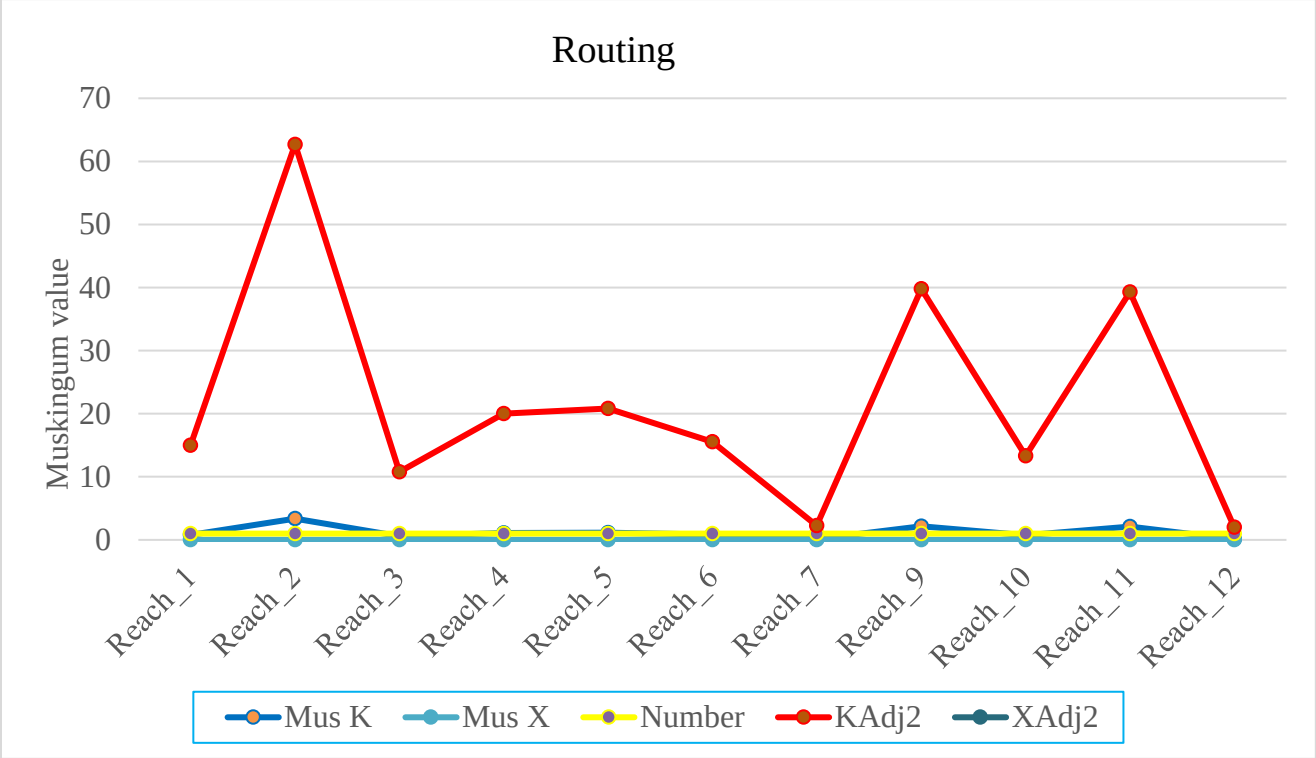

Figure 20. Before and after optimization HEC_HMS Model of Routing Muskingum

4. Base Flow

Subbasin-1: Baseflow with an initial flow rate of 0 $m^3/s/km^2$, a fraction of 0.76981, and a coefficient of 141.6. Subbasin-2: Baseflow with an initial flow rate of 0 $m^3/s/km^2$, a fraction of 0.5131, and a coefficient of 123.2. Subbasin-3: Baseflow with an initial flow rate of 0 $m^3/s/km^2$, a fraction of 0.25639, and a coefficient of 102.8. Subbasin-4: Baseflow with an initial flow rate of 0 $m^3/s/km^2$, a fraction of 0.20153, and a coefficient of 83. Subbasin-5: Baseflow with an initial flow rate of 0 $m^3/s/km^2$, a fraction of 0.0664738, and a coefficient of 138.2. Subbasin-6: Baseflow with an initial flow rate of 0 $m^3/s/km^2$, a fraction of 0.0167562, and a coefficient of 124.4. Subbasin-7: Baseflow with an initial flow rate of 0 $m^3/s/km^2$, a fraction of 0.0083129, and a coefficient of 132. Subbasin-8: Baseflow with an initial flow rate of 0 $m^3/s/km^2$, a fraction of 0.0050312, and a coefficient of 87. Subbasin-9: Baseflow with an initial flow rate of 0 $m^3/s/km^2$, a fraction of

0.0052556, and a coefficient of 72.6. Subbasin-10: Baseflow with an initial flow rate of 0 $m^3/s/km^2$, a fraction of 0.0036405, and a coefficient of 78.4. Subbasin-11: Baseflow with an initial flow rate of 0 $m^3/s/km^2$, a fraction of 0.0025582, and a coefficient of 66.2. Subbasin-12: Baseflow with an initial flow rate of 0 $m^3/s/km^2$, a fraction of 0.0014163, and a coefficient of 104. Subbasin-13: Baseflow with an initial flow rate of 0 $m^3/s/km^2$, a fraction of 0.0010027, and a coefficient of 68.8. Subbasin-14: Baseflow with an initial flow rate of 0 $m^3/s/km^2$, a fraction of 0.0040407, and a coefficient of 70. Subbasin-15: Baseflow with an initial flow rate of 0 $m^3/s/km^2$, a fraction of 0.0088854, and a coefficient of 61.4. Subbasin-16: Baseflow with an initial flow rate of 0 $m^3/s/km^2$, a fraction of 0.0180566, and a coefficient of 88.2. Subbasin-17: Baseflow with an initial flow rate of 0 $m^3/s/km^2$, a fraction of 0.0180566, and a coefficient of 75.4. These values represent various hydrological parameters related to groundwater flow in each subbasin. The coefficients and fractions play a role in modeling the flow dynamics.

Subbasin-1: Baseflow with a fraction of 0.76981 and a coefficient of 141.6. This suggests that the groundwater contribution is significant, and the coefficient indicates moderate flow potential. When considering soil erosion, areas with higher groundwater flow may have better soil stability due to consistent moisture levels. **Subbasin-2**: Baseflow with a fraction of 0.5131 and a coefficient of 123.2. Similar to Subbasin-1, this subbasin also has substantial groundwater flow potential. Soil erosion management should account for this consistent water supply. **Subbasin-3**: Baseflow with a fraction of 0.25639 and a coefficient of 102.8. The lower fraction indicates less groundwater contribution, but the coefficient still suggests moderate flow potential. Soil erosion control measures should consider both surface runoff and groundwater dynamics. **Subbasin-4**: Baseflow with a fraction of 0.20153 and a coefficient of 83. While the fraction is lower, the coefficient indicates a reasonable flow potential. Soil erosion prevention strategies should address both surface and subsurface water movement. **Subbasin-5**: Baseflow with a fraction of 0.0664738 and a coefficient of 138.2. The low fraction implies minimal groundwater contribution, but the high coefficient suggests rapid flow potential. Soil erosion management should focus on surface runoff control. **Subbasin-6 to Subbasin-17**: Similar considerations apply to the remaining subbasins. Evaluate the balance between groundwater flow, surface runoff, and soil erosion risk. Groundwater intercepts excess rainfall, reducing the intensity of surface runoff. It acts as a buffer, preventing

flash floods and soil erosion. Implement appropriate measures to maintain soil stability and prevent erosion.

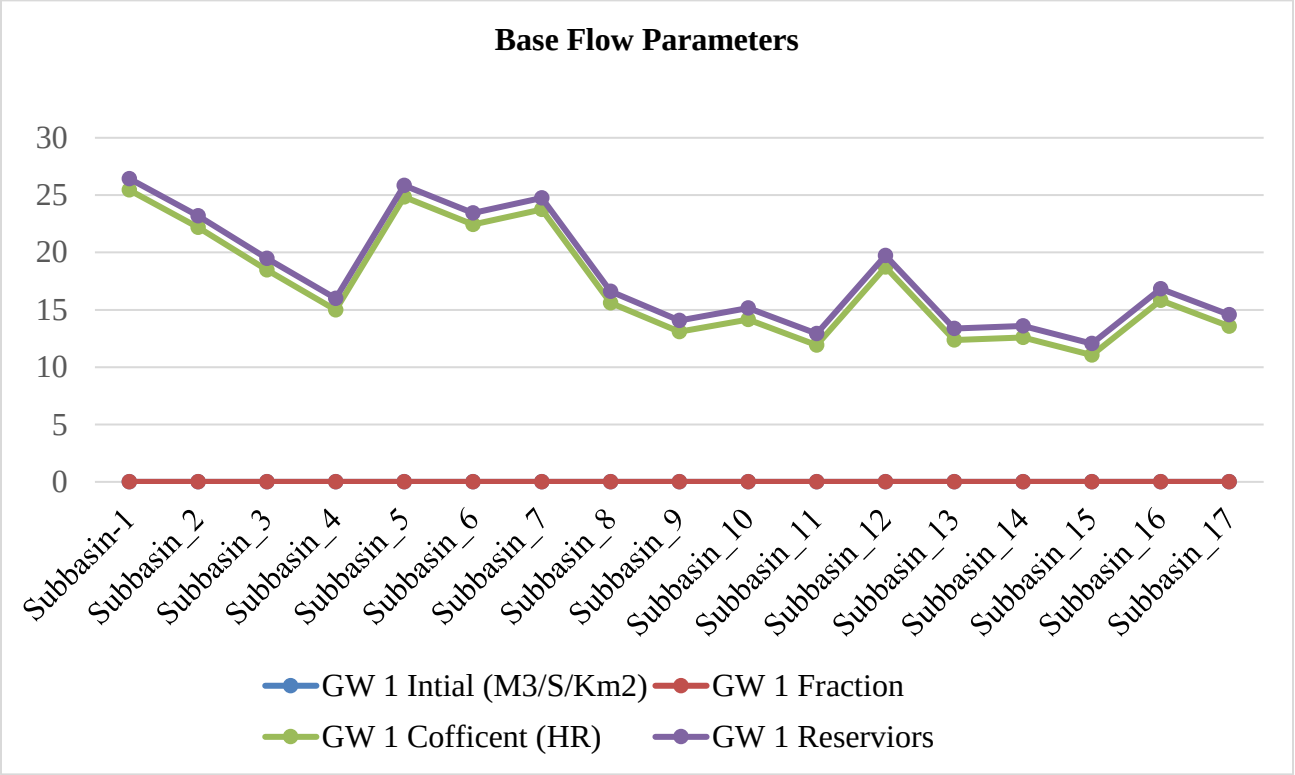

Figure 21: Base Flow parameter in Growndwater-1

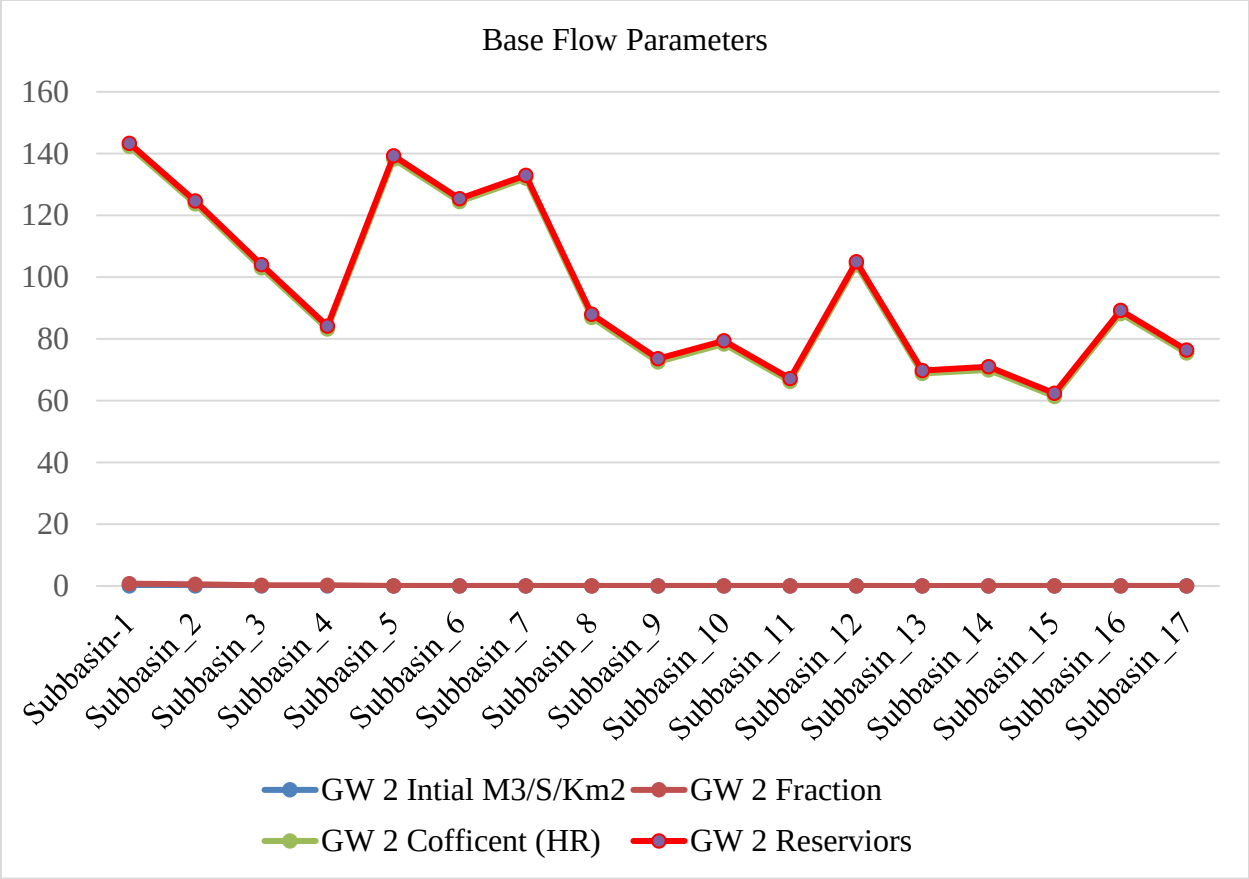

Figure 22: Base Flow parameter in Growndwater-2

5. Rate of Erosion

Erodibility Factor (K): This factor represents how susceptible the soil is to erosion. Lower values subbasin 1,2,3, and 5 (such as 0.1) indicate less erodible soil, while subbasin 4, 6 -17: higher values (such as 0.2) suggest higher susceptibility to erosion (more erodible soil). **Topographic Factor**: The topography of the land influences erosion. Higher values (e.g., Subbasin -1: 18.45) may indicate steeper slopes or other topographical features that contribute to erosion risk. **Curves Factor (Corves Factor)**: This factor likely relates to the shape or curvature of the land. A value of 0.2 suggests some influence on erosion processes. **Practice Factor**: The practice factor accounts for land management practices. A value of 1 indicates no specific practice adjustments, while other values may reflect different practices affecting erosion. **Threshold (M3/S)**: This threshold represents a critical flow rate (in cubic meters per second). It indicates the point at which erosion becomes significant. Values of 1 suggest a low threshold. **Exponent**: The exponent is a numerical value used in calculations. In this context, it likely affects the erosion model or equation.

Gradation Curve: The gradation curve may relate to particle size distribution in the soil. Overall, these factors collectively contribute to understanding soil erosion risk in different subbasins. Lower erodibility factors, appropriate land management practices, and understanding critical thresholds are essential for effective erosion control strategies.

Table 133: Erosion parameters

SUB BASIN	ERODIBILITY FACTOR (K)	TOPOGRAPHIC FACTOR	CORVES FACTOR	PRACTICE FACTOR	THRESHOLD (M3/S)	EXPONENT	GRADATION CURVE
Subbasin-1	0.1	18.45	0.2	1	1	0.5	Table 1
Subbasin_2	0.1	16.74	0.2	1	1	0.5	Table 1
Subbasin_3	0.1	7.26	0.2	1	1	0.5	Table 1
Subbasin_4	0.2	2.115	0.2	1	1	0.5	Table 1
Subbasin_5	0.1	16.08	0.2	1	1	0.5	Table 1
Subbasin_6	0.2	22.14	0.2	1	1	0.5	Table 1
Subbasin_7	0.2	14.37	0.2	1	0.1	0.5	Table 1
Subbasin_8	0.2	10.47	0.2	1	0.1	0.5	Table 1
Subbasin_9	0.2	4.92	0.2	1	0.1	0.5	Table 1
Subbasin_10	0.2	8.49	0.2	1	0.03	0.5	Table 1
Subbasin_11	0.2	4.92	0.2	1	0.03	0.5	Table 1
Subbasin_12	0.2	14.37	0.2	1	0.03	0.5	Table 1
Subbasin_13	0.2	7.74	0.2	1	0.03	0.5	Table 1
Subbasin_14	0.2	15.81	0.2	1	0.03	0.5	Table 1
Subbasin_15	0.2	9	0.2	1	0.1	0.5	Table 1
Subbasin_16	0.2	19.56	0.2	1	0.1	0.5	Table 1
Subbasin_17	0.2	16.8	0.2	1	0.1	0.5	Table 1

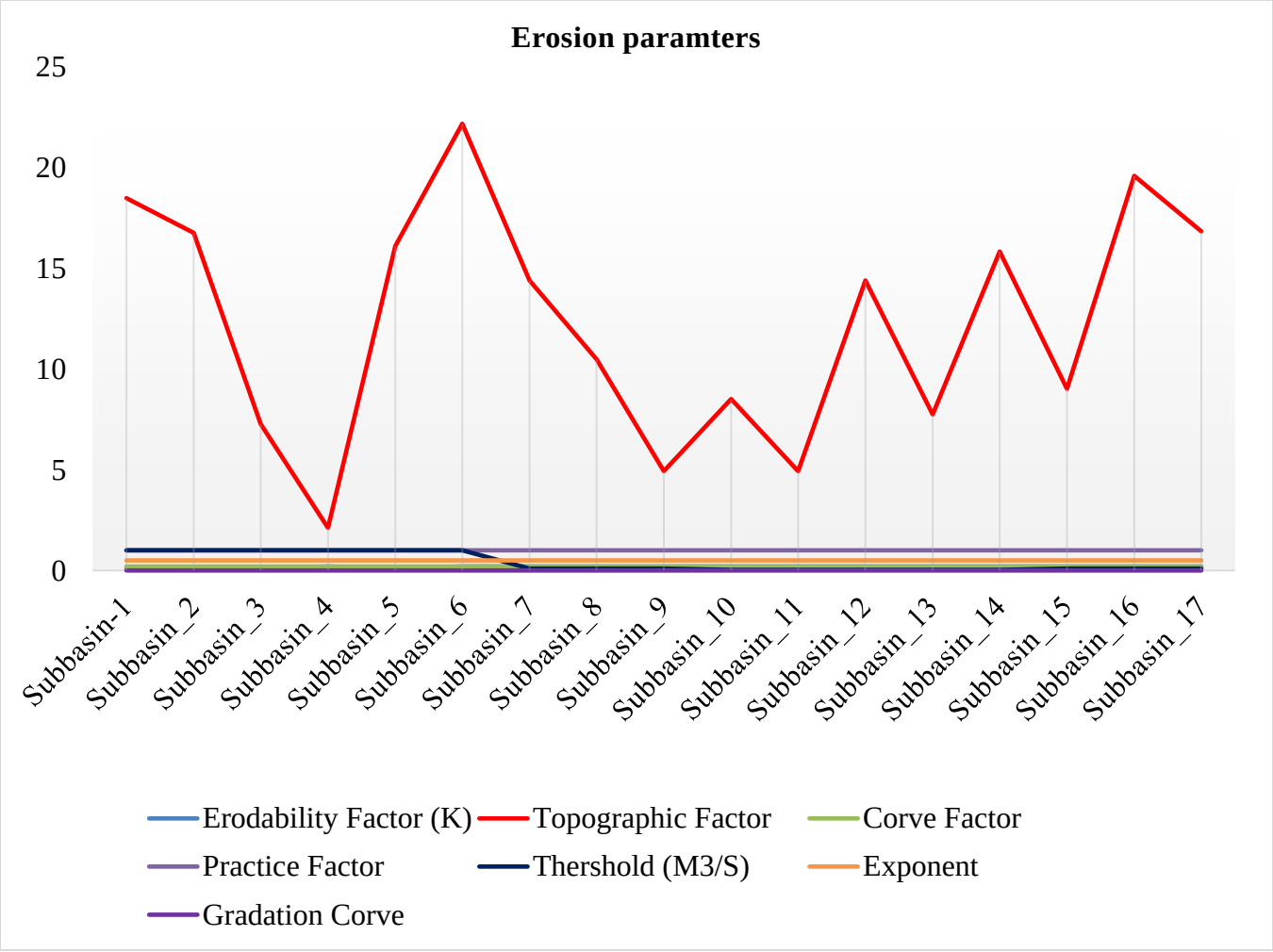

Figure 23: Erosion parameters

5.1.1. Sensitivity analysis of the Model

In this study sensitivity analysis of the model is being carried out on volume, Nash, and Peak with parameter change of ground water -1 fraction (GW1), ground water -2 fraction, coefficient, reservoir (GW2), time of concentration (TC), storage coefficient (SC), Muskingham K, Muskingham X. Sensitivity results are as showed in the (figure 24). It can be seen that Time of concentration and Storage coefficient and Muskingham X is the least sensitive parameters and the ground water -1 fraction (GW1), ground water -2 fraction, coefficient, reservoir (GW2), are the most sensitive parameters.

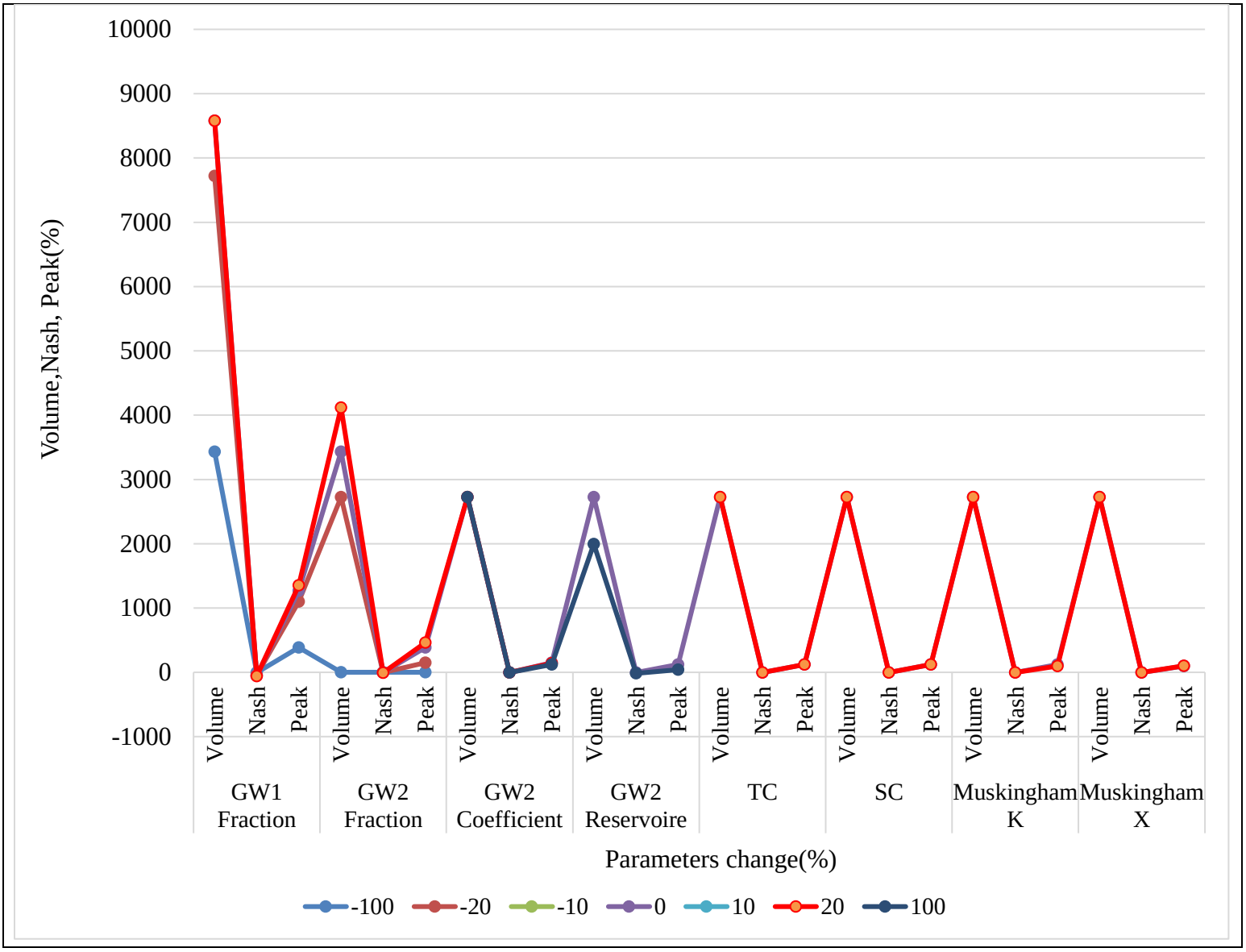

Figure 24: Sensitivity analysis of the model

5.2. Calibration (1990-2000)

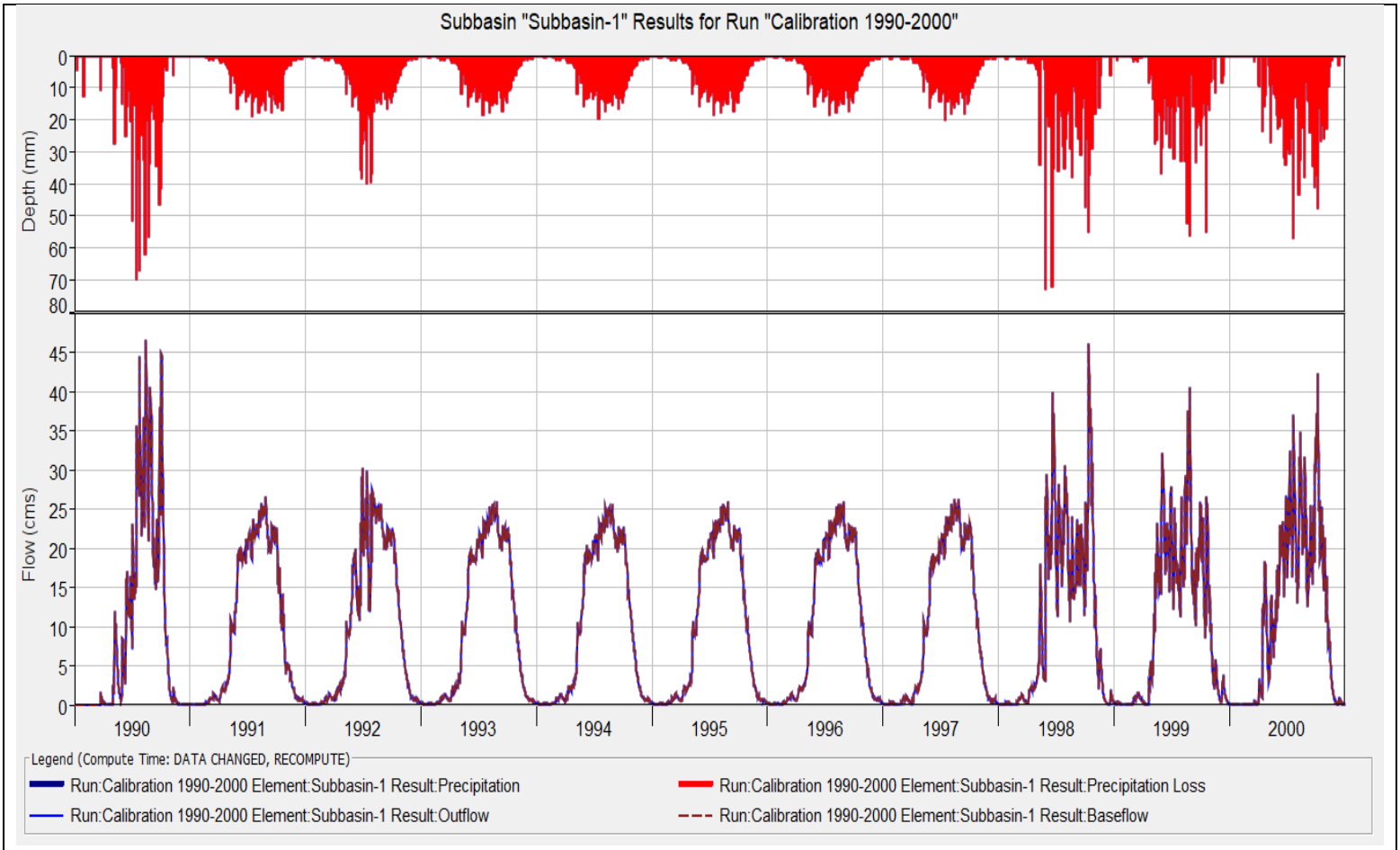

Figure 25. HEC-HMS Graph foe Sub-Basin-1 results for Run Calibration (1990-2000)

5.2.1. Analysis of Annual Calibration and Observed Flow Trends

Calibrated Flow value represents the average flow of water (in cubic meters per second, (m^3/s)) based on calibration or modeling. It indicates the expected flow based on calculations or simulations. **Observed Flow** value represents the actual observed flow of water (in cubic meters per second, (m^3/s)) in the natural environment. It reflects the real-world measurements taken from the field. Figure 24 and 26 shows that**, 1990 to 1994**: Both calibrated and observed flows show variations, but the observed flow tends to be lower than the calibrated flow. The difference between the two is more pronounced in some years (e.g., 1994). The observed flow (**1995 to 1997**) starts to increase significantly, surpassing the calibrated flow. This divergence suggests that natural

factors (e.g., climate, land use changes) are influencing the flow. The observed flow (**1998 to 2000**) continues to rise, reaching its peak in 2000. The calibrated flow also increases but remains slightly lower than the observed flow. Overall, the increasing trend in observed flow indicates changes in surface runoff, while the calibrated flow provides a reference based on modeling or historical data. The discrepancy between the two may be due to various factors affecting water availability and runoff patterns. Out flow, observed flow and residual flow found in appendix 10 for extra understanding.

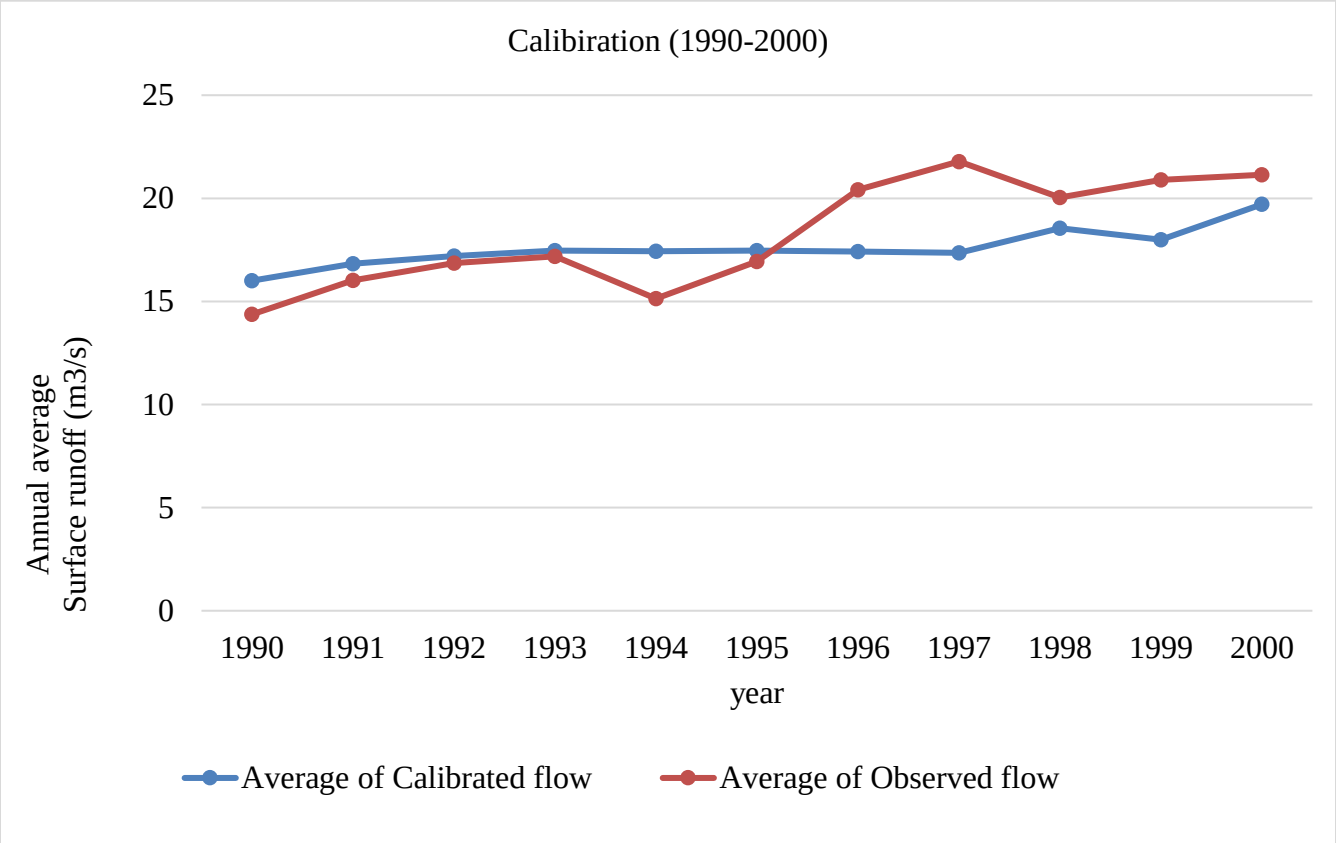

Figure 26: Annual average flow 1990-2000 calibration

5.2.2. Analysis of Monthly Calibration and Observed Flow Trends

The Figure 26, shown that of the calibration has been Monthly Variability**:** The lowest validated flow suggests minimal water availability in February (0.168 m^3/s). Cold temperatures and reduced precipitation likely contribute. **Augst (**41.96m^3/s**)**: The peak flow in Augst aligns with increased rainfall. Calibration flow informs water management decisions. It guides reservoir operations, irrigation planning, and environmental conservation efforts.

The Observed Flow reflects actual measurements on the ground. It considers natural variations, human interventions, and measurement errors: **August (**57.43 m^3/s**)**: The highest observed flow occurs in August. Monsoon rains, and seasonal factors contribute. However, discrepancies with calibrated flow raise questions. The lowest observed flow in February (2.198 m^3/s) indicates a dry season. Water scarcity during this period affects agriculture and ecosystems. The gap between calibrated and observed flow is crucial. Factors include: Human Interventions: Dams, diversions, and water withdrawals alter flow. Climate Change: Altered precipitation patterns impact both calibrated and observed flow. Accurate flow gauging is challenging, especially in remote areas. In summary, understanding the calibrated and observed flow variations across months is essential for effective water resource management, flood control, and ecological balance. Factors such as climate, topography, and human activities influence these flow dynamics, emphasizing the need for accurate monitoring and modeling.

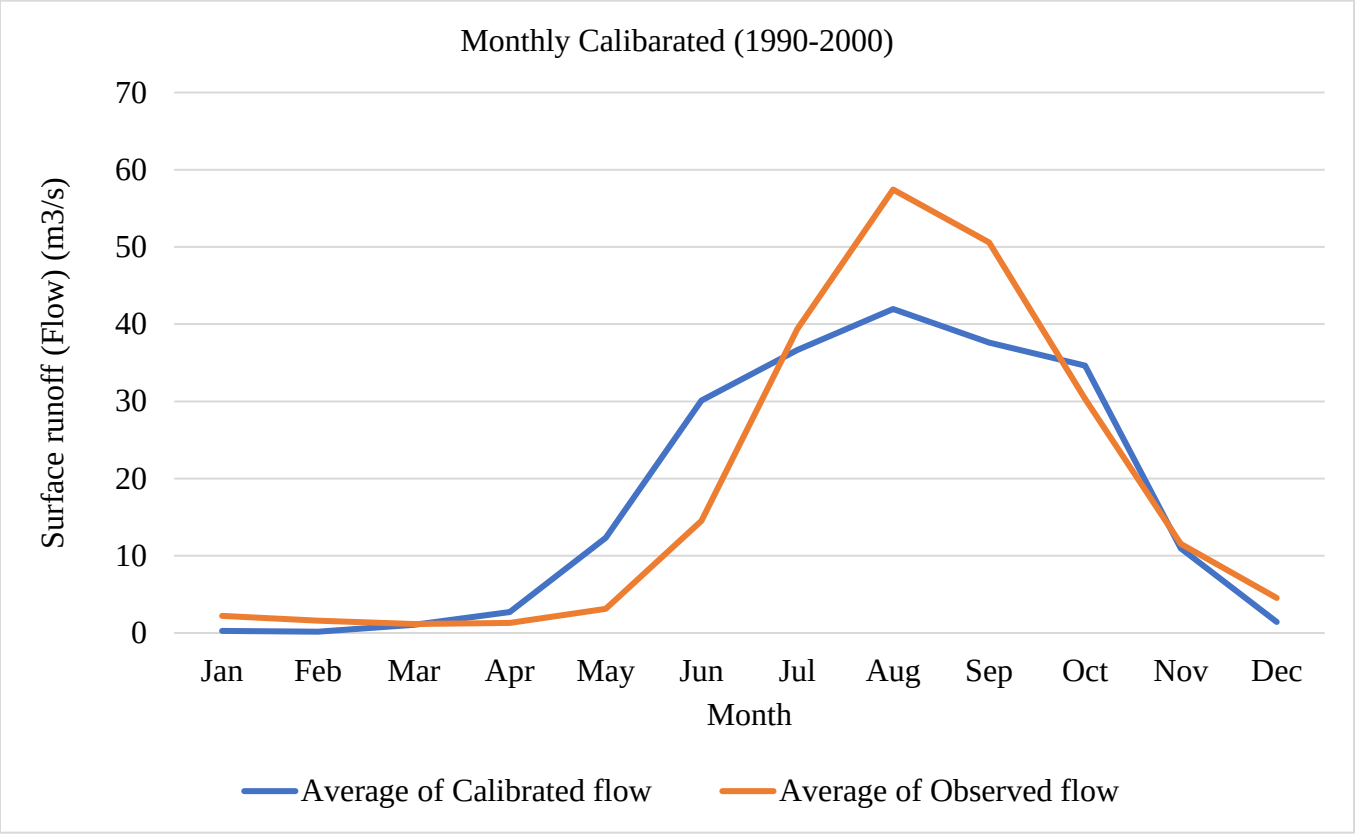

Figure 27: Monthly average flow 1990-2000 calibiration

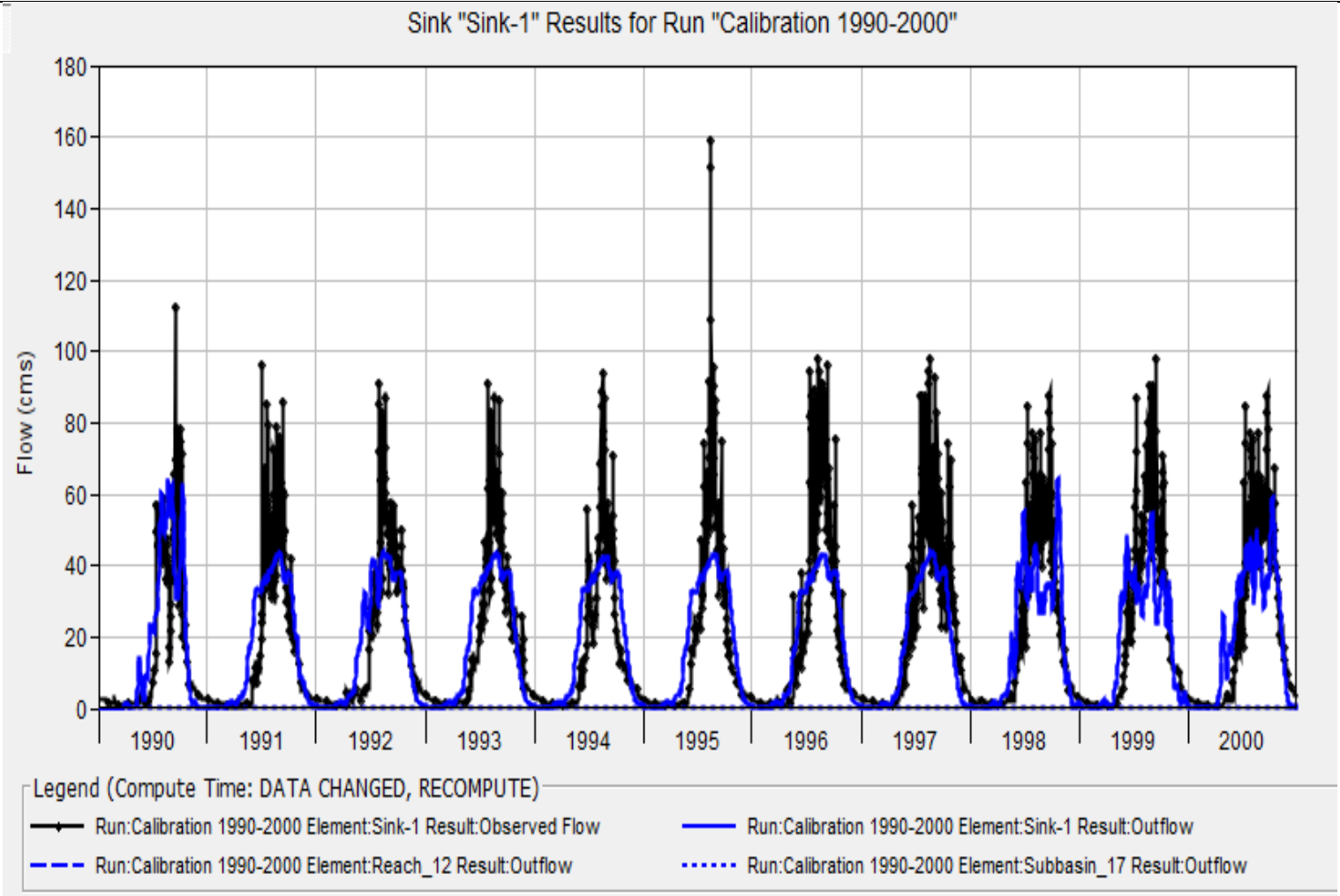

Figure 28. Calibration HEC_HMS Model Flow result from sinke (01 Jan 1990- 31 Dec 2000)

5.3. Validation (2001-1010)

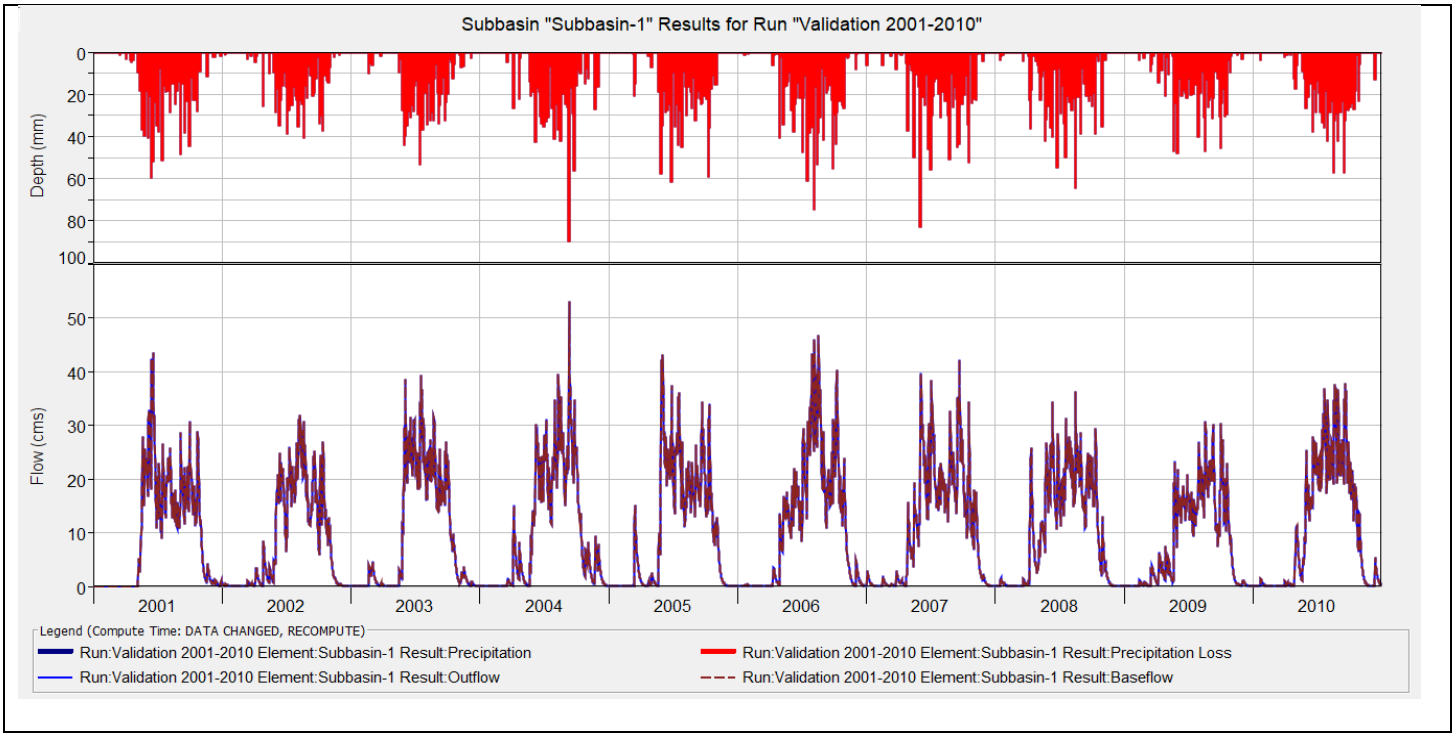

Figure 29. Graph for Sub-Basin-1 results for run Validation (2001-2010)

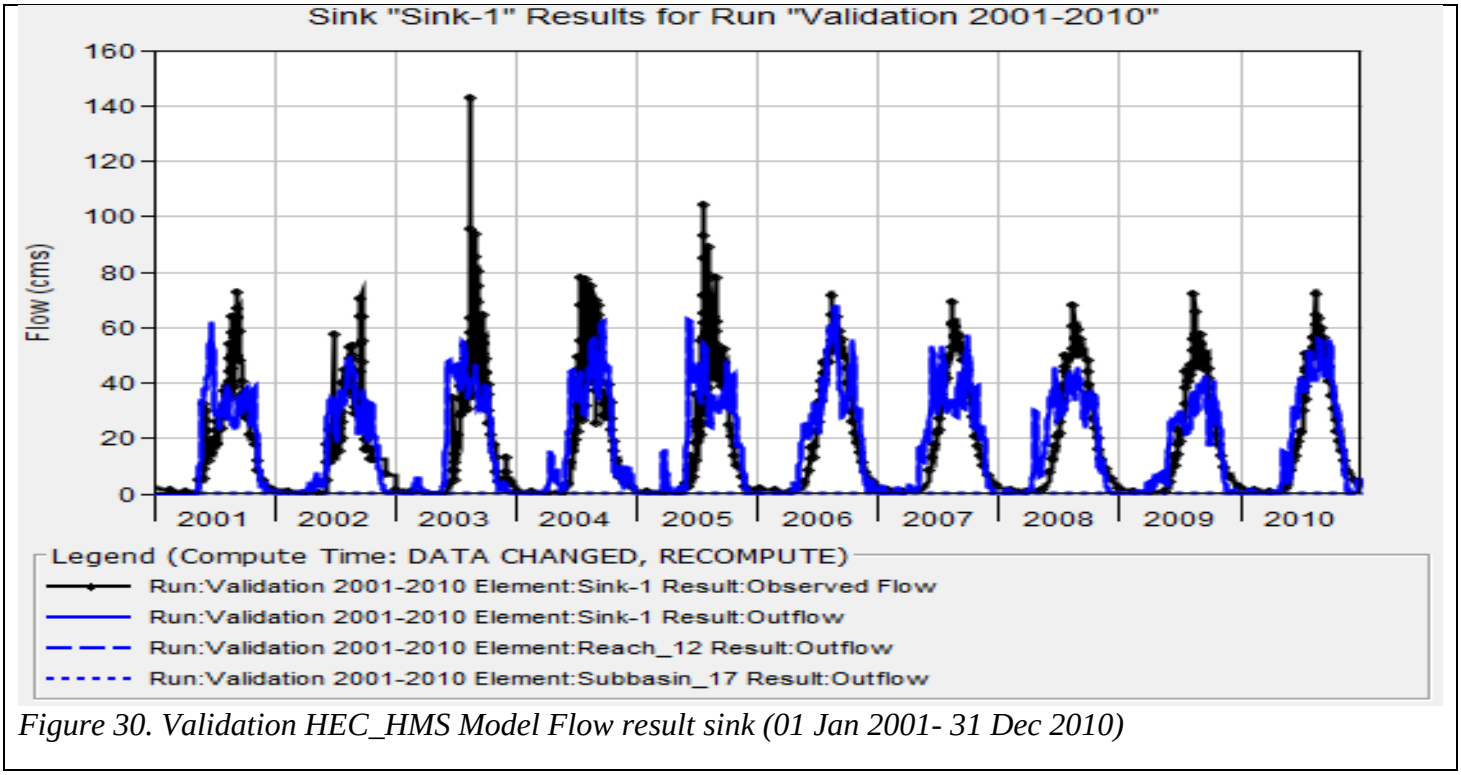

Figure 30. Validation HEC_HMS Model Flow result sink (01 Jan 2001- 31 Dec 2010)

4.4.1. Analysis of Annually Average Simulation and Observed Flow Trends

Water flow in rivers was a critical aspect of hydrological systems, impacting ecosystems, soil erosion, agriculture, and human settlements. Monitoring and understanding river flow patterns are essential for effective water resource management. In this study, we explore the trends in validated and observed flow data over the past decade.

Validated Flow refers to flow estimates obtained through rigorous modeling and calibration against ground measurements. These estimates are based on hydrological models and historical data. Observed Flow represents actual measurements collected from river gauges or other monitoring stations. These measurements provide direct information about the water flow. Overall, the validated and observed flow values exhibit a reasonable level of consistency. However, some variations exist, which warrant further investigation. Both validated and observed flows show annual fluctuations Figure 28 and 29. For instance:

- In 2006, the validated flow reached a peak of 19.39, indicating higher water availability and precipitation.
- Conversely, 2009 witnessed lower flows, with a validated average of 14.18.
- In 2006 and 2010, the observed flow reached a peak of 17.49 and 17.52 m^3/s, respectively. The overall overserved peak flow and lower flow is slightly variation.

Notably, the observed flow tends to be slightly lower than the validated flow in most years. This discrepancy could be attributed to factors such as measurement errors, unaccounted inflows, or changes in land use. Climate variability plays a significant role. Extreme weather events, and precipitation levels impact river flow. The observed flow may capture short-term variations missed by the validated model. Anthropogenic activities, such as dam construction, irrigation, and water withdrawals, can alter river flow. These interventions may not always be adequately accounted for in validated models. Spatial Considerations is essential to analyze flow trends at specific river segments or catchment areas. Local factors, such as topography and land cover, influence flow dynamics. The interplay between validated and observed flow data is crucial for sustainable water management. By integrating these approaches, we can better address the challenges posed by changing hydrological conditions.

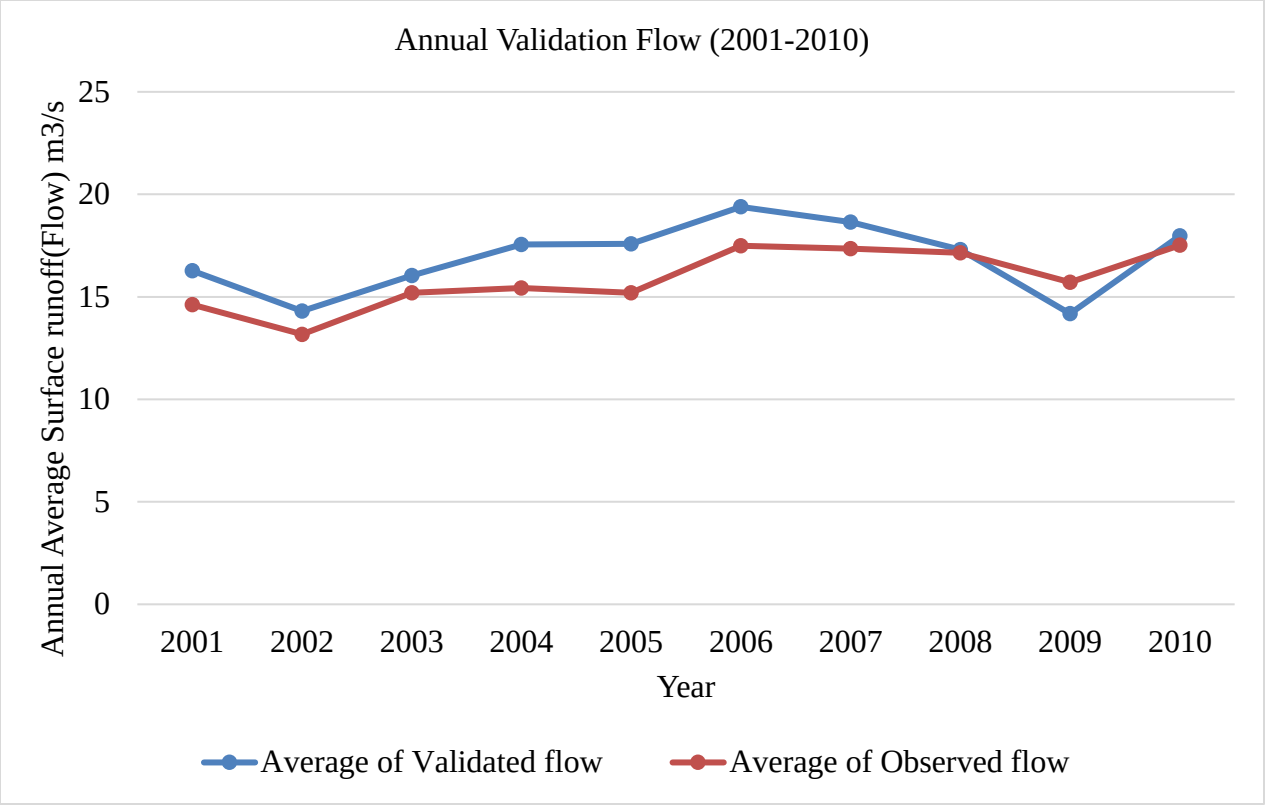

Figure 31:Annual Average of simulated and Observed flow

4.4.2. Analysis of Monthly Flow Data: Simulation vs. Observed

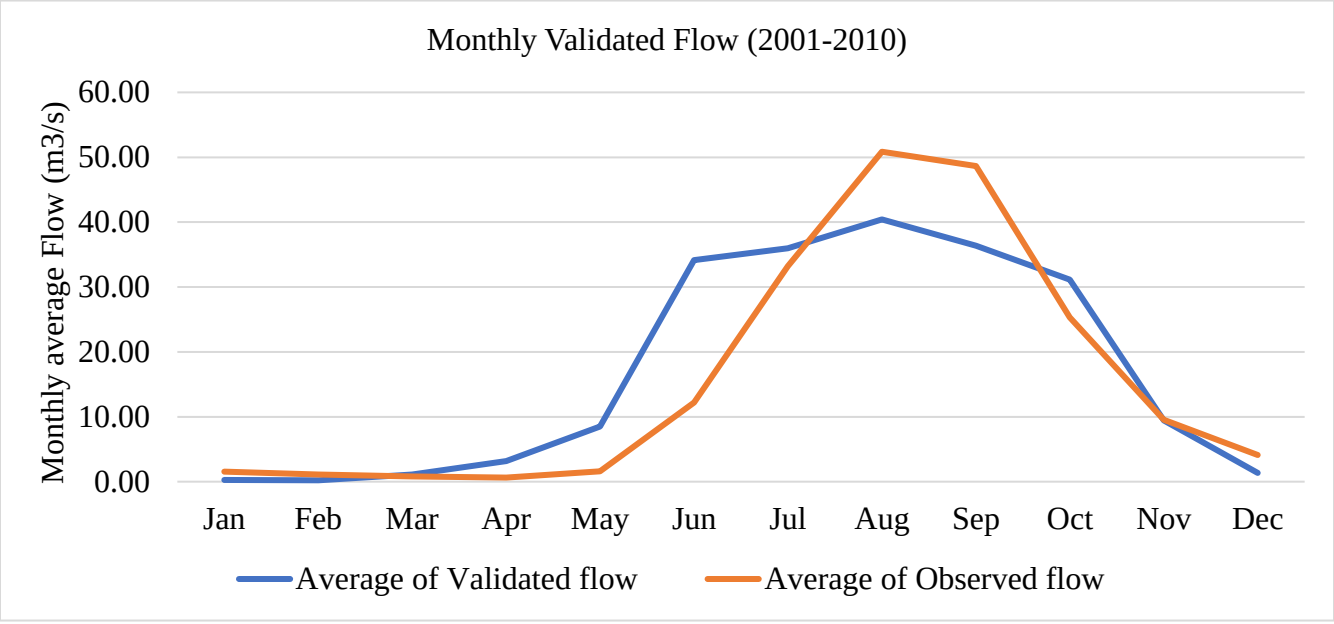

Figure 32: Monthly Average of Simulated and Observed flow

The Validated Flow represents the scientifically calculated flow based on models, historical data, and rigorous measurements. The Figure 31, result of the validation has been Monthly Variability**: January (0.2509)**: The lowest validated flow suggests minimal water availability. Cold temperatures and reduced precipitation likely contribute. The peak flow in Augst **(40.419)** aligns with increased rainfall. Validated flow informs water management decisions. It guides reservoir operations, irrigation planning, and environmental conservation efforts. Hydrologists use complex models to simulate flow under different scenarios.

The Observed Flow reflects actual measurements on the ground. It considers natural variations, human interventions, and measurement errors: **August (50.85)**: The highest observed flow occurs in August. Monsoon rains, and seasonal factors contribute. **April (0.631)**: The lowest observed flow in April indicates a dry season. Water scarcity during this period affects agriculture and ecosystems. The gap between validated and observed flow is crucial. Factors include: Human Interventions: Dams, diversions, and water withdrawals alter flow. Climate Change: Altered precipitation patterns impact both validated and observed flow. Accurate flow gauging is challenging, especially in remote areas. Understanding discrepancies helps ensure water security. Sustainable water use requires reconciling theoretical models with real-world observations.

4.5. Erosion Rate across Sub-Basin A Decades of Transformation

Erosion, the gradual wearing a way of land surfaces by natural forces, is a critical environmental phenomenon. Understanding erosion rates in Dura watershed is essential for sustainable land management and conservation efforts. In this study, we delve into the erosion rates observed in various sections (SB1 to SB17) over the years 1993, 2003, and 2010 (Figure 32). By analyzing these data points, we gain insights into the changing landscape and the impact of environmental factors. The erosion rates, expressed in tone per year, provide a quantitative measure of how much material is lost from specific sections.

Across all SB 1 to SB17 erosion rates have generally increased over the decade (Figure 32). In 1993, SB1 experienced an erosion rate of 4.56 t/yr. By 2010, this rate had more than doubled to 11.76 t ha/yr. This significant change suggests intensified environmental processes affecting this section. SB2 also witnessed a substantial increase, from 8.27 t/yr in 1993 to 10.79 t/yr in 2010.

The upward trend indicates heightened vulnerability. SB3 to SB17: Similar patterns emerge in other sections. For instance:

- SB3: 2.15 t/yr (1993) → 2.87 t/yr (2010)
- SB4: 2.37 t/yr (1993) → 3.46 t/yr (2010)
- SB5: 0.55 t/yr (1993) → 0.71 t/yr (2010)

Several factors contribute to erosion rates in the Dura watershed: Increased precipitation, extreme weather events, and temperature fluctuations impact erosion. Human activities, such as deforestation, agriculture, and construction, alter landscapes. Urbanization and agricultural practices likely play a role in the accelerated erosion rates. Vegetation acts as a natural buffer against erosion. Reduced vegetation cover due to land clearing or disturbances can exacerbate erosion.

The escalating erosion rates have implications for: Soil Health: Erosion depletes fertile topsoil, affecting agricultural productivity. Landscape Stability: Increased erosion threatens infrastructure, habitats, and ecosystems.

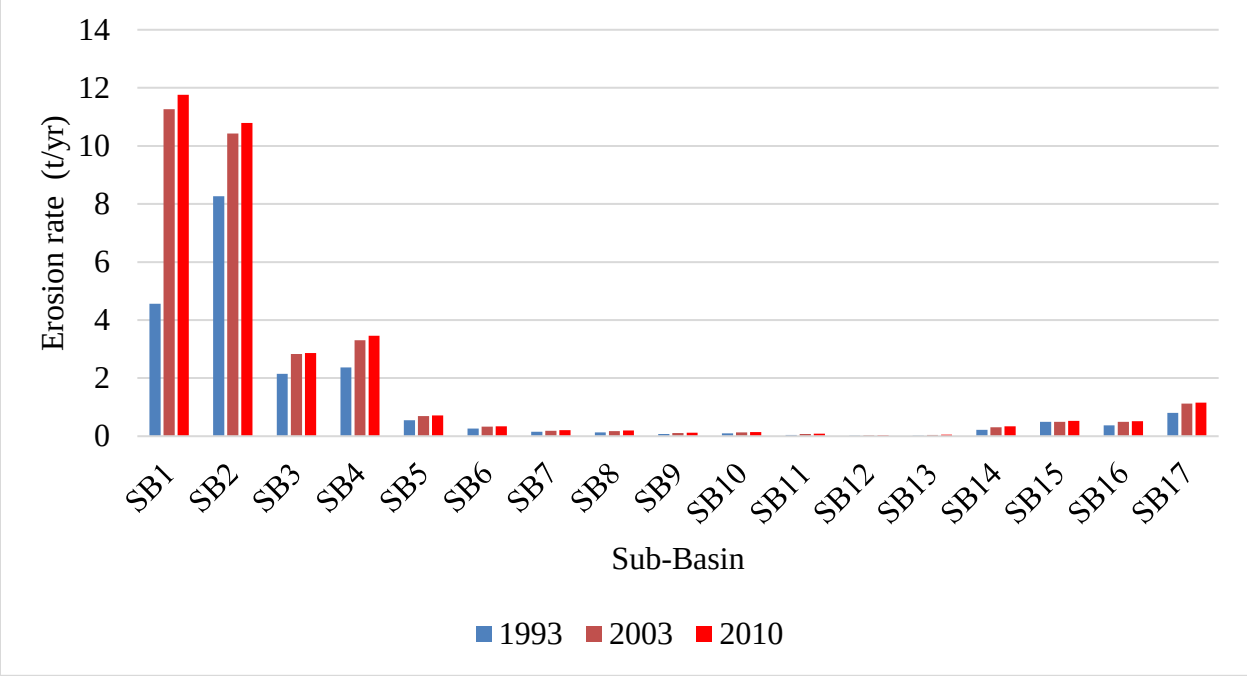

Figure 33: Erosion Rate across Sub-Basin a Three Decades of Transformation

4.5.1. Trends of sediment yield from the catchments of the watershed

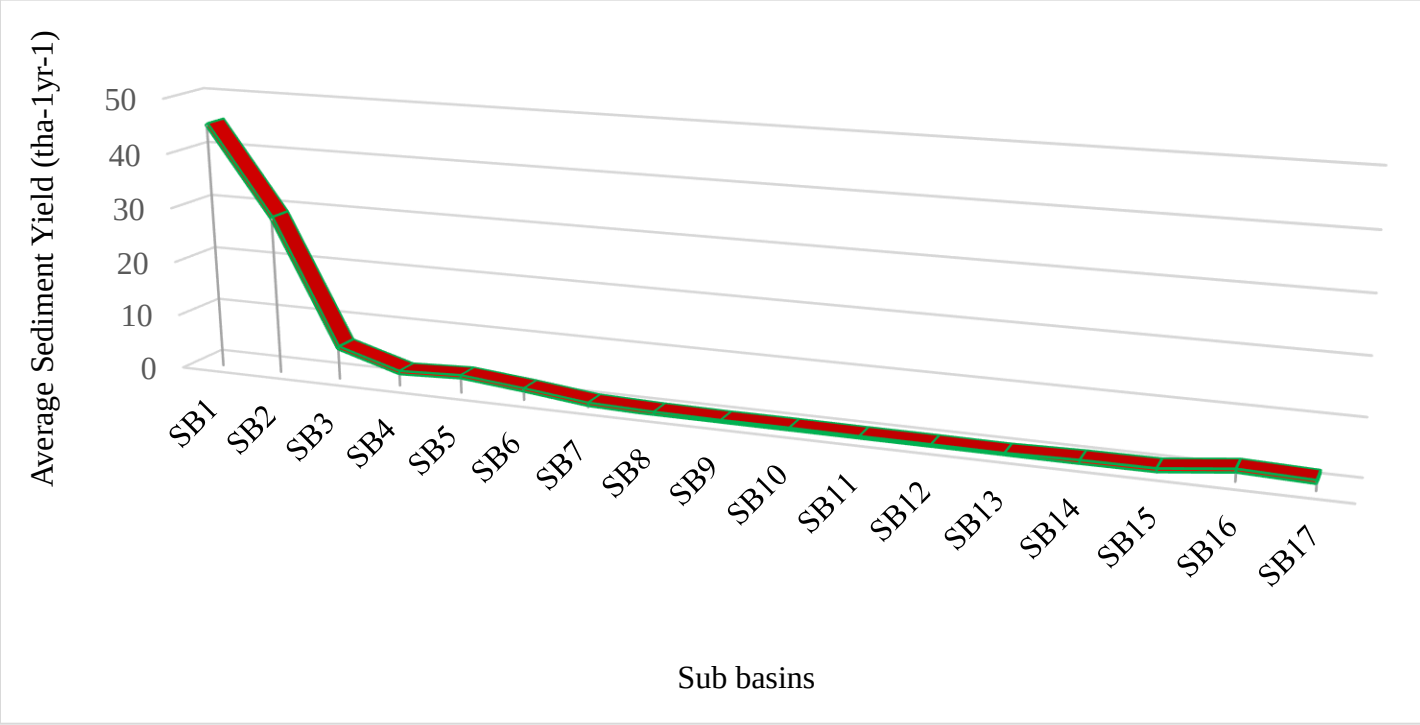

*Figure 34: Average Sediment Yield each Sub-Watershed (*t ha-*1yr-1)*

The sediment yield data for the sub-basins of the Dura watersheds shows in Figure 34 a distinct downward trend as we move from SB1 to SB17. SB1 has the highest sediment yield at 45.16 tha-1yr-1, indicating a potentially high rate of erosion or other geological activity. There is a significant drop from SB1 to SB2, and the trend continues to decline, with SB3 yielding only 5.81 tha-1yr-1. The lowest sediment yields are observed in the latter sub-basins, with SB13 at 0.0306 tha-1yr-1, suggesting lower erosion rates or more stable conditions. The overall pattern suggests that the upper sub-basins may be experiencing more intense sediment transport processes compared to the lower ones. This trend analysis could be useful for watershed management and conservation efforts, as it highlights areas that may require more attention due to higher sediment yields.

4.5.2. Prioritize and rank sub-Basin for appropriate management intervention

Table 144: Priority class for watershed management

Sub basin	Average Sediment load(tha-1yr-1)	Severity class	Priority Class	Source
SB1	45.15769087	Severe[1]	II	(Alemu Beyene et al., 2020) (Bewket and Teferi, 2009)
SB2	28.90020381	High [2]	IV	
SB3	5.808173625	Low [3]	VI	
SB4	2.425760807	Very low[4]		
SB5	2.929677663	Very low		
SB6	1.824373513	Very low		
SB7	0.521091928	Very low		
SB8	0.218905504	Very low		
SB9	0.115809254	Very low		
SB10	0.137659708	Very low		
SB11	0.074376977	Very low		
SB12	0.077622915	Very low		
SB13	0.030677604	Very low		
SB14	0.308114491	Very low		
SB15	0.382443168	Very low		
SB16	1.813986857	Very low		
SB17	1.446216539	Very low		

Table 14 The average sediment load in tone per hectare per year for each sub-basin in Dura watershed.

The table 14 shows the average sediment load in tons per hectare per year for each sub-basin. The highest sediment load is for **SB1** with **45.16** tons per hectare per year, and the lowest sediment load is for **SB13** with **0.03** tons per hectare per year. Based on the sediment load, it is possible to prioritize and rank sub-catchments for appropriate management intervention. The sub-basins with high sediment loads are more prone to soil erosion and high to severe Soil erosion risk and require immediate attention (Figure 34). Therefore, **SB1** with the highest sediment load should be prioritized for management intervention. Similarly, **SB2** with a sediment load of **28.90** tons per hectare per year and **SB3** with a sediment load of **5.81** tons per hectare per year should also be considered for management intervention. On the other hand, **SB 5_SB 17** with the lowest sediment

[1] Erosion rate >30 tha-1yr-1(Alemu et al, 2020; Bewket and Teferi, 2009)
[2] Erosion rate 18-30 tha-1yr-1(Alemu et al, 2020; Bewket and Teferi, 2009)
[3] Erosion rate 5-10 tha-1yr-1(Alemu et al, 2020; Bewket and Teferi, 2009)
[4] Erosion rate <5 tha-1yr-1(Alemu et al, 2020; Bewket and Teferi, 2009)

load requires less attention. This means those sub-basins have a low erosion risk rate in the Watershed.

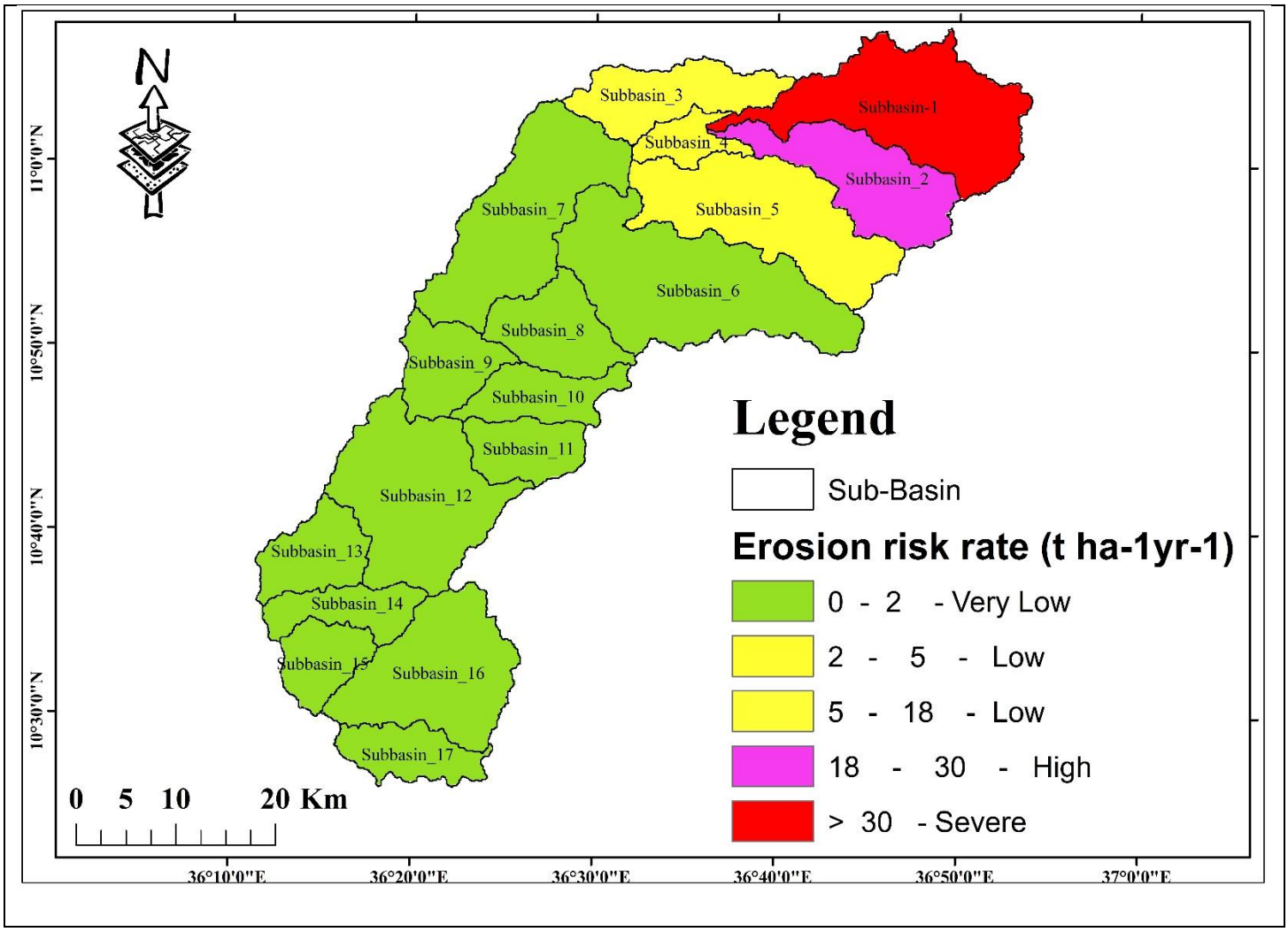

Figure 35: Erosion risk map of Dura Watershed

CHAPTER FIVE

CONCULUSION AND RECOMMENDATIONS

5.1. Conclusion

The Dura watershed result shows the changes in the area of four land use land cover classes from 1993 to 2023.In the year of 2023 is the most dominant conservation year compare to other trends. The most notable trends are the significant increase in bush land and the drastic decrease in bare land. These changes might be related to the environmental, economic, and social factors that affect land use. The forest and agricultural land are more stable, but still subject to fluctuations. The forest area has shown a net increase over the years, indicating positive efforts towards afforestation and conservation. The bush land area has experienced significant changes with substantial increases over time. The agricultural land area has shown mixed trends with an initial increase followed by a decrease in recent years. The bare land area has consistently decreased over time.

The sensitivity analysis revealed that the HEC-HMS model in the Dura watershed is most sensitive to changes in groundwater parameters (GW1, GW2 coefficient), followed by the reservoir coefficient. Conversely, the model exhibited the least sensitivity to time of concentration (TC), storage coefficient (SC), and Muskingum X. These findings highlight the crucial role of accurately representing groundwater interactions and reservoir characteristics for reliable model simulations in the Dura watershed.

In the simulation, the surface runoff modeling results in the HEC-HMS model were found to be adequate for the Dura watershed. This adequacy is manifested in both the calibration (Nash-Sutcliffe Efficiency, RMSE, Percent Bias and R^2,) 64.2, 0.6 -3.66, and 64, daily and 80.8, 0.6, -3.66, 64 monthly values, respectively and validation ((Nash-Sutcliffe Efficiency, RMSE, Percent Bias and R^2,) phases 60.4, 0.6, 6.54, 62 daily and 63.8, 0.6, 6.54, 62 monthly values, respectively. The daily and monthly Nash values close to each other was indicate another parameter are more accurate. Among the given parameters, the ground water fraction (GWF), Muskingum K, and time of concentration exhibit sensitivity, while the others are less sensitive. As we reflect on the erosion rates documented over this decade, we recognize the urgency of addressing environmental challenges. Monitoring and proactive measures are essential to safeguard our planet's delicate

balance. Let this data serve as a call to action a reminder that our actions today shape the landscape for generations to come.

Based on the result of the model analysis of sediment loads across various sub-basins reveals critical insights for management intervention. Sub-basins with high sediment loads, such as **SB1** (45.16 tons per hectare per year), warrant immediate attention due to their susceptibility to soil erosion. Additionally, **SB2** (28.90 tons per hectare per year) and **SB3** (5.81 tons per hectare per year) should also be prioritized for management efforts to increase infiltration and reduce soil erosion. Conversely, **SB13**, with the lowest sediment load (0.03 tons per hectare per year), requires less intervention.

5.2. **Recommendations**

The analysis of the Dura watershed has revealed valuable insights into the relationship between land cover changes and soil erosion modeling. Based on these findings, several critical recommendations can be made to ensure the long-term sustainability of the watershed and its resources:

Continuous Monitoring: Erosion rates within the Dura watershed should be consistently monitored to understand shifting patterns and identify areas particularly susceptible to erosion. This will allow for proactive management strategies. Investing in long-term monitoring programs is crucial for tracking trends in erosion and evaluating the effectiveness of implemented management interventions. This data is essential for adapting strategies over time.

Targeted Approach: Management efforts should be prioritized based on the severity of erosion. Sub-basins experiencing higher erosion rates and sediment yield (e.g., SB1, SB2, SB3) should be the primary focus for intervention.

Implementation of Practices: Erosion control practices such as terracing, contour farming, and reforestation should be implemented in areas experiencing rapid erosion, particularly in sub-basins SB1, SB2, and SB3. These techniques can significantly reduce soil loss and promote land health. Promoting afforestation and re-vegetation efforts in vulnerable sub-basins, especially alongside areas with high erosion rates, will enhance land cover and decrease soil vulnerability.

Sustainable Practices and Education: Encouraging land management practices like crop rotation and promoting soil conservation techniques among farmers and landowners is crucial for long-term sustainability. Educational programs can raise awareness about the importance of soil conservation within local communities. Collaborative Efforts: Erosion prevention efforts require the involvement of all stakeholders. Empowering stakeholders through participation and fostering collaboration are essential for effective action.

Research and Innovation: Investing in research to explore innovative erosion control methods can pave the way for future advancements in sustainable land management. Urgent Intervention: Sub-basins SB1, SB2, and SB3 require immediate attention. Implementing erosion control measures, stabilizing vulnerable areas, and preventing further sediment loss are critical steps to address the most pressing concerns.

Generally, these recommendations address the root causes of erosion and propose a multi-pronged approach. By prioritizing areas facing the greatest risks, implementing appropriate erosion control measures, and fostering a culture of sustainable land management, the long-term health and productivity of the Dura watershed can be secured. Continuous monitoring and research will ensure adaptability and the ongoing success of these efforts.

References

Abiye, W. (2022). Soil and Water Conservation Nexus Agricultural Productivity in Ethiopia. *Advances in Agriculture*, *2022*. https://doi.org/10.1155/2022/8611733

Addis, H. K., & Klik, A. (2015). Predicting the spatial distribution of soil erodibility factor using USLE nomograph in an agricultural watershed, Ethiopia. *International Soil and Water Conservation Research*, *3*(4), 282–290. https://doi.org/10.1016/j.iswcr.2015.11.002

Adhikari, P. (2020). *Application of HEC-HMS to the investigation of soil erosion and sediment yield by surface runoff*.

Ahmed, A. A., & Ismail, U. H. A. E. (2008). Sediment in the Nile River System. *Consultancy Study Requested by UNESCO*, *January*, 93 pp.

Alemayehu, B. (2015). *Gis And Remote Sensing Based Land Use/Land Cover Change Detection And Prediction In Fagita Lekoma Woreda, Awi Zone, North Western Ethiopia*. 85. https://doi.org/10.1371/journal.pone.0265071

Alemu, B. (2015). *The Effect of Land Use Land The Effect of Land Use Land Cover Change on Land Degradation in the Highlands of Ethiopia*. *5*(January 2015), 1–13. www.iiste.org

Alemu Beyene. (2023). *Soil erosion risk assessment in the Chaleleka wetland watershed, Central Rift Valley of Ethiopiantral Rift Valley of Ethiopia*.

Alemu Beyene Woldesenbet, Sebsebe Demisew Wudmatas. (2020). Enset-based land use land cover change detection and its impact on soil erosion in Meki river watershed, Western Lake Ziway Sub-Basin, Central Rift Valley of Ethiopia. *Environmental Systems Research*, *9*(1). https://doi.org/10.1186/s40068-020-00198-x

Ali, (2014). *The Impact of Soil Erosion in the Upper Blue Nile on Downstream Reservoir Sedimentation*.

Ananda, J., & Herath, G. (2003). Soil erosion in developing countries: A socio-economic appraisal. *Journal of Environmental Management*, *68*(4), 343–353. https://doi.org/10.1016/S0301-4797(03)00082-3

Andreev, D. V. (2020). The use of GIS technology in modern conditions. *IOP Conference Series: Earth and Environmental Science*, *421*(4). https://doi.org/10.1088/1755-1315/421/4/042001

Aneseyee, A. B., Elias, E., Soromessa, T., & Feyisa, G. L. (2020). Land use/land cover change effect on soil erosion and sediment delivery in the Winike watershed, Omo Gibe Basin, Ethiopia. *Science of the Total Environment*, *728*, 1–9. https://doi.org/10.1016/j.scitotenv.2020.138776

Arekhi, S., & Niazi, Y. (2012). *Soil erosion and sediment yield modeling using RS and GIS techniques : a case study , Iran*. 285–296. https://doi.org/10.1007/s12517-010-0220-4

Balabathina, V. N., Raju, R. P., Mulualem, W., & Tadele, G. (2020). Estimation of soil loss using remote sensing and GIS-based universal soil loss equation in northern catchment of

Lake Tana Sub-basin, Upper Blue Nile Basin, Northwest Ethiopia. *Environmental Systems Research*, *9*(1), 1–37. https://doi.org/10.1186/s40068-020-00203-3

Balasubramanian, A. (2017). Soil Erosion- Causes and Effects Soil Erosion – Causes and Effects By Prof . A . Balasubramanian Centre for Advanced Studies in Earth Science , University of Mysore , Mysore. *Centre for Advanced Studies in Earth Science*, *March*, 7. https://doi.org/10.13140/RG.2.2.26247.39841

Baláž, M., Danáčová, M., & Szolgay, J. (2011). On the use of the Muskingum method for the simulation of flood wave movements. *Slovak Journal of Civil Engineering*, *18*(3), 14–20. https://doi.org/10.2478/v10189-010-0012-6

Banasik, K., & Walling, D. E. (1996). Predicting sedimentgraphs for a small agricultural catchment. *Nordic Hydrology*, *27*(4), 275–294. https://doi.org/10.2166/nh.1996.0010

Barakat, A., Rafai, M., Mosaid, H., Islam, M. S., & Saeed, S. (2023). Mapping of Water-Induced Soil Erosion Using Machine Learning Models: A Case Study of Oum Er Rbia Basin (Morocco). *Earth Systems and Environment*, *7*(1), 151–170. https://doi.org/10.1007/s41748-022-00317-x

Barnett, V., Neter, J., & Wasserman, W. (1975). Applied Linear Statistical Models. In *Journal of the Royal Statistical Society. Series A (General)* (Vol. 138, Issue 2). https://doi.org/10.2307/2984653

Bartolini, S., Mecocci, A., Pozzebon, A., Zoppetti, C., Bertoni, D., Sarti, G., Caiti, A., Costanzi, R., Catani, F., Ciampalini, A., & Moretti, S. (2018). Augmented virtuality for coastal management: A holistic use of in situ and remote sensing for large scale definition of coastal dynamics. *ISPRS International Journal of Geo-Information*, *7*(3), 1–27. https://doi.org/10.3390/ijgi7030092

Bekele, T. (2019). Effect of Land Use and Land Cover Changes on Soil Erosion in Ethiopia. *International Journal of Agricultural Science and Food Technology*, *5*, 026–034. https://doi.org/10.17352/2455-815x.000038

Berihun, M. L., Tsunekawa, A., Haregeweyn, N., Meshesha, D. T., Adgo, E., Tsubo, M., Masunaga, T., Fenta, A. A., Sultan, D., & Yibeltal, M. (2019). Exploring land use/land cover changes, drivers and their implications in contrasting agro-ecological environments of Ethiopia. *Land Use Policy*, *87*(May), 104052. https://doi.org/10.1016/j.landusepol.2019.104052

Bettina Schaefl and, H. V. G. (2010). Advanced Bash-Scripting Guide An in-depth exploration of the art of shell scripting Table of Contents. *Okt 2005 Abrufbar Uber Httpwww Tldp OrgLDPabsabsguide Pdf Zugriff 1112 2005*, *2274*(November 2008), 2267–2274. https://doi.org/10.1002/hyp

Bewket, W. (2007). Soil and water conservation intervention with conventional technologies in northwestern highlands of Ethiopia: Acceptance and adoption by farmers. *Land Use Policy*, *24*(2), 404–416. https://doi.org/10.1016/j.landusepol.2006.05.004

Bewket, W., & Sterk, G. (2005). Dynamics in land cover and its effect on stream flow in the Chemoga watershed, Blue Nile basin, Ethiopia. *Hydrological Processes*, *19*(2), 445–458.

https://doi.org/10.1002/hyp.5542

Bitew G. Tassew, Mulugeta A. Belete and K.Miege , (2019) *Hydrology*, *6*(1), 1–17. https://doi.org/10.3390/hydrology6010021

Borji, T. T. (2013). Sedimentation and Sustainability of Hydropower Reservoirs: Cases of Grand Ethiopian Renaissance Dam on the Blue Nile River in Ethiopia. *Master Theses*, *June*.

Bryan, R. B. (2000). Soil erodibility and processes of water erosion on hillslope. *Geomorphology*, *32*(3–4), 385–415. https://doi.org/10.1016/S0169-555X(99)00105-1

Chow, V. Te, Maidment, D. R., Mays, L. W., & Ven Te Chow, David R. Maidment, L. W. M. (1998). *Applied Hydrology Chow 1988.pdf* (pp. 1–294). http://ponce.sdsu.edu/Applied_Hydrology_Chow_1988.pdf

Demissie, T. A. (2022). Land use and land cover change dynamics and its impact on watershed hydrological parameters: the case of Awetu watershed, Ethiopia. *Journal of Sedimentary Environments*, *7*(1), 79–94. https://doi.org/10.1007/s43217-021-00084-1

Devi, R., Tesfahune, E., Legesse, W., Deboch, B., & Beyene, A. (2008). Assessment of siltation and nutrient enrichment of Gilgel Gibe dam, Southwest Ethiopia. *Bioresource Technology*, *99*(5), 975–979. https://doi.org/10.1016/j.biortech.2007.03.013

Dibaba, W. T., Demissie, T. A., & Miegel, K. (2020a). *Drivers and Implications of Land Use/Land Cover Dynamics in Finchaa Catchment, Northwestern Ethiopia*. 1–20.

Dibaba, W. T., Demissie, T. A., & Miegel, K. (2020b). Watershed hydrological response to combined land use/land cover and climate change in highland ethiopia: Finchaa catchment. *Water (Switzerland)*, *12*(6). https://doi.org/10.3390/w12061801

Dobos, E., Micheli, E., Baumgardner, M. F., Biehl, L., & Helt, T. (2000). Use of combined digital elevation model and satellite radiometric data for regional soil mapping. *Geoderma*, *97*(3–4), 367–391. https://doi.org/10.1016/S0016-7061(00)00046-X

Durán Zuazo, V. H., & Rodríguez Pleguezuelo, C. R. (2008). Soil-erosion and runoff prevention by plant covers. A review. *Agronomy for Sustainable Development*, *28*(1), 65–86. https://doi.org/10.1051/agro:2007062

Easton, Z. M., Fuka, D. R., White, E. D., Collick, A. S., Biruk Ashagre, B., McCartney, M., Awulachew, S. B., Ahmed, A. A., & Steenhuis, T. S. (2010). A multi basin SWAT model analysis of runoff and sedimentation in the Blue Nile, Ethiopia. *Hydrology and Earth System Sciences*, *14*(10), 1827–1841. https://doi.org/10.5194/hess-14-1827-2010

Ebabu, K., Taye, G., Tsunekawa, A., Haregeweyn, N., Adgo, E., Tsubo, M., Fenta, A. A., Meshesha, D. T., Sultan, D., Aklog, D., Admasu, T., van Wesemael, B., & Poesen, J. (2023). Land use, management and climate effects on runoff and soil loss responses in the highlands of Ethiopia. *Journal of Environmental Management*, *326*(PA), 116707. https://doi.org/10.1016/j.jenvman.2022.116707

Esa, E., Assen, M., & Legass, A. (2018). Implications of land use/cover dynamics on soil erosion potential of agricultural watershed, northwestern highlands of Ethiopia. *Environmental Systems Research*, *7*(1). https://doi.org/10.1186/s40068-018-0122-0

Eskandari Damaneh, H., Khosravi, H., Habashi, K., Eskandari Damaneh, H., & Tiefenbacher, J. P. (2022). The impact of land use and land cover changes on soil erosion in western Iran. *Natural Hazards*, *110*(3), 2185–2205. https://doi.org/10.1007/s11069-021-05032-w

Gashaw, T. (2015). Soil erosion in Ethiopia: Extent, Conservation Efforts and Issues of Sustainability. *Palgo J.Agriculture*, *2*(2), 38–48.

Gashaw, T., Dile, Y. T., Worqlul, A. W., Bantider, A., Zeleke, G., Bewket, W., & Alamirew, T. (2021). Evaluating the Effectiveness of Best Management Practices On Soil Erosion Reduction Using the SWAT Model: for the Case of Gumara Watershed, Abbay (Upper Blue Nile) Basin. *Environmental Management*, *68*(2), 240–261. https://doi.org/10.1007/s00267-021-01492-9

Gashaw, T., Tulu, T., & Argaw, M. (2017). Erosion risk assessment for prioritization of conservation measures in Geleda watershed , Blue Nile basin , Ethiopia. *Environmental Systems Research*, 1–15. https://doi.org/10.1186/s40068-016-0078-x

Girma Addisu. (2010). *HYDROGEOLOGICAL AND HYDROGEOCHEMICAL CHARACTERIATION OF BELES RIVER BASIN, NORTHWESTERN ETHIOPIA*.

Gomiero, T. (2016). *Soil Degradation , Land Scarcity and Food Security : Reviewing a Complex Challenge*. 1–41. https://doi.org/10.3390/su8030281

Hajigholizadeh, M., Melesse, A. M., & Fuentes, H. R. (2018). Erosion and sediment transport modelling in shallowwaters: A review on approaches, models and applications. *International Journal of Environmental Research and Public Health*, *15*(3). https://doi.org/10.3390/ijerph15030518

Hans Hurni, Solomon Abate , Amare Bantider, Berhanu Debele , Eva Ludi, Brigitte Portner, Birru Yitaferu, and G. Z. (1998). Analysing degradation and rehabilitation for sustainable land management in the highlands of Ethiopia. *Land Degradation and Development*, *9*(6), 529–542. https://doi.org/10.1002/(SICI)1099-145X(199811/12)9:6<529::AID-LDR313>3.0.CO;2-O

Haregeweyn, N., Tsunekawa, A., Nyssen, J., Poesen, J., Tsubo, M., Tsegaye Meshesha, D., Schütt, B., Adgo, E., & Tegegne, F. (2015). Soil erosion and conservation in Ethiopia: A review. *Progress in Physical Geography*, *39*(6), 750–774. https://doi.org/10.1177/0309133315598725

Haregeweyn, N., Tsunekawa, A., Poesen, J., Tsubo, M., Meshesha, D. T., Fenta, A. A., Nyssen, J., & Adgo, E. (2017). Comprehensive assessment of soil erosion risk for better land use planning in river basins: Case study of the Upper Blue Nile River. *Science of the Total Environment*, *574*, 95–108. https://doi.org/10.1016/j.scitotenv.2016.09.019

Hurni H, Berhe WA, Chadhokar P, Daniel D, Gete Z, Grunder M, K. G. (2016). Soil and Water Conservation in Ethiopia (Guidelines for Development Agents). Ministry of Agriculture (MoA). Ethiopia 2016. In *Journal of Soils and Sediments* (Vol. 1, Issue 2). https://doi.org/https://www.researchgate.net/publication/324274153 Soil

Ismail, H., Kamal, M. R., Mojid, M. A., Abdullah, A. F. Bin, & Hin, L. S. (2022). Loss methods in HEC-HMS model for streamflow projection under climate change: a review.

International Journal of Hydrology Science and Technology, *13*(1), 23. https://doi.org/10.1504/IJHST.2022.119234

Jeevika and, & Jagritee. (2018). Rainfall-Runoff Simulation and Modelling Using HEC-HMS and HEC-RAS Models : Case Studies from Nepal and Sweden. *Lund University*, 1–69. www.tvrl.lth.se

Jemal, K. (2021). Review of Soil Erosion Risk For Soil and Water Conservation Planning Under Ethiopian Condition Agrotechnology. *Agrotechnology*, *10*(2168–9881), 11.

Jr, J. A., & Denil, M. (2006). Cartographic Perspectives. *… Perspectives*, *58*(44), 2001–2002. http://makingmaps.owu.edu/cp/cp53.pdf#page=2

Juraj M. and, & P., S. (2004). Calibration, verification and sensitivity analysis of HEC-HMS Model. In *Computer* (Issue August).

Kebede Wolka1*, Habitamu Tadesse1, E. G. and F. Y. (2015). Soil erosion risk assessment in the Chaleleka wetland watershed, Central Rift Valley of Ethiopia. *Environmental Systems Research*, *4*(1), 1–12. https://doi.org/10.1186/s40068-015-0030-5

Kgaphola, M. J., Ramoelo, A., Odindi, J., Mwenge Kahinda, J.-M., Seetal, A. R., & Musvoto, C. (2023). Impact of land use and land cover change on land degradation in rural semi-arid South Africa: case of the Greater Sekhukhune District Municipality. *Environmental Monitoring and Assessment*, *195*(6), 710. https://doi.org/10.1007/s10661-023-11104-0

Kidane, D., & Alemu, B. (2018). *The Effect of Upstream Land Use Practices on Soil Erosion and Sedimentation in the Upper Blue Nile Basin , Ethiopia*. *January 2015*.

Kidane, M., Bezie, A., Kesete, N., & Tolessa, T. (2019). The impact of land use and land cover (LULC) dynamics on soil erosion and sediment yield in Ethiopia. *Heliyon*, *5*(12), e02981. https://doi.org/10.1016/j.heliyon.2019.e02981

Kum, G., Sönmez, M., & Kargın, A. (2022). An Alternative Process for Determining Erosion Risk: The Fuzzy Method. *Coğrafya Dergisi / Journal of Geography*, *44*, 219–229. https://doi.org/10.26650/JGEOG2022-1058416

Kumarasinghe, U. (2021). A review on new technologies in soil erosion management. *Journal of Research Technology and Engineering*, *2*(1), 120–127.

Landau, S., Mitchell, R. A. C., Barnett, V., Colls, J. J., Craigon, J., & Payne, R. W. (2000). A parsimonious, multiple-regression model of wheat yield response to environment. *Agricultural and Forest Meteorology*, *101*(2–3), 151–166. https://doi.org/10.1016/S0168-1923(99)00166-5

Lisle, I. G., Sander, G. C., Parlange, J.-Y., Rose, C. W., Hogarth, W. L., Braddock, R. D., Stagnitti, F., Lockington, D. A., Jomaa, S., Cheraghi, M., & Barry, D. A. (2017). Transport Time Scales in Soil Erosion Modeling. *Vadose Zone Journal*, *16*(12), 1–13. https://doi.org/10.2136/vzj2017.06.0121

Majoro, F., Wali, U. G., Munyaneza, O., Naramabuye, F.-X., & Mukamwambali, C. (2020). On-site and Off-site Effects of Soil Erosion: Causal Analysis and Remedial Measures in Agricultural Land - a Review. *Rwanda Journal of Engineering, Science, Technology and*

Environment, *3*(2), 1–19. https://doi.org/10.4314/rjeste.v3i2.1

Manson, S. M., Burrough, P. A., & McDonnell, R. A. (1999). Principles of Geographical Information Systems: Spatial Information Systems and Geostatistics. *Economic Geography*, *75*(4), 422. https://doi.org/10.2307/144481

Mekuria, W., Veldkamp, E., Haile, M., Gebrehiwot, K., Muys, B., & Nyssen, J. (2009). Effectiveness of exclosures to control soil erosion and local community perception on soil erosion in Tigray, Ethiopia. *African Journal of Agricultural Research*, *4*(4), 365–377.

Meshesha, D. T., Tsunekawa, A., Tsubo, M., & Haregeweyn, N. (2012). Dynamics and hotspots of soil erosion and management scenarios of the Central Rift Valley of Ethiopia. *International Journal of Sediment Research*, *27*(1), 84–99. https://doi.org/10.1016/S1001-6279(12)60018-3

Mewded, M., Abebe, A., Tilahun, S., & Agide, Z. (2021). Impact of land use and land cover change on the magnitude of surface runoff in the endorheic Hayk Lake basin, Ethiopia. *SN Applied Sciences*, *3*(8). https://doi.org/10.1007/s42452-021-04725-y

Mosbahi, M., Benabdallah, S., & Boussema, M. R. (2013). Assessment of soil erosion risk using SWAT model. *Arabian Journal of Geosciences*, *6*(10), 4011–4019. https://doi.org/10.1007/s12517-012-0658-7

Nachtergaele, F., Velthuizen, H. Van, & Verelst, L. (2008). Harmonized world soil database. *Food and Agriculture …*, *May 2014*, 43. http://www.fao.org/nr/Water/docs/Harm-World-Soil-DBv7cv.pdf

Negese, A. (2021). Impacts of Land Use and Land Cover Change on Soil Erosion and Hydrological Responses in Ethiopia. *Proceedings of the National Academy of Sciences*, *2021*(11), 10. https://doi.org/10.1073/pnas.96.11.5995

Nejadhashemi, A. P., Shen, C., Wardynski, B. J., & Mantha, P. S. (2010). Evaluating the impacts of land use changes on hydrologic responses in the agricultural regions of Michigan and Wisconsin. *American Society of Agricultural and Biological Engineers Annual International Meeting 2010, ASABE 2010*, *3*, 2091–2119. https://doi.org/10.13031/2013.31927

PU I, A O C I E., & M.M., M. (2017). Soil Erosion: A Review of Models and Applications. *International Journal of Advanced Engineering Research and Science*, *4*(12), 138–150. https://doi.org/10.22161/ijaers.4.12.22

Pak, B, Ramos, K., Fleming, M., Scharffenberg, W. Gibson, (2015). Sensitivity Analysis For Sediment Transport In The Hydrologic Modeling System (Hec-Hms). 2013(December 2013).

Pandey, A., Himanshu, S. K., Mishra, S. K., & Singh, V. P. (2016). Physically based soil erosion and sediment yield models revisited. *Catena*, *147*, 595–620. https://doi.org/10.1016/j.catena.2016.08.002

Pandey, S., Kumar, P., Zlatic, M., Nautiyal, R., & Panwar, V. P. (2021). Recent advances in assessment of soil erosion vulnerability in a watershed. *International Soil and Water Conservation Research*, *9*(3), 305–318. https://doi.org/10.1016/j.iswcr.2021.03.001

Ramakrishnan, D., Bandyopadhyay, A., & Kusuma, K. N. (2009). SCS-CN and GIS-based approach for identifying potential water harvesting sites in the Kali Watershed, Mahi River Basin, India. *Journal of Earth System Science*, *118*(4), 355–368. https://doi.org/10.1007/s12040-009-0034-5

Rhodes, C. J. (2014). Soil erosion, climate change and global food security: Challenges and strategies. *Science Progress*, *97*(2), 97–153. https://doi.org/10.3184/003685014X13994567941465

Sahu, M. K., Shwetha, H. R., & Dwarakish, G. S. (2023). State-of-the-art hydrological models and application of the HEC-HMS model: a review. *Modeling Earth Systems and Environment*, *9*(3), 3029–3051. https://doi.org/10.1007/s40808-023-01704-7

Sanjay Shekar, N. C., & Vinay, D. C. (2021). Performance of hec-hms and swat to simulate streamflow in the sub-humid tropical hemavathi catchment. *Journal of Water and Climate Change*, *12*(7), 3005–3017. https://doi.org/10.2166/wcc.2021.072

Scharffenberg, W., Ely, P., Daly, S., Fleming, M., & Pak, J. (2010). Hydrologic Modeling System (Hec-Hms): Physically-Based Simulation Components. *2nd Joint Federal Interagency Conference*, 8.

Scholten, W. (2007). *Agricultural development and water use in the Central Rift Valley of Ethiopia : A rapid appraisal Agricultural development and water use in the Central Rift Valley of Ethiopia : A rapid appraisal*.

Senamaw, A., Gashaw, T., & Ehsan, M. A. (2022). Impacts of Land-Use/Land-Cover Changes on Water-Borne Soil Erosion Using Geospatial Technologies and RUSLE Model over Chimbel Watershed of Upper Blue Nile Basin in Ethiopia. *Earth Systems and Environment*, *6*(2), 483–497. https://doi.org/10.1007/s41748-021-00259-w

Shah, Z. C. and T. M. (1998). An Introduction to the Global Soil Status. *Environmental Studies*.

Sharu, E. H. (2020). Application of HEC-HMS Model for Flow Simulation for Dungun River Basin. *Advances in Agricultural and Food Research Journal*, *2*(January 2021), 1–16. https://doi.org/10.36877/aafrj.a0000169

Sidle, R. C., Ziegler, A. D., Negishi, J. N., Nik, A. R., Siew, R., & Turkelboom, F. (2006). Erosion processes in steep terrain - Truths, myths, and uncertainties related to forest management in Southeast Asia. *Forest Ecology and Management*, *224*(1–2), 199–225. https://doi.org/10.1016/j.foreco.2005.12.019

Strahler, A. N. (1957). *Quantitative Analysis of Watershed Geomorphology*. *6*.

Szatten, D., & Habel, M. (2020). Effects of land cover changes on sediment and nutrient balance in the catchment with cascade-dammed waters. *Remote Sensing*, *12*(20), 1–21. https://doi.org/10.3390/rs12203414

Taddese, G. (2001). Land degradation: A challenge to Ethiopia. *Environmental Management*, *27*(6), 815–824. https://doi.org/10.1007/s002670010190

Tadesse, T. B., Tefera, S. A., & Lambe, B. T. (2022). Soil erosion assessment in Ethiopia: a recent synthesis of modeling and plot-level studies. *Arabian Journal of Geosciences*,

15(18). https://doi.org/10.1007/s12517-022-10805-z

Tamene, L., Abera, W., Demissie, B., Desta, G., Woldearegay, K., & Mekonnen, K. (2022). Soil erosion assessment in Ethiopia: A review. *Journal of Soil and Water Conservation*, *77*(2), 144–157. https://doi.org/10.2489/jswc.2022.00002

Teketay, D. (2001). *ScholarWorks at WMU Deforestation , wood famine and environmental degradation in highland ecosystems of Ethiopia : urgent need for actions*.

Tesfaye, B., Lengoiboni, M., & Zevenbergen, J. (2021). *Mapping Land Use Land Cover Changes and Their Determinants in the Context of a Massive Free Labour Mobilisation Campaign : Evidence from South Wollo , Ethiopia*.

Thangarajah, V., & Saabith, S. (2021). International Journal of Advance Engineering and Research. *International Journal of Advance Engineering and Research Development*, *July*, 63–69. https://doi.org/10.13140/RG.2.2.21207.83364

Tilahun, B. (2013). *Valuing The Economic Benefits Of Controlling Off-Site Effects Of Soil Erosion: Empirical Evidence From The Eastern Highlands Of Ethiopia*.

Tsegaye, B. (2019). Effect of Land Use and Land Cover Changes on Soil Erosion in Ethiopia. *International Journal of Agricultural Science and Food Technology*, *5*, 26–34.

US Army Corps of Engineers. (2016). Hydrologic Modeling System, HEC-HMS, Quick Start Guide. *U.S. Army Corps of Engineers, Institute for Water Resources, Hydrologic Engineering Center*, *August*, 56. https://www.hec.usace.army.mil/software/hec-hms/documentation/HEC-HMS_QuickStart_Guide_4.2.pdf

US Army Corps of Engineers Hydrologic Engineering Center. (2000). Hydrologic Modeling System Technical Reference Manual. *Hydrologic Modeling System HEC-HMS Technical Reference Manual*, *March*, 148.

USDA, (1972). National engineering handbook, section 4: hydrology. *Washington, DC*, *August*, 127. http://scholar.google.com/scholar?hl=en&btnG=Search&q=intitle:National+Engineering+Handbook+Section+4+Hydrology#0%5Cnhttp://scholar.google.com/scholar?hl=en&btnG=Search&q=intitle:National+engineering+handbook,+section+4:+hydrology#0

Walling, D. E., He, Q., & Blake, W. (1999). Use of 7Be and 137Cs measurements to document soil erosion on agricultural land measurements have now been employed for assessing rates of soil redistribution on cultivated land in many areas of the world , of its much shorter should provide a basis inves. *Water Resources*, *35*(12), 3865–3874.

Wang, H. W., Kondolf, M., Tullos, D., & Kuo, W. C. (2018). Sediment management in Taiwan's reservoirs and barriers to implementation. *Water (Switzerland)*, *10*(8). https://doi.org/10.3390/w10081034

Wassie, S. B. (2020). Natural resource degradation tendencies in Ethiopia: a review. *Environmental Systems Research*, *9*(1), 1–29. https://doi.org/10.1186/s40068-020-00194-1

William W. Doe III! and Russell Harmon. (2022). Introduction to Soil Erosion and Landscape Evolution Modeling. *The Basics of Practical Optimization, Second Edition*, 1–27.

https://doi.org/10.1137/1.9781611977370.ch1

Wischmeier, W. H., and Smith, D. D. (1978). *Predicting ratnfall erosión iosses. USDA Agr. Res. Serv. Hand-book. 537*.

Woldai, T. (2020). The status of Earth Observation (EO) & Geo-Information Sciences in Africa–trends and challenges. In *Geo-Spatial Information Science* (Vol. 23, Issue 1). Taylor & Francis. https://doi.org/10.1080/10095020.2020.1730711

Wordofa, M. G., Okoyo, E. N., & Erkalo, E. (2020). Factors influencing adoption of improved structural soil and water conservation measures in Eastern Ethiopia. *Environmental Systems Research*, *9*(1), 13. https://doi.org/10.1186/s40068-020-00175-4

Yesuph, A. Y., & Dagnew, A. B. (2019). Soil erosion mapping and severity analysis based on RUSLE model and local perception in the Beshillo Catchment of the Blue Nile Basin, Ethiopia. *Environmental Systems Research*, *8*(1), 1–22. https://doi.org/10.1186/s40068-019-0145-1

Zegeye, H. (2017). Major Drivers and Consequences of Deforestation in Ethiopia. *Asian Journal of Science and Technology*, *8*(8), 5166–5175.

Zewide, I., & Achame, A. (2021). Review of on site and off site effects of soil erosion. *International Journal of Environment and Pollution Research*, *9*(August), 1–17. https://doi.org/10.37745/ijepr.13

Zhang, H., Wei, J., Yang, Q., Baartman, J. E. M., Gai, L., Yang, X., Li, S. Q., Yu, J., Ritsema, C. J., & Geissen, V. (2017). An improved method for calculating slope length (λ) and the LS parameters of the Revised Universal Soil Loss Equation for large watersheds. *Geoderma*, *308*(July), 36–45. https://doi.org/10.1016/j.geoderma.2017.08.006

Appendixes

Appendix.1 Climate data Analysis

Table 1. Monthly Average Maximum and Minimum temperature (1991-2020)

Row Labels	Addis Kidame station Average Minimum Temperature	Addis Kidame station Average Maximum Temperature	Chagni station Average minimum temperature	Chagni station Average of maximum Temperature	Bullen station Average minimum Temperature	Bullen station Average maximum Temperature
JAN	5.661307827	26.21739717	8.911639653	30.57942217	11.51327518	29.69022631
FEB	6.988504542	27.7838668	10.93270283	32.28855258	13.5210142	31.61730813
MAR	8.790062724	28.41365591	12.8967687	32.86004489	15.63201067	32.35800161
APR	10.6658858	28.13022222	14.86313146	32.32447534	17.41474891	31.87623207
MAY	11.77773297	26.10608528	15.85820667	29.42349969	16.93270525	29.01603775
JUN	11.80291204	23.76522222	15.3690903	26.38923457	15.94104743	25.91601277
JUL	11.67073029	21.86978495	15.28307948	24.90315093	15.55889198	24.17016098
AGU	11.34121864	22.0511828	14.99815443	24.978162	15.57934201	24.22439876
SEP	10.61261111	23.3423268	14.41802714	25.92433541	15.19647373	25.73799242
OCT	9.51437276	24.04180898	13.95089514	27.08821532	14.74292839	26.64161624
NOV	7.163740741	24.8044902	11.4170157	28.62150504	12.81159063	27.95084671
DEC	5.457855475	25.50674664	9.690300245	29.5010138	11.6666104	28.71005455

Table 2. Monthly Average Rainfall in three-gauge station (1990-2020)

Row Labels	**Addis Kidame Station Average Rainfall in(mm)**	**Chagni Station Average Rainfall (mm)**	**Bullen Station Average Rainfall(mm)**
JAN	2.00	0.60	0.00
FEB	0.80	0.80	0.70

MAR	5.00	4.40	4.20
APR	14.20	10.40	11.20
May	66.00	53.60	47.30
JUN	122.10	94.90	73.90
JUL	153.10	105.50	87.30
AGU	152.80	111.70	83.60
SEP	126.60	99.00	69.50
OCT	54.90	67.80	44.00
NOV	22.80	13.00	7.90
DEC	5.00	2.50	1.40

Appendix. 2. Land Use Land Cover Change Analysis

Table 3 Area of Land Use Land cover types in Dura Watershed 1993 to 2023

Class Name	**1993**	**2003**	**2013**	**2023**
	Area(ha)	Area(ha)	Area(ha)	Area(ha)
Forest	44970.1	47394	40073.4	50565.6
Bush land	59528.7	49929.3	75565.3	109942
Agricultural Land	50282.2	73600.1	80002.7	61608.1
Bare land	70305.8	54163.6	29444.5	2960.3

Table 15: LULCC matrix in hectare (ha)

Change in Hectare (ha)				
Land Use Type	1993-2003	2003-2013	2013-2023	1993-2023
Forest	2423.9	-7320.6	10492.2	5595.5
Bush land	-9599.4	25636	34376.7	50413.3
Agricultural land	23317.9	6402.6	-18394.6	11325.9
Bare land	-16142.2	-24719.1	-26484.2	-67345.5

Appendix. 3. Calibration and Validation Summary Results

Table 3.1. calibration Summery results for run

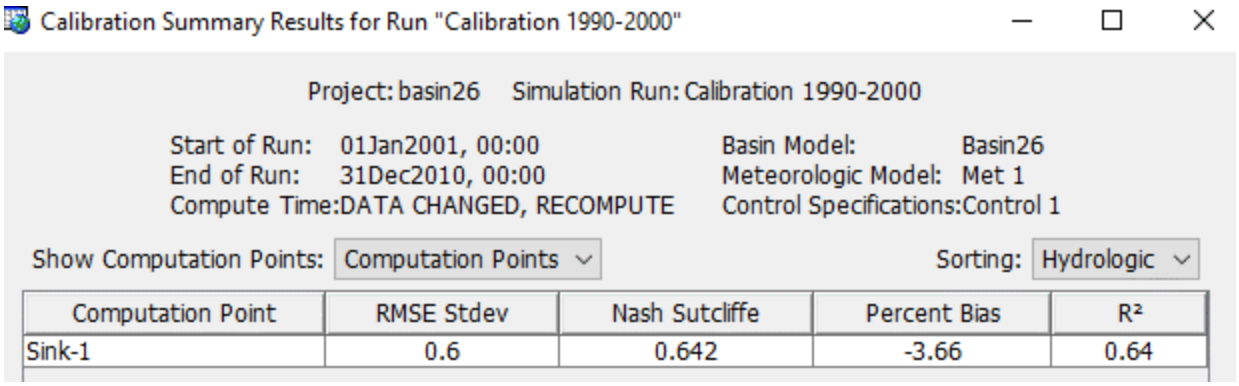

Table 3.2. Global Summery Results run calibration 1990-2000

Hydrologic Element	Derange Area (Km^2)	Peak discharge (m^3/s)	Volume (mm)
Subbasin-1	237.34	46.6	14702.94
Subbasin_2	143.27	19.7	9799.95
J10	380.61	66.1	12857.34
Reach_1	380.61	62.7	12857.33
Subbasin_3	107.07	8	4896.93
Subbasin_4	38.446	2.5	3849.13
J7	526.126	72.1	10579.08
Reach_2	526.126	64	10579.05
Subbasin_5	218.25	3.7	1269.61
J11	218.25	3.7	1269.61
Reach_3	218.25	3.6	1269.61
Subbasin_6	285.88	1.3	320.03

J9	504.13	4.8	731.13
Reach_4	504.13	4.6	731.13
J8	504.13	4.6	731.13
Reach_5	504.13	4.4	731.13
Subbasin_7	223	0.5	158.77
Subbasin_8	94.29	0.1	96.09
J6	1347.546	68.9	4436.93
Reach_6	1347.546	68.2	4436.92
Subbasin_9	78.628	0.1	100.38
J5	1426.174	68.3	4197.84
Reach_7	1426.174	68.3	4197.84
Subbasin_10	70.363	0.1	69.53
Subbasin_11	67.012	0.1	48.86
J4	1563.549	68.3	3834.23
Reach_9	1563.549	65.6	3834.22
Subbasin_12	228.41	0.1	27.05
Subbasin_13	75.767	0	19.15
J3	1867.726	65.6	3213.86
Reach_10	1867.726	65.4	3213.86
Subbasin_14	63.516	0.1	77.18
Subbasin_15	60.045	0.2	169.71
J2	1991.287	65.5	3022.02
Reach_11	1991.287	63.9	3022
Subbasin_16	187.93	1.1	344.87
J1	2179.217	64.3	2791.13
Reach_12	2179.217	64.3	2791.13
Subbasin_17	66.196	0.4	344.87
Sink-1	2245.413	64.5	2719.01

Table 3.3. Calibration Summery results for run validation (2001-2010)

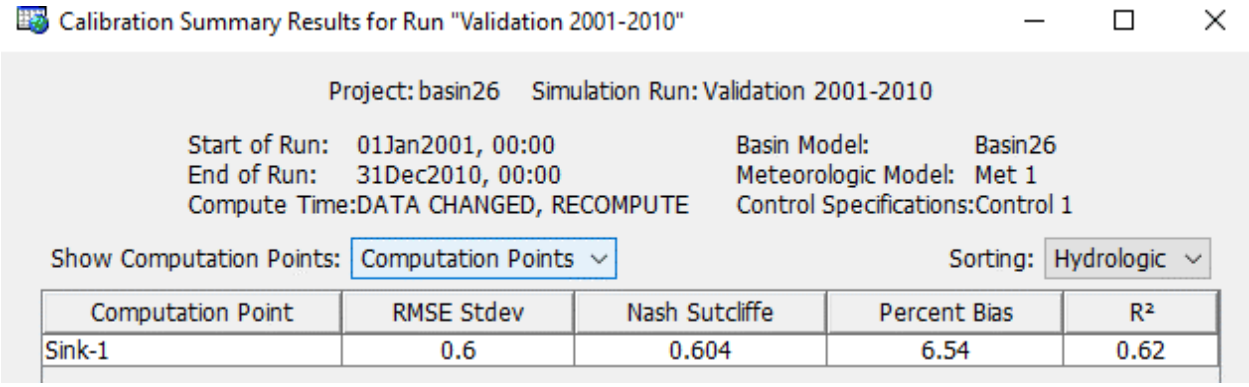

Table Global Summery results to run validation (2001-2000)

Hydrologic Element	Derange Area (Km^2)	Peak discharge (m^3/s)	Volume (mm)
Subbasin-1	237.34	53.1	12864.48
Subbasin_2	143.27	23	8574.69
J10	380.61	76.1	11249.71
Reach_1	380.61	68.8	11249.65
Subbasin_3	107.07	9.5	4284.74
Subbasin_4	38.446	3	3367.97
J7	526.126	78.8	9256.3
Reach_2	526.126	67.5	9256.06
Subbasin_5	218.25	4.3	1110.86
J11	218.25	4.3	1110.86
Reach_3	218.25	4	1110.86
Subbasin_6	285.88	1.5	280.02
J9	504.13	5.2	639.71
Reach_4	504.13	4.8	639.71
J8	504.13	4.8	639.71
Reach_5	504.13	4.6	639.7
Subbasin_7	223	0.6	138.92
Subbasin_8	94.29	0.2	84.08
J6	1347.546	72.6	3882.06
Reach_6	1347.546	71.8	3882.02
Subbasin_9	78.628	0.2	87.83
J5	1426.174	71.9	3672.84
Reach_7	1426.174	71.9	3672.84
Subbasin_10	70.363	0.1	60.84
Subbasin_11	67.012	0.1	42.75
J4	1563.549	72	3354.71

Reach_9	1563.549	68.7	3354.6
Subbasin_12	228.41	0.1	23.67
Subbasin_13	75.767	0	16.76
J3	1867.726	68.8	2811.84
Reach_10	1867.726	68.6	2811.81
Subbasin_14	63.516	0.1	67.53
Subbasin_15	60.045	0.2	148.49
J2	1991.287	68.8	2643.96
Reach_11	1991.287	66.8	2643.83
Subbasin_16	187.93	1.3	301.76
J1	2179.217	67.4	2441.86
Reach_12	2179.217	67.4	2441.85
Subbasin_17	66.196	0.5	301.76
Sink-1	2245.413	67.6	2378.76

Appendix 4. Model parameters

Table 4.1. loss parameters

Subbasin	Initial Deficit (MM)	Maximum Storage (MM)	Constante Rate (MM/HR)
Subbasin-1	22.892	26.382	36.842
Subbasin_2	22.892	26.382	36.842
Subbasin_3	22.892	26.382	36.842
Subbasin_4	22.892	26.382	36.842
Subbasin_5	22.892	26.382	36.842
Subbasin_6	22.892	26.382	36.842
Subbasin_7	22.892	26.382	36.842
Subbasin_8	22.892	26.382	36.842
Subbasin_9	22.892	26.382	36.842
Subbasin_10	22.892	26.382	36.842
Subbasin_11	22.892	26.382	36.842
Subbasin_12	22.892	26.382	36.842
Subbasin_13	22.892	26.382	36.842
Subbasin_14	22.892	26.382	36.842
Subbasin_15	22.892	26.382	36.842
Subbasin_16	22.892	26.382	36.842

Subbasin_17	22.892	26.382	36.842

Table 4.2. Transform parameters

Subbasin	Time of Concentration (HR)	Storage Coefficient (HR)
Subbasin-1	55.3485342	55.158
Subbasin_2	48.156	48
Subbasin_3	40.182	40.211
Subbasin_4	32.443	32.463
Subbasin_5	54.02	53.895
Subbasin_6	48.625	48.842
Subbasin_7	51.596	51.789
Subbasin_8	34.007	34.021
Subbasin_9	28.378	28.337
Subbasin_10	30.645	30.611
Subbasin_11	25.8762215	25.895
Subbasin_12	40.6514658	40.674
Subbasin_13	26.893	26.947
Subbasin_14	27.362	27.411
Subbasin_15	24	24
Subbasin_16	34.476	34.526
Subbasin_17	29.4723127	29.474

Table 4.3. Base Flow parameters

Subbasin	GW 1 Flow Type	GW 1 Initial (M3/S/Km2)	GW 1 Fraction	GW 1 Coefficient (HR)	GW 1 Reservoirs
Subbasin-1	Baseflow	0	0	25.44	1
Subbasin_2	Baseflow	0	0	22.2	1
Subbasin_3	Baseflow	0	0	18.48	1
Subbasin_4	Baseflow	0	0	15	1
Subbasin_5	Baseflow	0	0	24.84	1
Subbasin_6	Baseflow	0	0	22.44	1
Subbasin_7	Baseflow	0	0	23.76	1
Subbasin_8	Baseflow	0	0	15.6	1
Subbasin_9	Baseflow	0	0	13.08	1
Subbasin_10	Baseflow	0	0	14.16	1

Subbasin_11	Baseflow	0	0	11.928	1
Subbasin_12	Baseflow	0	0	18.72	1
Subbasin_13	Baseflow	0	0	12.36	1
Subbasin_14	Baseflow	0	0	12.6	1
Subbasin_15	Baseflow	0	0	11.052	1
Subbasin_16	Baseflow	0	0	15.84	1
Subbasin_17	Baseflow	0	0	13.56	1

Table.4.4. Base Flow parameters

Subbasin	**GW 2 Flow Type**	**GW 2 Initial M3/S/Km2**	**GW 2 Fraction**	**GW 2 Coefficient (HR)**	**GW 2 Reservoirs**
Subbasin-1	Baseflow	0	0.76981	141.6	1
Subbasin_2	Baseflow	0	0.5131	123.2	1
Subbasin_3	Baseflow	0	0.25639	102.8	1
Subbasin_4	Baseflow	0	0.20153	83	1
Subbasin_5	Baseflow	0	0.0664738	138.2	1
Subbasin_6	Baseflow	0	0.0167562	124.4	1
Subbasin_7	Baseflow	0	0.0083129	132	1
Subbasin_8	Baseflow	0	0.0050312	87	1
Subbasin_9	Baseflow	0	0.0052556	72.6	1
Subbasin_10	Baseflow	0	0.0036405	78.4	1
Subbasin_11	Baseflow	0	0.0025582	66.2	1
Subbasin_12	Baseflow	0	0.0014163	104	1
Subbasin_13	Baseflow	0	0.0010027	68.8	1
Subbasin_14	Baseflow	0	0.0040407	70	1
Subbasin_15	Baseflow	0	0.0088854	61.4	1
Subbasin_16	Baseflow	0	0.0180566	88.2	1
Subbasin_17	Baseflow	0	0.0180566	75.4	1

Table 16: Erosion parameters

SUB BASIN	ERODIBILITY FACTOR (K)	TOPOGRAPHIC FACTOR	CORVES FACTOR	PRACTICE FACTOR	THRESHOLD (M3/S)	EXPONENT	GRADATION CURVE
SUBBASIN-1	0.1	18.45	0.2	1	1	0.5	Table 1
SUBBASIN_2	0.1	16.74	0.2	1	1	0.5	Table 1
SUBBASIN_3	0.1	7.26	0.2	1	1	0.5	Table 1
SUBBASIN_4	0.2	2.115	0.2	1	1	0.5	Table 1
SUBBASIN_5	0.1	16.08	0.2	1	1	0.5	Table 1
SUBBASIN_6	0.2	22.14	0.2	1	1	0.5	Table 1
SUBBASIN_7	0.2	14.37	0.2	1	0.1	0.5	Table 1
SUBBASIN_8	0.2	10.47	0.2	1	0.1	0.5	Table 1
SUBBASIN_9	0.2	4.92	0.2	1	0.1	0.5	Table 1
SUBBASIN_10	0.2	8.49	0.2	1	0.03	0.5	Table 1
SUBBASIN_11	0.2	4.92	0.2	1	0.03	0.5	Table 1
SUBBASIN_12	0.2	14.37	0.2	1	0.03	0.5	Table 1
SUBBASIN_13	0.2	7.74	0.2	1	0.03	0.5	Table 1
SUBBASIN_14	0.2	15.81	0.2	1	0.03	0.5	Table 1
SUBBASIN_15	0.2	9	0.2	1	0.1	0.5	Table 1
SUBBASIN_16	0.2	19.56	0.2	1	0.1	0.5	Table 1
SUBBASIN_17	0.2	16.8	0.2	1	0.1	0.5	Table 1

Appendix 5 Sensitivity analysis of the model

Table 5.1. *Sensitivity analysis of the model*

Parameters change	Sensitivity of the model								
		-100	**-20**	**-10**	**0**	**10**	**20**	**100**	**Remark**
GW1 Fraction	Volume	3431.43	7720.77		8578.64		8578.68		S
	Nash	-4.451	-42.052		-54.113		-57.363		S
	Peak	384.9	1100.8		1269.1		1351.8		S
GW2 Fraction	Volume	NA	2725.94		3431.43		4117.71		S
	Nash	NA	-1.741		-4.451		-7.881		S
	Peak	NA	147.7		384.9		461.9		S
GW2 Coefficient	Volume				2725.94		2725.93	2725.84	S
	Nash				-1.741		-1.699	-1.591	S
	Peak				147.7		140.5	121.8	S
GW2 Reservoir	Volume				2725.84			1994.89	S
	Nash				-1.591			-16.568	S
	Peak				121.8			42.9	S
TC	Volume				2725.84		2725.84		NS
	Nash				-1.591		-1.591		NS
	Peak				121.8		121.8		NS
SC	Volume				2725.84		2725.84		NS
	Nash				-1.591		-1.591		NS
	Peak				121.8		121.8		NS
Muskingham K	Volume				2725.84		2725.6		S
	Nash				-1.591		-1.468		S
	Peak				121.8		99		S
Muskingham X	Volume				2725.6		2725.61		NS
	Nash				-1.468		-1.474		NS
	Peak				99		99.8		NS

Appendix 6 Model optimization trial

Table 6.1 Optimized Value

Elements	Parameters	Units	Initial value	Optimized value
All Subbasins	Deficit and Constant - Maximum Deficit Scale Factor		1	100
All Subbasins	Deficit and Constant - Initial Deficit Scale Factor		1	100
All Subbasins	Deficit and Constant - Constant Rate Scale Factor		1	100
Reach_1	Muskingum - x		0.25	0.5
Reach_1	Muskingum - K	HR	14.992	48
Reach_2	Muskingum - K	HR	48	48
Reach_3	Muskingum - K	HR	10.768	48
Reach_4	Muskingum - K	HR	19.994	48
Reach_5	Muskingum - K	HR	20.842	48
Reach_6	Muskingum - K	HR	15.533	48
Reach_7	Muskingum - K	HR	2.2417	48
Reach_9	Muskingum - K	HR	39.803	48
Reach_10	Muskingum - K	HR	13.3042264	48
Reach_11	Muskingum - K	HR	39.291	48
Reach_12	Muskingum - K	HR	2	48
Reach_2	Muskingum - x		0.25	0.001
Reach_3	Muskingum - x		0.25	0.001
Reach_4	Muskingum - x		0.25	0.001
Reach_5	Muskingum - x		0.25	0.001
Reach_6	Muskingum - x		0.25	0.001
Reach_7	Muskingum - x		0.25	0.001
Reach_9	Muskingum - x		0.25	0.001
Reach_10	Muskingum - x		0.25	0.001
Reach_11	Muskingum - x		0.25	0.001
Reach_12	Muskingum - x		0.25	0.001

Table 6.2. Loss before and after Optimization

Initial Deficit (mm)	Maximum storage (mm)	Constant rate (mm)	Optimize. Initial Deficit (mm)	Optimize Maximum storage (mm)	Optimize Constant rate (mm)

11.446	13.191	18.421	22.892	26.382	36.842
11.446	13.191	18.421	22.892	26.382	36.842
11.446	13.191	18.421	22.892	26.382	36.842
11.446	13.191	18.421	22.892	26.382	36.842
11.446	13.191	18.421	22.892	26.382	36.842
11.446	13.191	18.421	22.892	26.382	36.842
11.446	13.191	18.421	22.892	26.382	36.842
11.446	13.191	18.421	22.892	26.382	36.842
11.446	13.191	18.421	22.892	26.382	36.842
11.446	13.191	18.421	22.892	26.382	36.842
11.446	13.191	18.421	22.892	26.382	36.842
11.446	13.191	18.421	22.892	26.382	36.842
11.446	13.191	18.421	22.892	26.382	36.842
11.446	13.191	18.421	22.892	26.382	36.842
11.446	13.191	18.421	22.892	26.382	36.842
11.446	13.191	18.421	22.892	26.382	36.842
11.446	13.191	18.421	22.892	26.382	36.842

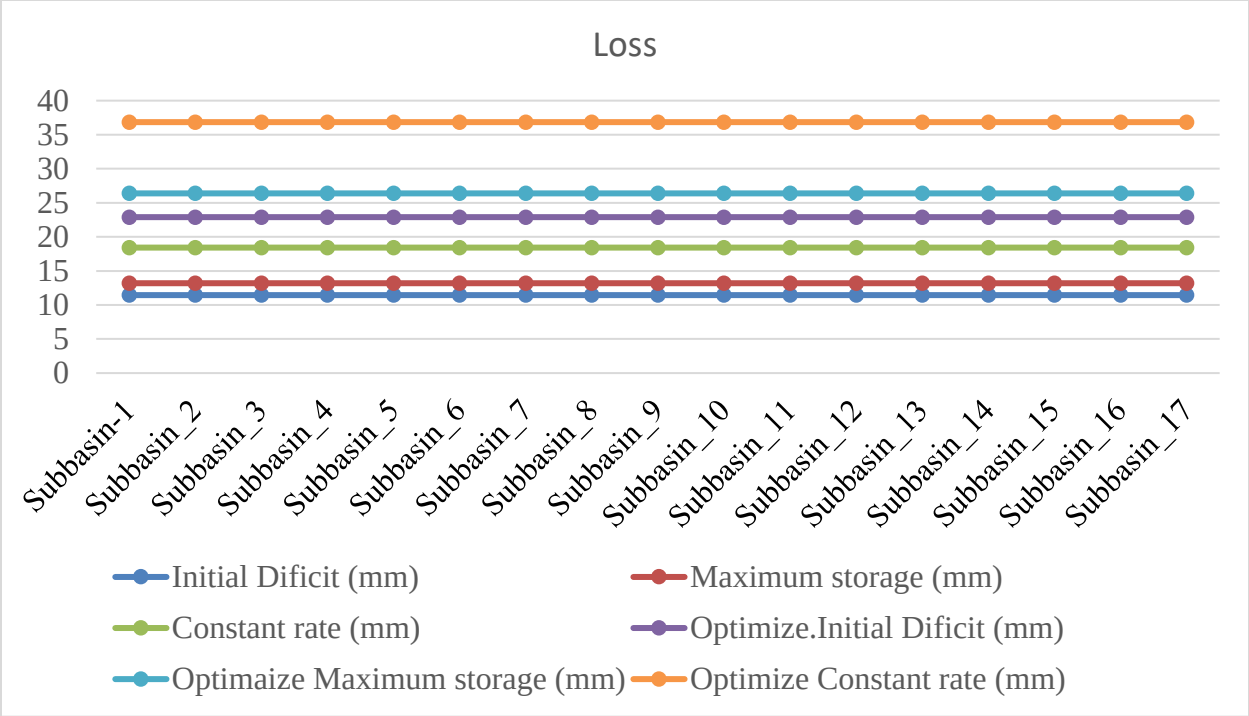

Figure Before and after optimization HEC_HMS Model of loss

Table. 6.3. Optimization trial in Muskingum

Reach	Initial type	Initial discharge	Mus K	Mus X	Number	KAdj2
Reach_1	Discharge = Inflow		0.8052	0.01	1	14.99162
Reach_2	Discharge = Inflow		3.3674	0.01	1	62.69596
Reach_3	Discharge = Inflow		0.57834	0.01	1	10.76783
Reach_4	Discharge = Inflow		1.0739	0.01	1	19.99441
Reach_5	Discharge = Inflow		1.1194	0.01	1	20.84156
Reach_6	Discharge = Inflow		0.83429	0.01	1	15.53323
Reach_7	Discharge = Inflow		0.1204	0.01	1	2.241668

Reach_9	Discharge = Inflow		2.1378	0.01	1	39.80264
Reach_10	Discharge = Inflow		0.71457	0.01	1	13.30423
Reach_11	Discharge = Inflow		2.1103	0.01	1	39.29063
Reach_12	Discharge = Inflow		0.10742	0.01	1	2

Table 6.4. Before and after Opt. Transformation

	TC	SC	TCAdj24	SCAdj24
Subbasin-1	7.08	13.1	55.34853	55.15789
Subbasin_2	6.16	11.4	48.15635	48
Subbasin_3	5.14	9.55	40.18241	40.21053
Subbasin_4	4.15	7.71	32.443	32.46316
Subbasin_5	6.91	12.8	54.01954	53.89474
Subbasin_6	6.22	11.6	48.62541	48.84211
Subbasin_7	6.6	12.3	51.59609	51.78947
Subbasin_8	4.35	8.08	34.00651	34.02105
Subbasin_9	3.63	6.73	28.37785	28.33684
Subbasin_10	3.92	7.27	30.64495	30.61053
Subbasin_11	3.31	6.15	25.87622	25.89474
Subbasin_12	5.2	9.66	40.65147	40.67368
Subbasin_13	3.44	6.4	26.89251	26.94737
Subbasin_14	3.5	6.51	27.36156	27.41053
Subbasin_15	3.07	5.7	24	24
Subbasin_16	4.41	8.2	34.47557	34.52632
Subbasin_17	3.77	7	29.47231	29.47368

Appendix 7 Stream flow

Table 7.1. Average observed and Simulated flow

Row Labels	Average of Simulated	Average of Observed
1991	**16.59232877**	**16.0260274**
1	0	1.922580645
2	0	1.35
3	0	0.819354839

4	1.123333333	0.86
5	11.83870968	1.277419355
6	31.05666667	9.596666667
7	36.4483871	46.0516129
8	41.23870968	51.59677419
9	38.51	45.23
10	28.1	21.96451613
11	7.993333333	7.093333333
12	1.590322581	3.087096774
1992	**17.19781421**	**16.85601093**
1	0.34516129	2.216129032
2	0.265517241	1.489655172
3	1.380645161	0.94516129
4	2.59	2.426666667
5	12.13870968	3.606451613
6	26.93	7.263333333
7	37.19032258	33.51935484
8	42.11612903	53.09032258
9	38.25333333	44.46333333
10	32.19032258	33.95806452
11	10.64333333	12.93
12	1.548387097	5.361290323
1993	**17.47178082**	**17.18547945**
1	0.332258065	2.864516129
2	0.264285714	1.814285714
3	1.380645161	1.435483871
4	2.59	1.723333333
5	12.13870968	2.529032258
6	30.98333333	13.26
7	36.8	33.78064516
8	41.78387097	54.64516129
9	38.47666667	46.02333333
10	31.64193548	27.22580645
11	10.46333333	14.73333333
12	1.548387097	4.929032258
1994	**17.43616438**	**15.13068493**
1	0.325806452	2.687096774
2	0.246428571	1.678571429
3	1.316129032	1.209677419
4	2.46	1.066666667
5	11.57741935	2.077419355
6	31.16333333	14.44666667
7	36.37419355	27.84516129

8	41.28387097	57.0483871
9	38.29666667	44.22666667
10	32.20322581	15.38387097
11	11.11666667	8.576666667
12	1.635483871	4.270967742
1995	**17.46958904**	**16.93041096**
1	0.351612903	1.9
2	0.257142857	1.55
3	1.341935484	1.212903226
4	2.506666667	1.02
5	11.59677419	1.480645161
6	30.59	14.30333333
7	36.6	33.12580645
8	41.65483871	73.8516129
9	38.63333333	44.52333333
10	32.21290323	18.10322581
11	11.00333333	7.03
12	1.635483871	3.548387097
1996	**17.42349727**	**20.4136612**
1	0.34516129	1.9
2	0.265517241	1.562068966
3	1.374193548	1.438709677
4	2.59	1.566666667
5	12.14516129	6.996774194
6	30.99333333	18.13666667
7	36.79354839	48.37741935
8	41.78064516	71.96129032
9	38.46	54.36
10	31.63548387	26.87741935
11	10.46	7.123333333
12	1.54516129	3.432258065
1997	**17.35780822**	**21.78657534**
1	0.219354839	2.216129032
2	0.217857143	1.7
3	1.019354839	1.474193548
4	2.14	1.383333333
5	12.10645161	5.364516129
6	30.52	25.63666667
7	36.80645161	45.02903226
8	42.26129032	61.51935484
9	38.60333333	51.5
10	31.79032258	37.51935484
11	10.08666667	20.05

12	1.248387097	6.470967742
1998	**18.55041096**	**20.04739726**
1	0.158064516	1.741935484
2	0.221428571	1.982142857
3	1.074193548	1.54516129
4	2.29	1.313333333
5	10.8516129	2.761290323
6	36.56666667	16.72
7	38.12258065	44.46774194
8	35.95806452	53.32258065
9	32.21	60.40666667
10	45.90967742	35.94193548
11	16.38	14.30333333
12	1.516129032	4.719354839
1999	**17.99643836**	**20.8909589**
1	0.522580645	2.096774194
2	0.028571429	1.389285714
3	1.277419355	0.909677419
4	1.05	0.723333333
5	19.79032258	3.264516129
6	38.66666667	21.64
7	33.01290323	43.43548387
8	37.32580645	61.63225806
9	34.67666667	53.01
10	32.62903226	42.32903226
11	13.14333333	12.82333333
12	2.596774194	5.7
2000	**19.71038251**	**21.14945355**
1	0.15483871	2.096774194
2	0	1.379310345
3	0.129032258	0.896774194
4	8.61	0.766666667
5	15.19354839	2.935483871
6	30.26	16.72
7	41.38064516	44.82903226
8	40.67741935	53.42258065
9	35.11	60.87333333
10	46.27419355	46.41612903
11	16.99	17.06666667
12	0.864516129	5.464516129
2001	**16.50575342**	**14.62383562**
1	0.038709677	2.019354839
2	0	1.167857143

3	0.096774194	1.003225806
4	1.486666667	0.713333333
5	12.06129032	2.722580645
6	46.97333333	16.60666667
7	30.01290323	22.7483871
8	31.08709677	39.91935484
9	29.45333333	49.08
10	31.70322581	25.83870968
11	12.93	10.23333333
12	1.429032258	2.716129032
2002	**14.30986301**	**13.17369863**
1	0.54516129	1.435483871
2	0.014285714	0.864285714
3	0.325806452	0.461290323
4	1.76	0.316666667
5	4.077419355	0.264516129
6	25.59	12.53
7	29.57741935	23.24193548
8	43.10967742	42.36451613
9	30.20333333	40.51666667
10	26.01612903	15.98709677
11	9.096666667	12.40333333
12	0.322580645	6.929032258
2003	**16.0460274**	**15.19506849**
1	0	1.04516129
2	0.314285714	1.035714286
3	3.022580645	0.887096774
4	0.25	0.343333333
5	0.996774194	0.216129032
6	38.75666667	4.463333333
7	45.03225806	27.06774194
8	40.37741935	51.45806452
9	34.14333333	56.65666667
10	24.26451613	27.12580645
11	3.483333333	5.483333333
12	0.790322581	5.387096774
2004	**17.55819672**	**15.43879781**
1	0.016129032	1.025806452
2	0.024137931	0.848275862
3	0.390322581	0.4
4	7.256666667	0.41
5	3.7	0.429032258
6	31.16333333	9.943333333

7	35.96451613	40.18064516
8	47.22580645	50.60967742
9	46.47666667	46.15666667
10	26.65806452	24.01290323
11	6.203333333	7.523333333
12	5.161290323	2.858064516
2005	**17.58246575**	**15.19972603**
1	0.058064516	0.883870968
2	0.032142857	0.657142857
3	5.103225806	0.44516129
4	1.666666667	0.213333333
5	2.632258065	0.816129032
6	44.98666667	9.58
7	43.65483871	39.6516129
8	31.28387097	52.80645161
9	34.74666667	45.47
10	34.84516129	22.12580645
11	10.81333333	6.77
12	0.174193548	1.609677419
2006	**19.38931507**	**17.48684932**
1	0.048387097	1.838709677
2	0.139285714	1.353571429
3	0	1.025806452
4	1.433333333	0.89
5	16.5516129	2.416129032
6	26.82666667	14.79
7	35.02580645	36.22580645
8	59.30645161	55.76451613
9	34.09666667	50.28333333
10	40.99354839	28.2483871
11	14.24666667	11.17666667
12	2.109677419	4.5
2007	**18.65315068**	**17.35835616**
1	1.193548387	1.861290323
2	0.482142857	1.371428571
3	0.567741935	1.009677419
4	1.71	0.976666667
5	15.36451613	2.419354839
6	36.45333333	13.96333333
7	40.00645161	36.51935484
8	31.61935484	55.43225806
9	42.05	49.63
10	35.23225806	28.25483871

11	16.95666667	11.05
12	1.170967742	4.464516129
2008	**17.30027322**	**17.15027322**
1	0.464516129	1.916129032
2	0.303448276	1.386206897
3	0.203225806	0.993548387
4	12.79	1.016666667
5	15.24516129	2.596774194
6	35.54666667	13.77666667
7	33.75483871	37.27419355
8	40.7	54.52258065
9	32.39	49.38666667
10	29.2	27.46774194
11	6.363333333	10.41666667
12	0.122580645	4.225806452
2009	**14.17890411**	**15.7139726**
1	0	1.509677419
2	0.357142857	1.085714286
3	1.474193548	0.787096774
4	4.353333333	0.62
5	7.651612903	1.45483871
6	26.40666667	11.81666667
7	25.11290323	32.69032258
8	33.64516129	50.34193548
9	33.18333333	48.48333333
10	29.8	25.03548387
11	6.676666667	9.453333333
12	0.596774194	4.116129032
2010	**17.9739726**	**17.51589041**
1	0.183870968	1.703225806
2	0.442857143	1.289285714
3	0	0.970967742
4	0.61	0.81
5	7.85483871	2.377419355
6	28.72	14.56
7	41.72258065	36.73225806
8	45.84193548	55.29032258
9	47.15	50.77
10	32.57419355	28.94516129
11	7.513333333	10.95333333
12	1.767741935	4.44516129
Grand Total	**17.33555099**	**17.26429843**

Table 7.2. Monthly Average calibrated and observed flow

Month	**Average of Calibrated Flow**	**Average of Observed Flow**
Jan	0.250439883	2.198826979
Feb	0.168810289	1.597749196
Mar	1.070087977	1.163049853
Apr	2.703333333	1.301212121
May	12.32228739	3.13313783
Jun	30.10333333	14.52969697
Jul	36.6431085	39.39970674
Aug	41.96041056	57.43225806
Sep	37.62545455	50.58333333
Oct	34.62170088	30.31583578
Nov	10.95333333	11.55606061
Dec	1.435190616	4.534604106

Table 7.3. Annually Average Calibration and observed flow

	Average of Calibrated flow	Average of Observed flow
1990	16.0060274	14.37013699

1991	16.82328767	16.0260274
1992	17.19781421	16.85601093
1993	17.47178082	17.18547945
1994	17.43616438	15.13068493
1995	17.46958904	16.93041096
1996	17.42349727	20.4136612
1997	17.35780822	21.78657534
1998	18.55041096	20.04739726
1999	17.99643836	20.8909589
2000	19.71038251	21.14945355

Table7.4. Monthly Average Validated flow (200-2010)

Month	**Average of Validated Flow (m^3/s)**	**Average of Observed Flow (m^3/s)**
Jan	0.250967742	1.523870968
Feb	0.210638298	1.106028369
Mar	1.108709677	0.798387097
Apr	3.183	0.631
May	8.496774194	1.571290323
Jun	34.141	12.203
Jul	35.98645161	33.23322581
Aug	40.41967742	50.85096774
Sep	36.38933333	48.64333333

Month	Average of Validated Flow (m^3/s)	Average of Observed Flow (m^3/s)
Oct	31.12870968	25.30419355
Nov	9.428333333	9.546333333
Dec	1.364516129	4.12516129

Table 7.5. Annually Average Validation and observed flow

Year	Average of Validated Flow	Average of Observed Flow
2001	16.27	14.62
2002	14.31	13.17
2003	16.05	15.20
2004	17.56	15.44
2005	17.58	15.20
2006	19.39	17.49
2007	18.65	17.36

Year	Average of Validated Flow	Average of Observed Flow
2008	17.30	17.15
2009	14.18	15.71
2010	17.97	17.52

Appendix.8 Erosion rate

Table 8.1. Erosion Rate across Sub-Basin A Decades of Transformation

Sub-Basin	1993	2003	2010
	Erosion rate (t/yr)		
SB1	4.56	11.26	11.76
SB2	8.27	10.43	10.79
SB3	2.15	2.83	2.87
SB4	2.37	3.31	3.46

Sub-Basin	1993	2003	2010
	Erosion rate (t/yr)		
SB5	0.55	0.69	0.71
SB6	0.26	0.33	0.34
SB7	0.15	0.19	0.21
SB8	0.13	0.18	0.20
SB9	0.08	0.11	0.12
SB10	0.10	0.13	0.14
SB11	0.04	0.08	0.09
SB12	0.02	0.03	0.03
SB13	0.02	0.04	0.05
SB14	0.22	0.31	0.34
SB15	0.49	0.49	0.53
SB16	0.37	0.50	0.52
SB17	0.80	1.12	1.16

Appendix.9 Sediment yield

Table 9.1 Average Sediment Yield (tha-1yr-1) In Dura-Sub Watershed (1991-2010)

Sub basin	Average Sediment Yield(tha-1yr-1)
SB1	45.15769087
SB2	28.90020381
SB3	5.808173625
SB4	2.425760807
SB5	2.929677663
SB6	1.824373513
SB7	0.521091928
SB8	0.218905504
SB9	0.115809254
SB10	0.137659708
SB11	0.074376977
SB12	0.077622915
SB13	0.030677604
SB14	0.308114491
SB15	0.382443168
SB16	1.813986857
SB17	1.446216539

Table 9.2. Sum of sediment Yield for each Sub basin.

Year	Sum of SB1	Sum of SB2	Sum of SB3	Sum of SB4	Sum of SB5	Sum of SB6	Sum of SB7	Sum of SB8	Sum of SB9	Sum of SB10	Sum of SB11	Sum of SB12	Sum of SB13	Sum of SB14	Sum of SB15	Sum of SB16	Sum of SB17
1991	20.63	23.39	4.54	1.80	2.38	1.45	0.42	0.16	0.08	0.08	0.04	0.06	0.01	0.19	0.26	1.36	1.04
1992	21.40	26.14	5.20	2.14	2.63	1.62	0.46	0.18	0.09	0.13	0.06	0.06	0.03	0.28	0.31	1.60	1.25
1993	21.62	23.71	4.60	1.83	2.42	1.47	0.42	0.16	0.08	0.08	0.03	0.06	0.01	0.18	0.25	1.39	1.06
1994	21.52	23.47	4.55	1.81	2.40	1.46	0.42	0.16	0.08	0.08	0.03	0.06	0.01	0.18	0.25	1.37	1.04
1995	21.62	23.70	4.60	1.82	2.42	1.47	0.42	0.16	0.08	0.08	0.03	0.06	0.01	0.18	0.25	1.39	1.06

1996	21.62	23.68	4.60	1.82	2.42	1.47	0.42	0.16	0.08	0.08	0.03	0.06	0.01	0.18	0.25	1.39	1.06
1997	43.68	23.83	4.66	1.87	2.44	1.50	0.42	0.16	0.08	0.09	0.03	0.06	0.02	0.18	0.25	1.39	1.06
1998	62.11	35.03	7.05	2.94	3.49	2.18	0.61	0.28	0.14	0.21	0.10	0.09	0.05	0.48	0.46	2.16	1.89
1999	56.66	31.44	6.29	2.61	3.18	1.99	0.56	0.23	0.13	0.14	0.09	0.08	0.03	0.35	0.45	1.93	1.53
2000	61.27	33.93	6.74	2.74	3.43	2.11	0.60	0.26	0.14	0.16	0.10	0.10	0.04	0.34	0.46	2.06	1.74
2001	56.32	31.18	6.23	2.67	3.14	2.00	0.56	0.23	0.14	0.17	0.10	0.08	0.03	0.35	0.47	1.97	1.53
2002	43.58	23.95	4.80	2.04	2.48	1.52	0.45	0.25	0.13	0.14	0.06	0.09	0.03	0.30	0.43	1.53	1.18
2003	53.46	29.89	6.06	2.55	2.99	1.89	0.53	0.21	0.11	0.12	0.07	0.08	0.04	0.25	0.37	1.88	1.49
2004	65.24	36.86	8.00	3.50	3.88	2.52	0.71	0.31	0.16	0.17	0.10	0.11	0.05	0.38	0.55	2.68	2.15
2005	58.04	34.73	7.17	3.02	3.47	2.17	0.61	0.26	0.14	0.16	0.10	0.09	0.04	0.44	0.44	2.22	1.75
2006	64.38	35.56	7.19	3.01	3.58	2.26	0.64	0.26	0.13	0.21	0.10	0.09	0.05	0.47	0.44	2.22	1.75
2007	59.07	33.23	6.88	2.94	3.39	2.10	0.59	0.27	0.15	0.19	0.12	0.10	0.04	0.48	0.52	2.15	1.72
2008	52.48	29.49	5.97	2.52	2.93	1.84	0.52	0.26	0.14	0.15	0.11	0.10	0.04	0.33	0.47	1.96	1.77
2009	42.62	23.87	4.90	2.23	2.40	1.53	0.46	0.19	0.13	0.16	0.08	0.07	0.02	0.38	0.38	1.67	1.34
2010	55.82	30.93	6.15	2.66	3.12	1.93	0.57	0.24	0.12	0.13	0.08	0.08	0.05	0.27	0.40	1.96	1.53

Appendix 10. Model Figure

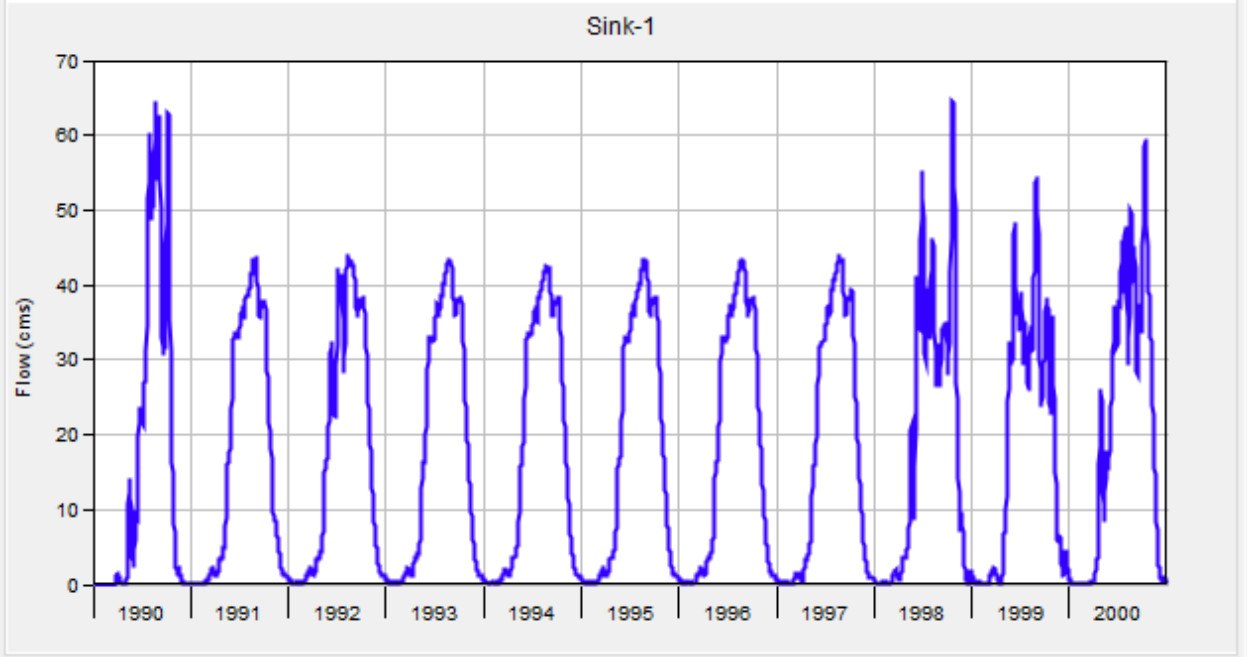

Figure 10.1 Sink outflow results for run to calibration (1990-2000)

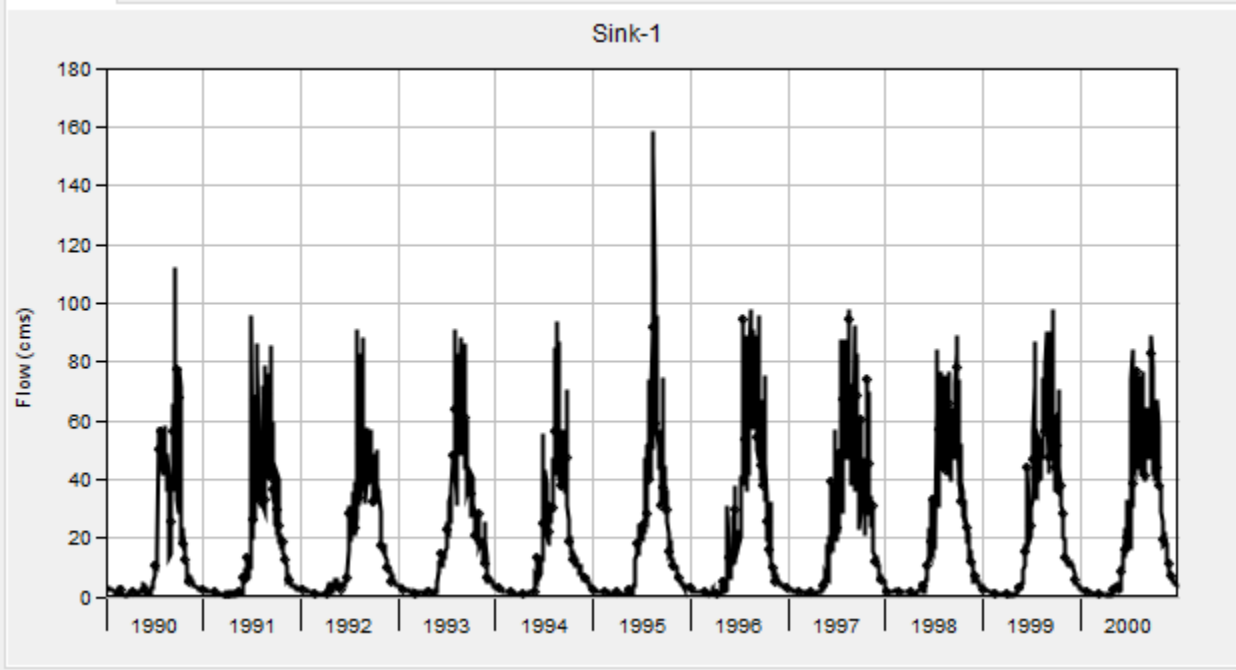

Figure 10.2 Sink observed flow results for run to calibration (1990-2000)

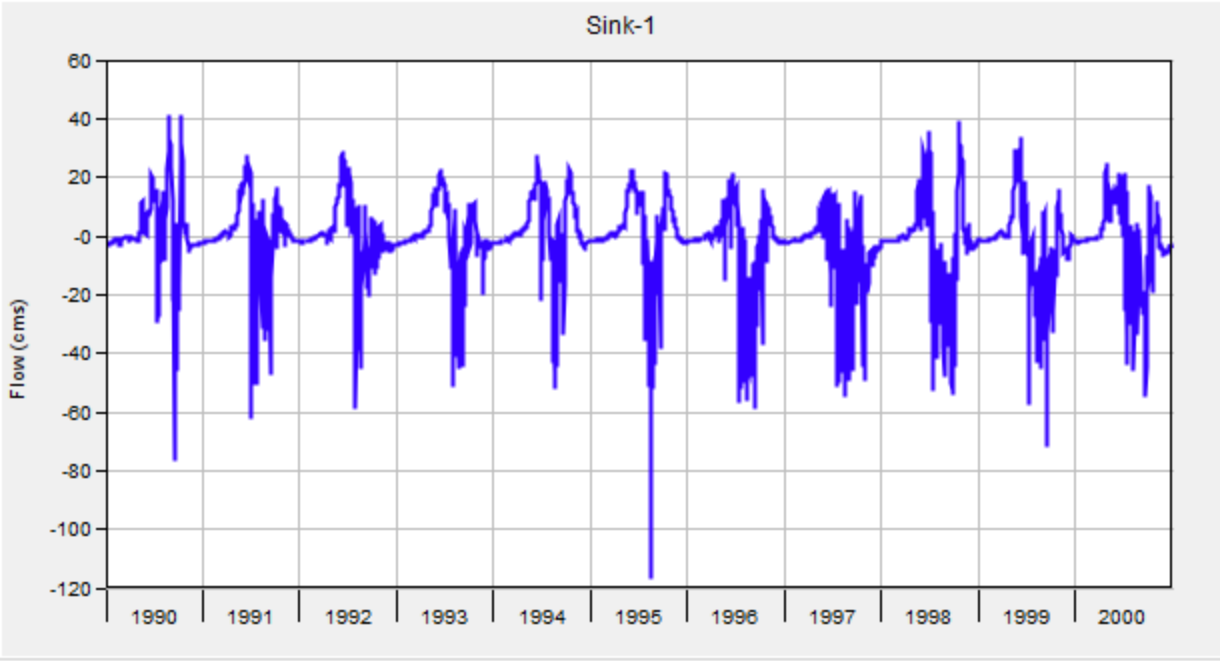

Figure 10.3 Sink Residual flow results for run to calibration (1990-2000)